

GEOLOGY of the SOUTH MOUNTAINS, CENTRAL ARIZONA

Stephen J. Reynolds

Bulletin 195
1985

Arizona Bureau of Geology
and Mineral Technology
Geological Survey Branch

ARIZONA BUREAU OF GEOLOGY AND MINERAL TECHNOLOGY

The Arizona Bureau of Geology and Mineral Technology was established in 1977 by an act of the State legislature. Under this act, the Arizona Bureau of Mines, created in 1915, was renamed and reorganized and its mission was redefined and expanded.

The Bureau of Geology and Mineral Technology, a division of the University of Arizona administered by the Arizona Board of Regents, is charged by the legislature to conduct research and provide information about the geologic setting of the State, including its mineral and energy resources, its natural attributes, and its natural hazards and limitations. In order to carry out these functions, the Bureau is organized into two branches.

Geological Survey Branch. Staff members conduct research, do geologic mapping, collect data, and provide information about the geologic setting of the State to (a) assist in developing an understanding of the geologic factors that influence the locations of metallic, nonmetallic, and mineral fuel resources in Arizona, and (b) assist in developing an understanding of the geologic materials and processes that control or limit human activities in the State.

Mineral Technology Branch. Staff members conduct research and provide information about exploration, mining, and metallurgical processes that are needed in the development of potential metallic, nonmetallic, and mineral fuel resources in Arizona. Guidance is directed toward the recovery and treatment of these resources by methods that are safe, efficient, and compatible with the environmental needs of the State.

Office of the Director

Richard A. Swalin, Director
William P. Cosart, Associate Director

Geological Survey Branch (Arizona Geological Survey)

Larry D. Fellows, State Geologist
and Assistant Director

Mineral Technology Branch

J. Brent Hiskey
Assistant Director

Mining and Mineral Resources Research Institute

Orlo E. Childs, Director

GEOLOGY of the SOUTH MOUNTAINS, CENTRAL ARIZONA

by

Stephen J. Reynolds

Bulletin 195

1985

Arizona Bureau of Geology
and Mineral Technology
Geological Survey Branch

Geological Survey Branch

Larry D. Fellows, Assistant Director and State Geologist

H. Wesley Peirce, Principal Geologist

Stephen J. Reynolds, Assistant Geologist

Jon E. Spencer, Assistant Geologist

Thomas G. McGarvin, Research Assistant II

Elaine Falls, Secretary I

Michael Settle, Secretary III

Evelyn M. VandenDolder, Associate Editor

Joseph R. LaVoie, Research Equipment Technician

Kenneth Matesich, Graphic Artist III

Preface

The geologic map and accompanying text that compose Bulletin 195 represent an important contribution to our understanding of the geologic framework of Arizona. The South Mountains are among the recently recognized "metamorphic core complexes" of western North America and, as such, are similar in age and origin to other core complexes in Arizona, including the Rawhide, Buckskin, Harquahala, Harcuvar, White Tank, Picacho, Tortolita, Santa Catalina, and Rincon Mountains. The accessibility and comparative geologic simplicity of the South Mountains make them an ideal area in which to study the characteristics and origin of these important complexes.

Prior to Dr. Reynolds' work in the area, geologists believed that the South Mountains were largely composed of 1.6- to 1.7-b.y.-old Precambrian gneiss. Dr. Reynolds, however, has demonstrated that the entire eastern half of the range is actually composed of sheared granitic rocks that are only 25 m.y. in age. He has also discovered a major, previously unrecognized, low-angle detachment fault that projects into the subsurface beneath Phoenix, Tempe, and Mesa.

This bulletin also documents for the first time that gold, silver, and copper mineralization in the South Mountains is middle Tertiary in age, not older, as previously thought. Ores mined between 1913 and 1942 yielded metals that would have been worth more than \$2.7 million at 1984 prices.

The classic geologic relationships of this area, which is surrounded by the State's major population center, will provide an excellent natural laboratory for geology students, mineral explorationists, prospectors, scout organizations, and other persons interested in the geologic history of Arizona.

Dr. Larry D. Fellows
State Geologist and Assistant Director
Arizona Bureau of Geology and
Mineral Technology

Acknowledgments

The author gratefully acknowledges the encouragement and support of Professors Peter J. Coney and George H. Davis, both of whom directed the University of Arizona Ph.D. research upon which this publication is largely based. The original dissertation was significantly improved through reviews by H. Wesley Peirce, Paul E. Damon, and John M. Guilbert. Sincere thanks are given to Paul Damon and M. Shafiqullah of the Laboratory of Isotope Geochemistry, University of Arizona, for their unending cooperation in the geochronologic aspects of this research. Dan Lynch, Arend Meijer, and Robert Butcher also provided assistance with isotope geochemistry. All phases of this research were financially supported by the Arizona Bureau of Geology and Mineral Technology.

The conclusions expressed in this publication are partly the result of research done in conjunction with Dr. Gordon S. Lister of the Australian Bureau of Mineral Resources. Gordon has been instrumental in helping to decipher the sense of shear in the mylonitic rocks and in critically evaluating the relative importance of coaxial and noncoaxial deformation. Gordon's research in the United States was made possible through a grant from the National Science Foundation.

The author has greatly benefited from a series of discussions and field trips with J. L. Anderson, P. J. Coney, G. A. Davis, G. H. Davis, H. W. Day, Ed DeWitt, W. R. Dickinson, E. G. Frost, S. P. Gillatt, H. W. Green, Warren Hamilton, S. B. Keith, Falk Koenemann, T. G. McGarvin, H. W. Peirce, D. M. Ragan, W. A. Rehrig, S. M. Richard, L. T. Silver, and J. E. Spencer.

Preparation of this bulletin was aided by several staff members of the Arizona Bureau of Geology and Mineral Technology. The text was clarified by thoughtful reviews by Jon E. Spencer, the late Anne M. Candea, and Evelyn M. VandenDolder, who edited the final manuscript and spent countless hours at the terminal to enhance the aesthetics of the computer-generated copy. The colored geologic map and final layout were prepared by Ken Matesich, under the supervision of Joe LaVoie. Most of the remaining figures were drafted by Jenny Laber. The manuscript was typed by Cheryl Wachter, Clara Garcia, Jennifer Fogle, and Alinda Carter. Finally, the author is grateful for the full support of Larry D. Fellows, State Geologist, and H. Wesley Peirce, Principal Geologist, both with the Bureau.

Table of Contents

PREFACE	iii
ACKNOWLEDGMENTS	iv
LIST OF TABLES AND ILLUSTRATIONS	vii
ABSTRACT	xi
INTRODUCTION	1
Location and Physiography	1
Geologic Studies	4
Cordilleran Metamorphic Core Complexes	5
Nomenclature	5
REGIONAL GEOLOGIC SETTING	6
GENERALIZED GEOLOGIC RELATIONSHIPS	7
PRECAMBRIAN ROCKS	13
Estrella Gneiss	13
Lithology	13
Metamorphic Grade and Protoliths	14
Komatke Granite	14
MIDDLE TERTIARY ROCKS	15
South Mountains Granodiorite	15
Field Relations	15
Lithology	15
Related Rock Types	16
Telegraph Pass Granite	16
Field Relations	16
Lithology	17
Related Rock Types	17
Dobbins Alaskite	17
Field Relations	17
Lithology	18
Mylonitic Gneiss and Schist	18
Lithology	18
Dikes and Sills	19
Chloritic Breccia and Microbreccia	21
Chloritic Breccia	21
Microbreccia	22
LATE TERTIARY-QUATERNARY SURFICIAL DEPOSITS	22
GEOCHRONOLOGY	23
Introduction	23
Geologic Constraints	23
Rb-Sr Geochronology	24
Estrella Gneiss	24
South Mountains Granodiorite	24
Telegraph Pass Granite	25
K-Ar Geochronology	26
Estrella Gneiss	26
South Mountains Granodiorite and Telegraph Pass Granite	26
Microdiorite Dike	27
U-Pb Geochronology	27
Geochronologic Summary	27

STRUCTURAL GEOLOGY	28
Precambrian Deformation	28
Character and Orientation	28
Age and Kinematics	28
Middle Tertiary Dilation Associated With Plutonism	28
South Mountains Granodiorite and Telegraph Pass Granite	29
Dikes and Sills	31
Kinematics	31
Middle Tertiary Mylonitic Deformation	32
Mylonitic Fabrics	32
Mineralogic Response to Mylonitization	33
Minor Structures	35
Gash Fractures	35
Pinch-and-Swell Structures	35
Folds	35
Orientation	36
Precambrian Rocks	36
Middle Tertiary Rocks	36
Relationship to Preexisting Features	36
Age	42
Conditions of Mylonitization	42
Kinematics	43
Middle Tertiary Fracturing, Brecciation, and Detachment Faulting	44
Chloritic Fracture Zones Within South Mountains Granodiorite	45
Transitional Zone Between Unfractured Granodiorite and Chloritic Breccia	45
Chloritic Breccia and Microbreccia	47
Detachment Fault	48
Kinematics	48
Age	49
Middle(?) Tertiary Arching	50
Late Tertiary Basin and Range Deformation	51
ECONOMIC GEOLOGY	52
SUMMARY AND CONCLUSIONS	54
Geologic Evolution of the South Mountains	54
Relationship Between Mylonitization, Brecciation, and Detachment Faulting	55
Implications for the Origin of Cordilleran Metamorphic Core Complexes	55
REFERENCES CITED	58
APPENDIX	61

List of Tables and Illustrations

Table	Page
1. Rb-Sr analyses	24
2. Rb-Sr model ages for aplites in South Mountains Granodiorite and Telegraph Pass Granite	25
3. K-Ar analyses	26
4. Modal orientations of crystalloblastic foliation in Precambrian domains	29
5. Modal and mean orientations of middle Tertiary igneous structures	30
6. Modal and mean orientations of mylonitic fabric . .	37
7. Modal and mean orientations of chloritic fracture zones and striations in chloritic breccia	45

Plate	Page
1. Geologic map of the South Mountains, central Arizona (pocket)	

Figure	Page
1. Map showing location of South Mountains and adjacent ranges	1
2. Aerial photograph of the South Mountains, looking southwest	2
3. Physiographic features of the South Mountains . . .	3
4. Aerial photograph showing profile of eastern South Mountains, looking southeast	3
5. Aerial photograph of northern edge of Main Ridge . .	4
6. Generalized geologic map and cross section of the South Mountains	8
7. Generalized geologic map of Telegraph Pass and vicinity	9
8. Schematic cross section of Telegraph Pass, Mount Suppoa, and Dobbins Lookout	9
9. Schematic cross section of Entrance Ridge and adjacent Main Ridge	10
10. Generalized geologic map of central Southern Foothills and Boundary Hills	10
11. Schematic cross section of central Southern Foothills and Boundary Hills	11

Figure	Page
12. Generalized geologic map of Pima and Ahwatukee Ridges	11
13. Schematic cross section of Pima and Ahwatukee Ridges	12
14. Photograph of Precambrian Estrella Gneiss below zone of intense mylonitization	13
15. Photograph of strongly deformed Komatke Granite in the Southern Foothills	14
16. Photograph of inclusion-rich South Mountains Granodiorite along the north edge of Main Ridge . .	15
17. Photograph of undeformed Telegraph Pass Granite near Telegraph Pass	17
18. Photograph of mylonitic Dobbins Alaskite near Mount Suppoa	18
19. Photograph of mylonitic gneiss and schist south of Mount Suppoa	18
20. Photomicrograph of mylonitic gneiss under crossed nicols	19
21. Photograph of middle Tertiary microdiorite dikes intruding South Mountains Granodiorite north of Telegraph Pass	20
22. Photomicrographs of dikes under crossed nicols . . .	20
23. Photograph of chloritic breccia on Two Peaks	21
24. Photomicrograph of chloritic breccia under crossed nicols	21
25. Photograph of microbreccia on the northeast end of Main Ridge	22
26. Photomicrograph of microbreccia under crossed nicols	22
27. Schematic cross section illustrating contact relationships	23
28. Rb-Sr whole-rock isochrons for South Mountains Granodiorite and Telegraph Pass Granite	25
29. Contoured equal-area plots of poles to crystallo- blastic foliation in Precambrian rocks	29
30. Strike-frequency diagram of crystalloblastic foliation that dips 60° or more	29
31. Contoured equal-area plots of poles to crystalloblastic and mylonitic foliations in Precambrian rocks	30
32. Strike-frequency diagram of aplite dikes in South Mountains Granodiorite	30
33. Strike-frequency diagrams of mineralized fractures in Telegraph Pass Granite, South Mountains Granodiorite, and Dobbins Alaskite	31
34. Trend-frequency diagrams of dikes in western and eastern dike swarms	31
35. Histogram of dike trends in both swarms	32
36. Trend-frequency diagram of microdiorite dikes . . .	32

Figure	Page
37. Photograph of mylonitic South Mountains Granodiorite with foliated quartz veins and aplite dikes	32
38. Photographs of mylonitic fabric	33
39. Photomicrographs of mylonitic fabric	34
40. Photograph of mylonitic lineation in South Mountains Granodiorite	34
41. Photograph of low-angle, mylonitic fabric cutting steep, crystalloblastic foliation in Precambrian Estrella Gneiss	35
42. Contoured equal-area plot of poles to mylonitic foliation in all Precambrian domains	38
43. Contoured equal-area plots of mylonitic fabric in individual Precambrian domains	38
44. Trend-frequency diagram of mylonitic lineation in all Precambrian domains	38
45. Contoured equal-area plot of mylonitic lineation in all Precambrian domains	39
46. Trend-frequency diagrams of mylonitic lineation in Precambrian rocks	39
47. Trend-frequency diagram of fold axes in mylonitically deformed, Precambrian rocks	39
48. Contoured equal-area plots of poles to mylonitic foliation in South Mountains Granodiorite	39
49. Trend-frequency diagrams of mylonitic lineation in middle Tertiary rocks	40
50. Contoured equal-area plots of mylonitic fabric in middle Tertiary rocks	41
51. Contoured equal-area plot of mylonitic fabric in dikes and sills	41
52. Trend-frequency diagram of long axes of deformed inclusions in South Mountains Granodiorite and Telegraph Pass Granite	42
53. Photomicrographs of undeformed and deformed dikes	42
54. Photograph of tension gash in mylonitic Estrella Gneiss	43
55. Photograph of S-C relationships in a cut slab of South Mountains Granodiorite	44
56. Strike-frequency diagram of chloritic fracture zones in South Mountains Granodiorite	45
57. Photograph of Main Ridge near Two Peaks, looking southwest	46
58. Photographs of structure in chloritic breccia	46
59. Strike-frequency diagrams of fracture zones in chloritic breccia	47
60. Trend-frequency diagram of striations in chloritic breccia	47
61. Histogram of striation trends in chloritic breccia on eastern ends of Main and Ahwatukee Ridges	48

Figure	Page
62. Stereographic projection showing rotation of mylonitic foliation and lineation by brecciation . .	48
63. Aerial photograph of South Mountains, looking southwest	49
64. Map showing attitude of mylonitic foliation in the South Mountains	50
65. Distribution of gold mines and prospects in the South Mountains	52
66. Strike-frequency diagram of gold-bearing veins in and near the Delta Mine	53
67. Chronology of geologic events in the South Mountains	54
68. Schematic diagram depicting an evolving-shear-zone model for Cordilleran metamorphic core complexes	56

Abstract

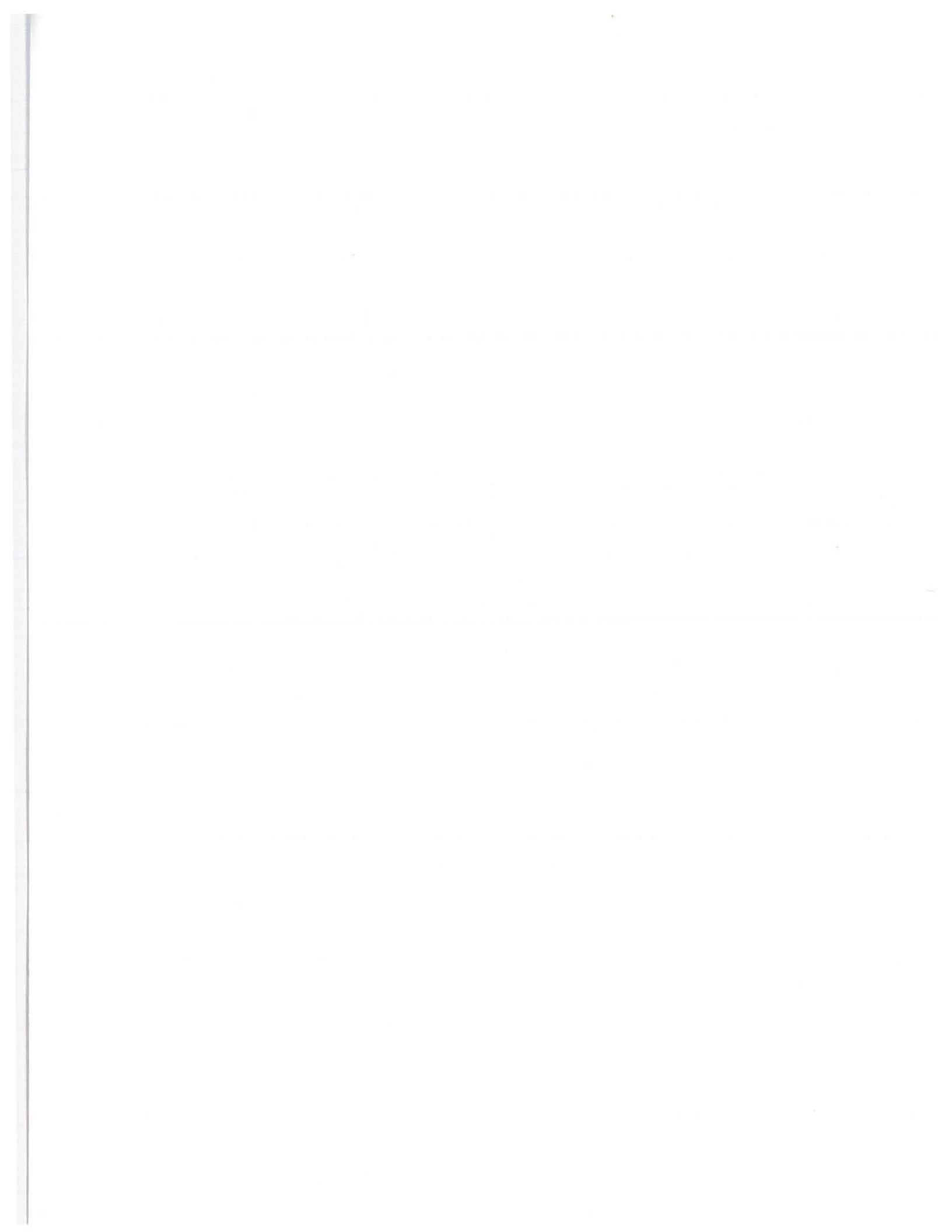
The South Mountains of central Arizona are a typical, but geologically simple, metamorphic core complex. The western half of the range is underlain by Precambrian metamorphic and granitic rocks, whereas the eastern half is primarily a composite middle Tertiary pluton. The Precambrian terrane is composed of two rock units, Estrella Gneiss and Komatke Granite, both of which were involved in a major episode of middle Proterozoic metamorphism and deformation that produced a steep crystalloblastic foliation. The composite Tertiary pluton has three semicontemporaneous phases: (1) South Mountains Granodiorite, the oldest and most widely distributed phase; (2) Telegraph Pass Granite; and (3) Dobbins Alaskite. Both the Precambrian terrane and the composite Tertiary pluton have been intruded by numerous, north-northwest-trending, middle Tertiary dikes.

Middle Tertiary plutonism was accompanied by intense mylonitization that affected Precambrian and middle Tertiary rocks alike. Mylonitization was associated with each intrusive pulse at 25 m.y. B.P. Mylonitization generally produced a low-angle foliation and east-northeast-trending lineation. The attitude of mylonitic foliation defines a broad, east-northeast-trending antiform that controls the topographic axis of the range. Structurally low rocks in the core of the antiform are nonmylonitic, but the intensity of mylonitic fabric progressively increases toward higher structural levels. Mylonitic Tertiary plutonic rocks are exposed as a gently dipping carapace overlying their less deformed equivalents. Mylonitic fabric cuts through the Precambrian terrane as a broad, west-dipping zone. Rocks above and below this mylonitic zone are lithologically identical and generally retain their Precambrian structure. Fabrics in all rock types indicate that mylonitization was accompanied by extension parallel to east-northeast-trending lineation and by flattening

perpendicular to subhorizontal foliation. Small-scale structures indicate that most mylonitic rocks were formed by noncoaxial, east-northeast-directed shear parallel to lineation. Other mylonitic rocks may have formed by localized coaxial deformation (i.e., pure shear). Mylonitization occurred under conditions of elevated temperature, but relatively low to moderate confining pressure; both temperature and pressure probably decreased during successive phases of mylonitization.

Mylonitization was succeeded by more brittle deformation that produced chloritic breccia and microbreccia in the footwall of a major detachment fault that dips gently to the east. The detachment fault and underlying breccia were formed by low-angle normal faulting and brittle extension in an east-northeast direction. Rocks above and directly below the detachment fault were antithetically rotated during faulting. The South Mountains detachment fault or an unexposed, higher detachment fault probably continues at depth a significant distance to the northeast in order to account for the southwest dip of Tertiary supracrustal rocks near Tempe.

Geologic and geochronologic data strongly suggest that mylonitization and detachment faulting represent a continuum of middle Tertiary shear and extension. Mylonitization and detachment faulting both involved extension and shear in an east-northeast direction and both are middle Tertiary in age based on Rb-Sr, U-Pb, and K-Ar geochronology. There is a complete spectrum of rocks transitional in character between mylonitic schist and microbreccia. Documentation of a continuum between mylonitization and detachment faulting has important implications regarding the evolution of Cordilleran metamorphic core complexes. Specifically, the complexes may represent the ductile to brittle evolution of normal-slip shear zones of crustal proportions.



Introduction

Location and Physiography

The South Mountains are located in central Arizona, 20 km east-southeast of the confluence of the Salt and Gila Rivers (Figure 1). They lie immediately south of metropolitan Phoenix and are mostly contained within the City of Phoenix South Mountain Park, the world's largest municipal park. Southwestern and southern parts of the range are in the Gila River Indian Reservation or International Harvester's Phoenix Proving Grounds. The South Mountains are referred to as the Salt River Mountains on some topographic maps.

The South Mountains are an isolated range surrounded by broad plains of unconsolidated surficial deposits (Figure 2). The range is 18 km long and varies in elevation from approxi-

mately 400 to 800 m (1,200-2,500 ft) above sea level. The dominant physiographic feature is a large, northeast-trending ridge, herein referred to as Main Ridge (Figure 3). Telegraph Pass, a pronounced topographic notch, occurs near the midpoint of the ridge.

The physiographic characteristics of Main Ridge show marked differences on either side of the pass. Northeast of the pass, Main Ridge exhibits an archlike topography with a relatively flat top and moderately steep, northwest and southeast flanks (Figures 2 and 4). This area displays a well-developed north-northwest topographic grain defined by numerous linear drainages and ridges (Figure 5). Southwest of Telegraph Pass, Main Ridge bifurcates into a series of southwest-trending ridges that have steep, rocky slopes and serrated crests. Most large drainages in this area flow to the southwest, parallel to the ridges.

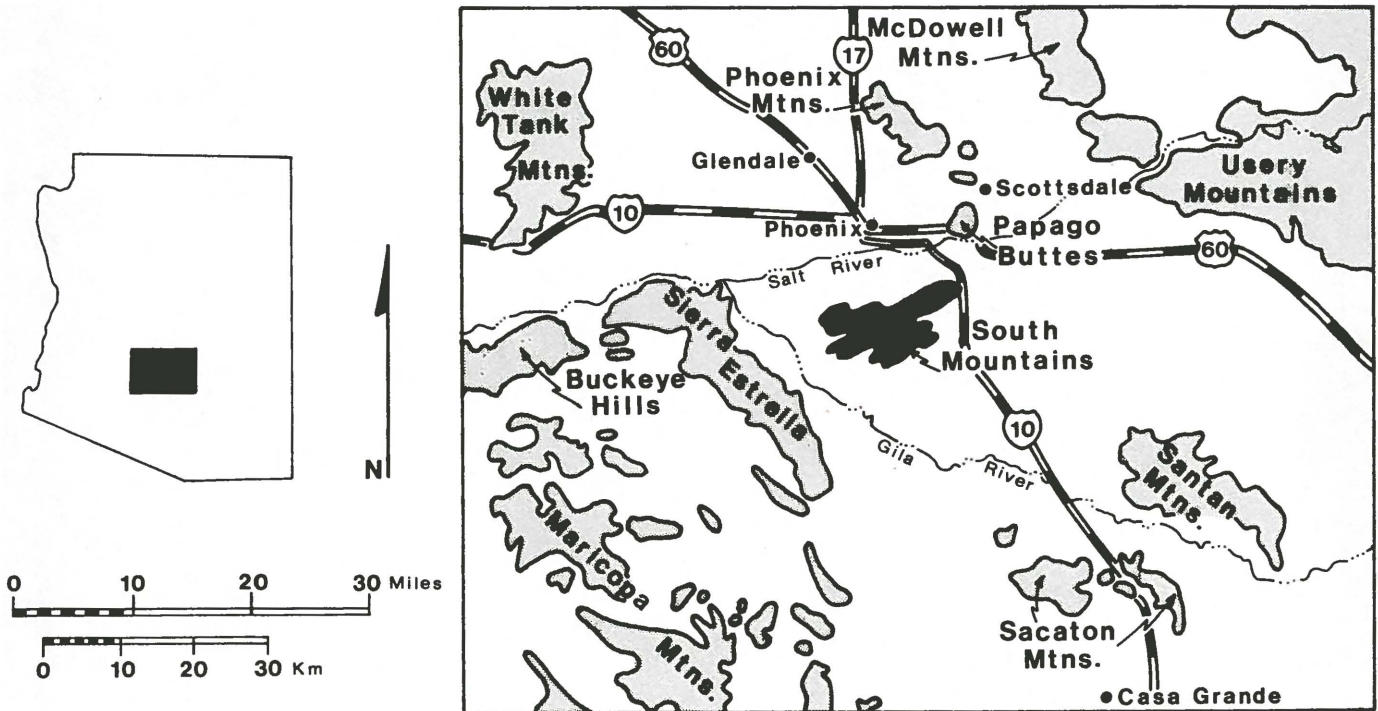


Figure 1. Map showing location of the South Mountains and adjacent ranges.



Figure 2. Aerial photograph of the South Mountains, looking southwest. Visible in the photograph are the Southern Foothills and International Harvester's

Phoenix Proving Grounds (both left center), Main Ridge (center), Alta Ridge (right center), and Sierra Estrella (background).

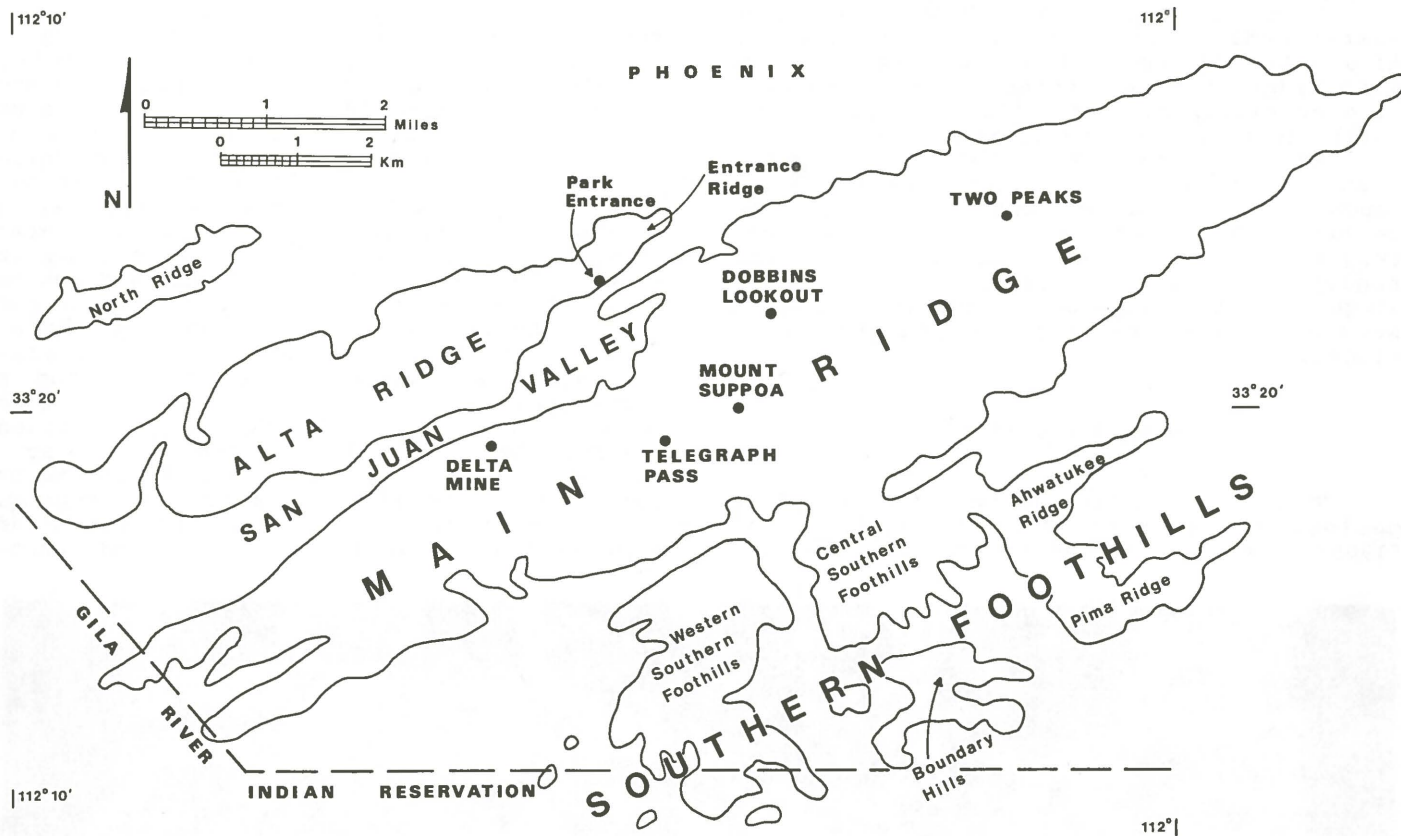


Figure 3. Physiographic features of the South Mountains.



Figure 4. Aerial photograph showing profile of eastern South Mountains, looking southeast. Telegraph Pass and Mount Suppoa are near the right edge of the photograph. The abrupt change in the topographic profile of the range on the left side of the photograph corresponds with the boundary between generally unbrecciated grano-

diorite to the right (southwest) and brecciated, chloritic granodiorite to the left (northeast). Mountain ranges in the distance are, from front to back, the Sacaton and San Tan Mountains, Picacho Mountains, and Santa Catalina Mountains (top left of photograph).

Lying northwest of Main Ridge is a north-east-trending ridge, herein referred to as Alta Ridge (Figure 3). Near the park entrance, Alta Ridge adjoins Entrance Ridge, a succession of small, rounded hills. The low-relief North Ridge lies northwest of Alta Ridge.

South of Main Ridge are irregularly shaped hills and ridges that constitute the Southern Foothills. The Southern Foothills can be subdivided into the following five sections (Figure 3): (1) western half; (2) central region; (3) Boundary Hills; (4) Ahwatukee Ridge; and (5) Pima Ridge. These physiographic subdivisions are referred to throughout this report.

Geologic Studies

This investigation is the first complete geologic study of the South Mountains. Lee (1905) briefly mentioned the range while dis-

cussing the geology of the lower Salt River region. Darton (1925) noted the presence of chloritic schist, phyllite, and biotite granite. The Geologic Map of Maricopa County (Wilson and others, 1957) depicts the range as Precambrian gneiss intruded by a narrow, northwest-trending Laramide pluton near Telegraph Pass. Wilson (1969) briefly described rock types and scattered gold occurrences in the Southern Foothills. Avedisian (1966) studied petrology of Precambrian metamorphic rocks, Tertiary granite, and Tertiary dikes in the western half of the range. He mapped the contact between the granite and Precambrian gneiss, and noted, but did not map, a gradational contact between the granite and a foliated, more mafic pluton to the east. Like Wilson and others (1957), Avedisian assigned the foliated mafic pluton a Precambrian age, suggesting that it had been emplaced before or during the Precambrian Mazatzal orogeny. Champine (1982), following the study of Reynolds (1982), studied mesoscopic and micro-

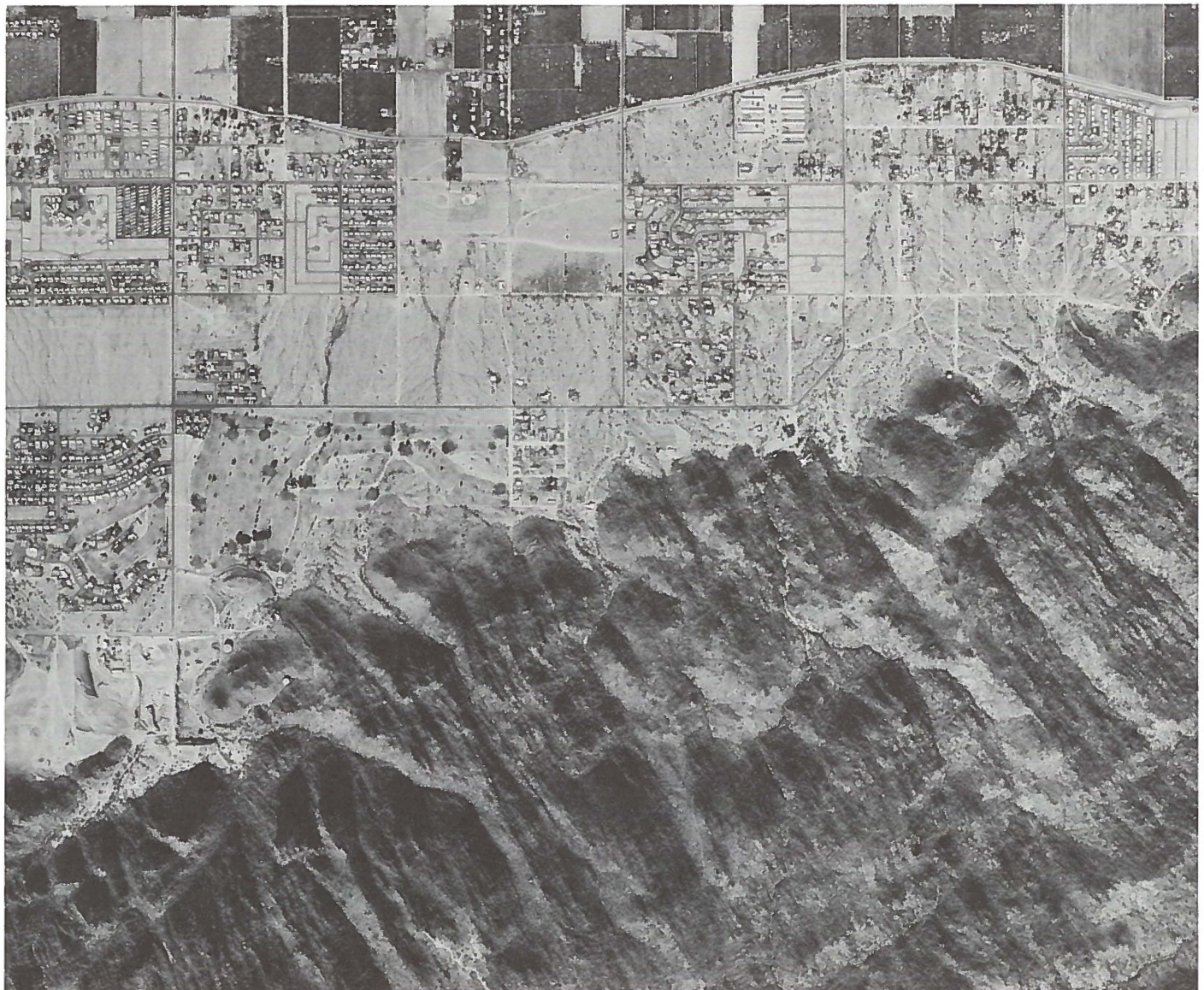


Figure 5. Aerial photograph of northern edge of Main Ridge. North is toward top of photograph. Note the

pronounced north-northwest-trending topographic grain.

scopic structures in the northeastern end of the range.

Mapping for the present study was carried out between 1977 and 1981, utilizing U.S. Geological Survey 7.5-minute quadrangles as a topographic base (Plate 1, in pocket). Detailed structural analysis was performed at many localities, and key rock types were collected for petrographic and geochronologic studies. Rb-Sr and K-Ar isotopic analyses were done in cooperation with M. Shafiqullah and Paul E. Damon of the Laboratory of Isotope Geochemistry, University of Arizona. Preliminary reports of this research have been published elsewhere (Reynolds and others, 1978; Reynolds and Rehrig, 1980; Reynolds, 1982, 1983). Additional discussion of the microstructures and structural evolution of the South Mountains is presented in S. J. Reynolds and G. S. Lister (in preparation). The preliminary U-Pb ages discussed in this report were determined by Ed DeWitt of the USGS, and are reported in S. J. Reynolds, M. Shafiqullah, P. E. Damon, and Ed DeWitt (in preparation).

Cordilleran Metamorphic Core Complexes

The term "metamorphic core complex" has been proposed for more than 20 mountain ranges or groups of ranges in western North America that contain a distinctive assemblage of rocks and structures (Coney, 1973, 1980; Davis, G. H., and Coney, 1979). Metamorphic core complexes are characterized by a central terrane of metamorphic, plutonic, and mylonitic rocks overlain by a marginal zone of brittle deformation and detachment faulting (see descriptions in Crittenden and others, 1980). The South Mountains not only contain rocks and structures typical of metamorphic core complexes, but they are also one of the most geologically simple core complexes known. The South Mountains have the characteristic mylonitic rocks and a detachment fault, but they lack a complicating Mesozoic history that makes interpretation of most other complexes so difficult. In the South Mountains, the origins of mylonitic rocks and a detachment fault can be evaluated in their most simple

geologic setting. Also, clear relationships between mylonitization and plutonism enable the age of mylonitization to be determined using isotope geochronology. The resulting age determinations provide the first unequivocal documentation for middle Tertiary mylonitization in Arizona (Reynolds and Rehrig, 1980; Reynolds, 1982).

Nomenclature

Usage of the names Estrella Gneiss, Komatke Granite, South Mountains Granodiorite, Telegraph Pass Granite, and Dobbins Alaskite has been approved by the USGS Geologic Nomenclature Committee (M. E. MacLachlan, 1981, written communication). Plutonic rock nomenclature employed in this study is that adopted by Streckeisen (1976). The term **mylonitic** is used to describe foliated and lineated rocks in which some minerals have deformed brittlely and some have deformed ductilely or have recrystallized. These rocks are very similar to hand specimens and photomicrographs of protomylonite, mylonite, and mylonite gneiss, as presented in the classification of Higgins (1971). In the present report, a tabular intrusion is referred to as a **dike** if it dips more than 45° and as a **sill** if it dips less than 45°. The term **microdiorite dike** refers to a distinctive set of dioritic dikes that are very fine to moderately coarse grained. Finally, the term **detachment fault** is used to describe a low-angle normal fault that represents a major structural discontinuity with at least one of the following four characteristics: (1) it is a zone of major displacement as revealed by a pronounced lithologic mismatch between upper and lower plates; (2) it separates rocks with contrasting structural styles; faulted, rotated, and brittlely distended upper-plate rocks are juxtaposed against less faulted lower-plate rocks; (3) the upper plate contains normal faults that are cut by or merge with the detachment fault; and (4) it is underlain by a zone of hydrothermally altered breccia and microbreccia derived from lower-plate rocks.

Regional Geologic Setting

The South Mountains are situated within the southern Basin and Range physiographic province, a region characterized by alternating mountain ranges and intermontane valleys. Most of the valleys are underlain by variable thicknesses of late Cenozoic clastic sediments, evaporitic units, and subordinate volcanic rocks. Mountain ranges near the South Mountains are composed of Precambrian or Phanerozoic metamorphic and granitic rocks that are generally overlain by Cenozoic volcanic and sedimentary rocks, with no intervening Paleozoic or Mesozoic supracrustal rocks. Therefore, the Precambrian and Cenozoic geologic history of the South Mountains region can be studied directly, but the Paleozoic and Mesozoic history must be extrapolated from elsewhere in Arizona.

The oldest rocks exposed near the South Mountains are middle Proterozoic (1.6-1.7 b.y. B.P.), amphibolite-grade, metamorphic rocks that typically possess a northeast-striking foliation with steep to moderate dips. The metamorphic rocks have been intruded by middle Proterozoic granitic to granodioritic plutons that are variously pre-, syn-, and postmetamorphic. No middle Proterozoic sedimentary rocks equivalent to the Apache Group have been reported near the South Mountains, although diabasic intrusions of approximately the same age may locally occur.

Exposures of Paleozoic rocks near the South Mountains are small and insufficiently studied (Wilson, 1969). Judging from Paleozoic rocks elsewhere in Arizona, most of central Arizona was probably overlain at one time by a cratonic sequence of Paleozoic clastic and carbonate rocks (Peirce, 1976a), but such rocks are believed to have been eroded from the region during the Mesozoic and early Cenozoic (Harshbarger and others, 1957).

There are virtually no exposures of Mesozoic sedimentary or volcanic rocks within 100 km of the South Mountains. Evidence of middle Mesozoic volcanism, sedimentation, plutonism, and deformation is preserved in west-central Arizona (Reynolds, 1980) and in southern Arizona (Hayes and Drewes, 1978; Haxel and others, 1980). Although it is unclear how

this Mesozoic tectonic activity affected central Arizona, it is probable that central Arizona was part of an uplifted area (Mogollon Highlands) that shed detritus northward during part of the Mesozoic (Harshbarger and others, 1957; Cooley and Davidson, 1963).

During the Late Cretaceous and early Tertiary Laramide orogeny, southern Arizona was the site of widespread magmatism, sedimentation, and compressional deformation (Drewes, 1978; Davis, G. H., 1979). One manifestation of this orogeny in central Arizona was emplacement of Late Cretaceous granitoids that are associated with porphyry-copper mineralization, such as in the Sacaton Mountains (Figure 1). In the early Tertiary, classic Laramide orogenesis was followed by emplacement of muscovite-bearing, peraluminous granites (Keith and Reynolds, 1980; Reynolds and Keith, 1983).

In the middle Tertiary, widespread sedimentation, volcanism, and plutonism occurred throughout the Basin and Range Province of Arizona. Middle Tertiary sedimentary and volcanic rocks rest unconformably on a variety of older rocks, indicating widespread erosion in early Tertiary time. Tilting and normal faulting of middle Tertiary sections were in many areas synchronous with sedimentation and volcanism. Middle Tertiary metamorphism, mylonitization, and uplift locally accompanied plutonism in metamorphic core complexes of southern and western Arizona (Crittenden and others, 1980).

Late Tertiary Basin-and-Range block faulting formed many of the present-day basins and ranges between 14 and 5 m.y. B.P. (Eberly and Stanley, 1978; Scarborough and Peirce, 1978; Shafiqullah and others, 1980). Variably sized clastics were shed into relatively down-dropped basins while adjacent mountain ranges were denuded by erosion. Evaporites accumulated in some closed basins, including the Luke Basin near Phoenix (Peirce, 1976b). As Basin-and-Range faulting waned, integrated drainage systems of the Salt and Gila Rivers became well established and assisted in the final sculpturing of the region.

Generalized Geologic Relationships

The South Mountains are composed of two fundamentally different geologic terranes (Plate 1 and Figure 6). The western half of the range consists of Precambrian metamorphic and granitic rocks, whereas the eastern half is dominated by a composite middle Tertiary pluton. Both terranes have been intruded by numerous, north-northwest-trending, middle Tertiary dikes.

The Precambrian terrane has been subdivided into two rock units: Estrella Gneiss and Komatke Granite. Estrella Gneiss is a widely exposed sequence of gneiss, amphibolite, schist, and granitic rocks. Along the western end of the range, the gneiss has been intruded by Precambrian Komatke Granite. Both rock units contain steep, crystalloblastic foliation that strikes northeast to east-west. The Precambrian rock units and their associated foliation have been subsequently overprinted by Tertiary mylonitization, especially in the eastern half of the Precambrian terrane. The mylonitic fabric is best developed in a diffuse, southwest-dipping zone that is both underlain and overlain by less-mylonitic rocks that largely retain their Precambrian crystalloblastic foliation.

The eastern half of the South Mountains is underlain by a composite middle Tertiary pluton that has three major phases: South Mountains Granodiorite, Telegraph Pass Granite, and Dobbins Alaskite. South Mountains Granodiorite, the most widely exposed phase, has intruded overlying Estrella Gneiss along a subhorizontal contact on Entrance Ridge, on Mount Suppoa, and in the central Southern Foothills (Figures 7-11). In most other areas, however, the granodiorite and gneiss are separated by an intervening body of Telegraph Pass Granite. The granite both intrudes and grades into South Mountains Granodiorite. Dobbins Alaskite, a complex assemblage of alaskite, fine-grained granite, and felsite, represents

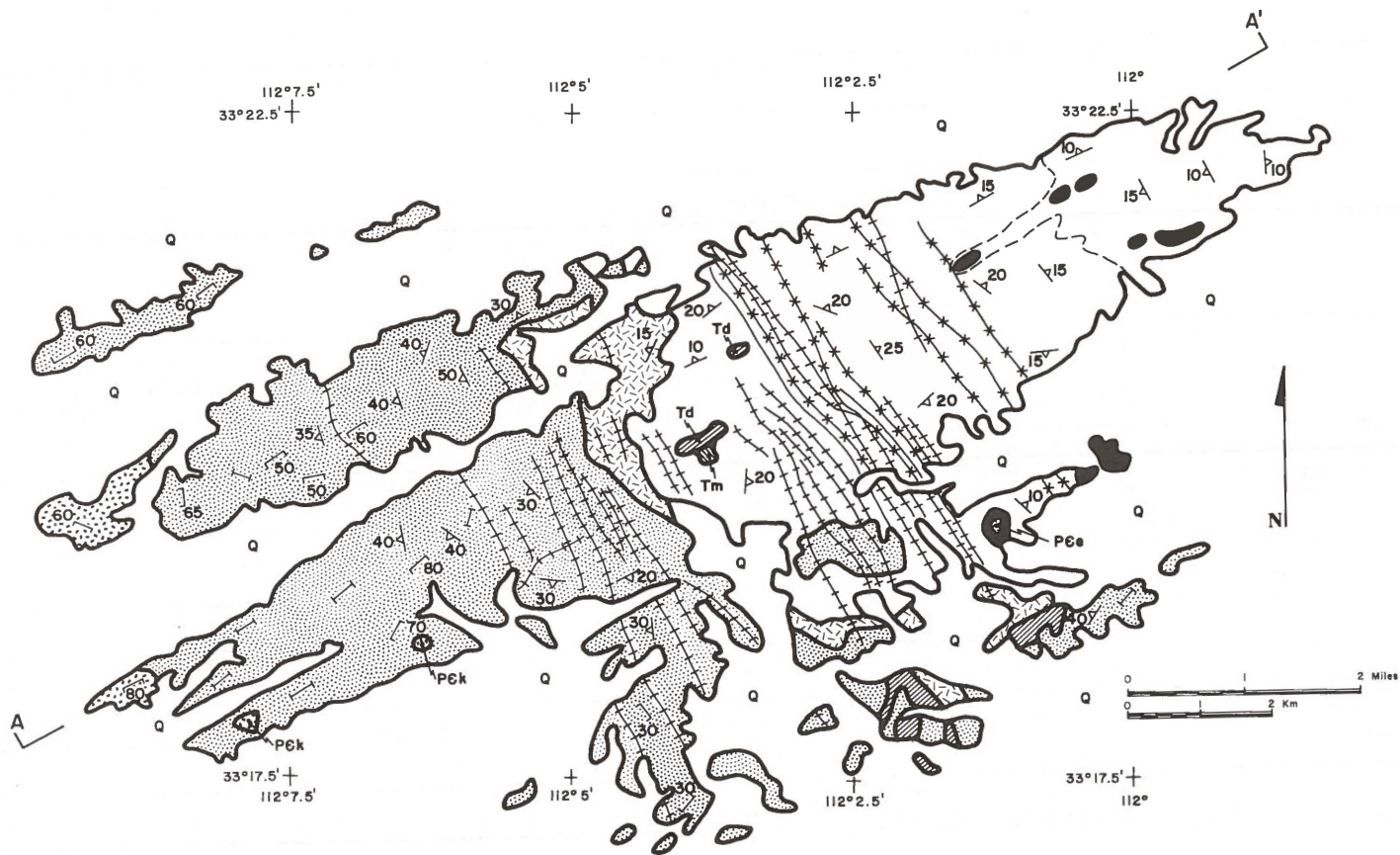
a border phase of the granite (Figures 12 and 13). Field relationships and geochronologic studies indicate that the granodiorite, granite, and alaskite are essentially contemporaneous and approximately 25 m.y. old.

All three phases of the composite middle Tertiary pluton have been overprinted to some degree by middle Tertiary mylonitization. Mylonitic foliation in the plutonic rocks dips gently off the range and defines a broad antiformal trend that trends east-northeast, parallel to the topographic crest of the range. The plutonic rocks are undeformed in the structurally low core of the antiformal trend, but are increasingly mylonitic toward higher structural levels. Penetrative mineral and slickenside-style lineation in the mylonitic rocks consistently trends east-northeast.

Numerous north-northwest-trending dikes intrude Precambrian and middle Tertiary rocks in the center of the range. The dikes range in composition from granite to diorite and were emplaced approximately 25 m.y. ago. Nearly half of the dikes contain a well-developed mylonitic fabric. The youngest intrusions in the range are microdiorite dikes that do not possess any mylonitic fabric.

A major episode of brecciation, fracturing, and detachment faulting is represented by a gently dipping chloritic breccia that gradationally overlies, and has been derived from, South Mountains Granodiorite on the northeast end of the range (Figures 6, 12, and 13). Chloritic breccia is locally capped by a thin, resistant ledge of microbreccia. On Ahwatukee Ridge, the microbreccia ledge is overlain by a low-angle detachment fault whose upper plate contains Precambrian Estrella Gneiss and several middle Tertiary dikes.

Relatively flat-lying, late Tertiary-Quaternary surficial deposits surround the range and were deposited nonconformably over all rock types and structures described above.



ROCK UNITS		SYMBOLS		
Late Tertiary- Quaternary	Q	-surficial deposits	—	-contact
		-chloritic breccia	—+—+—	-intermediate to felsic dike of middle Tertiary age
Middle Tertiary		-mylonitic gneiss and schist	*—*	-microdiorite dike of middle Tertiary age
		-Dobbins Alaskite	↖80	-strike and dip of crystalloblastic foliation
		-Telegraph Pass Granite	↖20	-strike and dip of mylonitic foliation
Precambrian		-South Mountains Granodiorite	— — —	-strike of vertical crystalloblastic foliation
		-Komatke Granite		
		-Estrella Gneiss		



Precambrian		-Estrella Gneiss	Middle Tertiary		-South Mountains Granodiorite
		-Komatke Granite			-Telegraph Pass Granite
		-crystalloblastic foliation			-Dobbins Alaskite
				-chloritic breccia	
				-mylonitic foliation	

Figure 6. Generalized geologic map and cross section of the South Mountains.

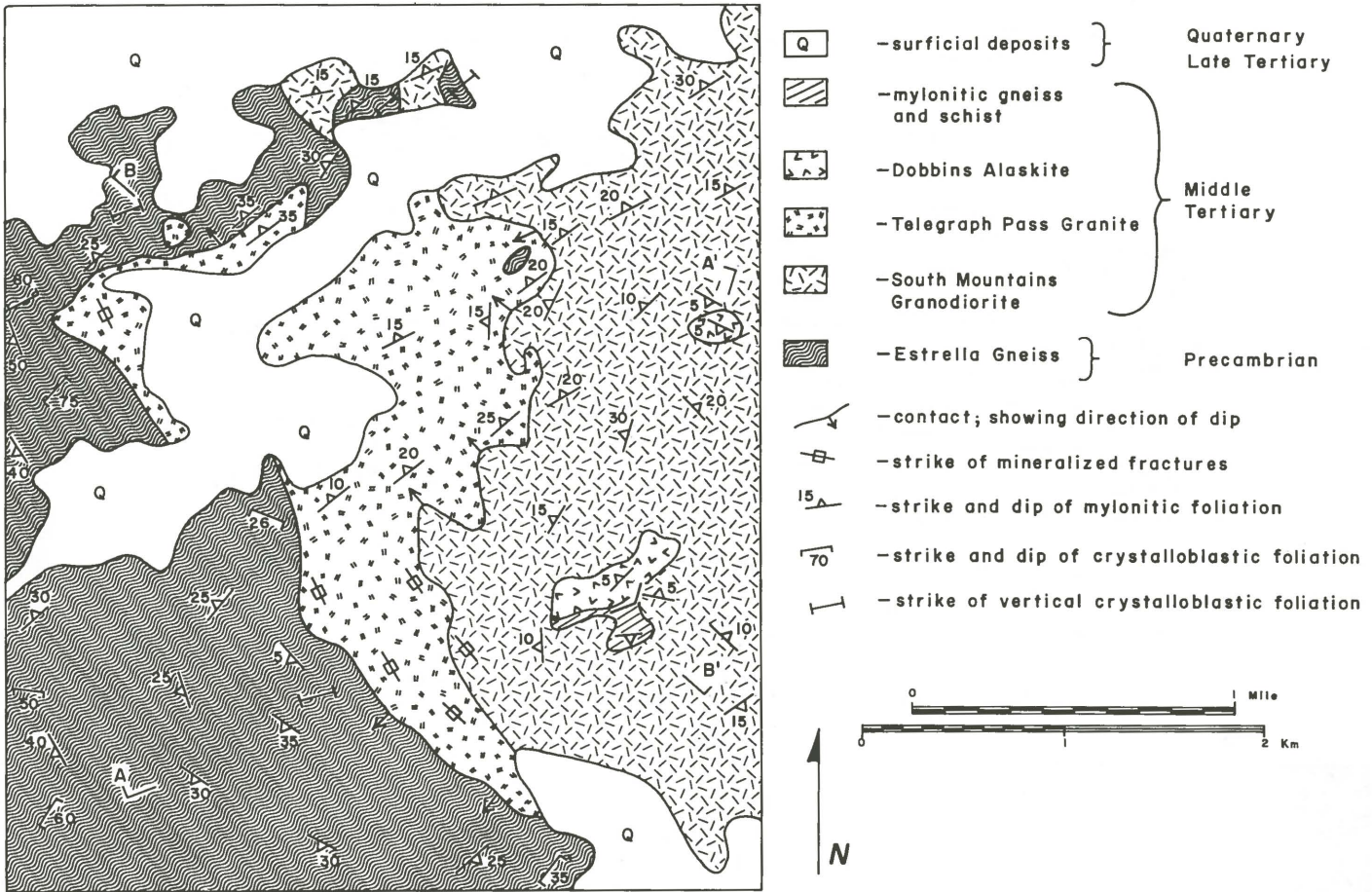


Figure 7. Generalized geologic map of Telegraph Pass and vicinity.

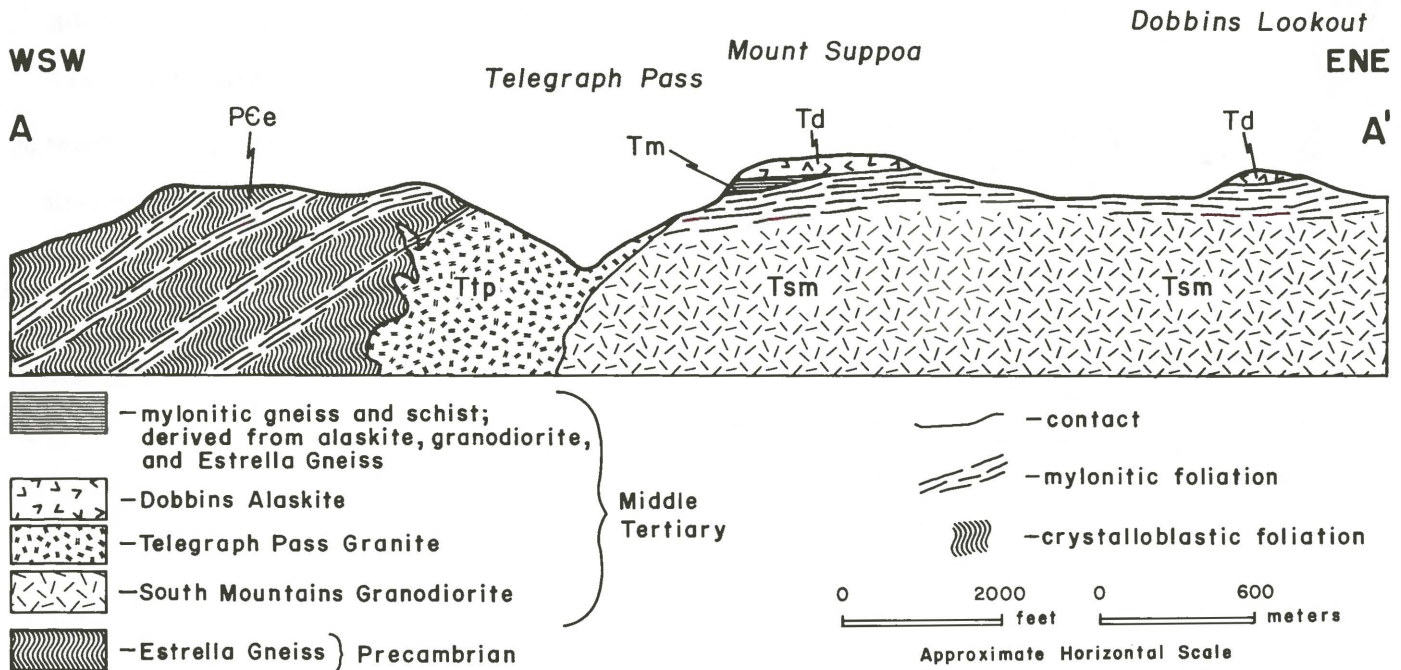


Figure 8. Schematic cross section of Telegraph Pass, Mount Suppoa, and Dobbins Lookout.

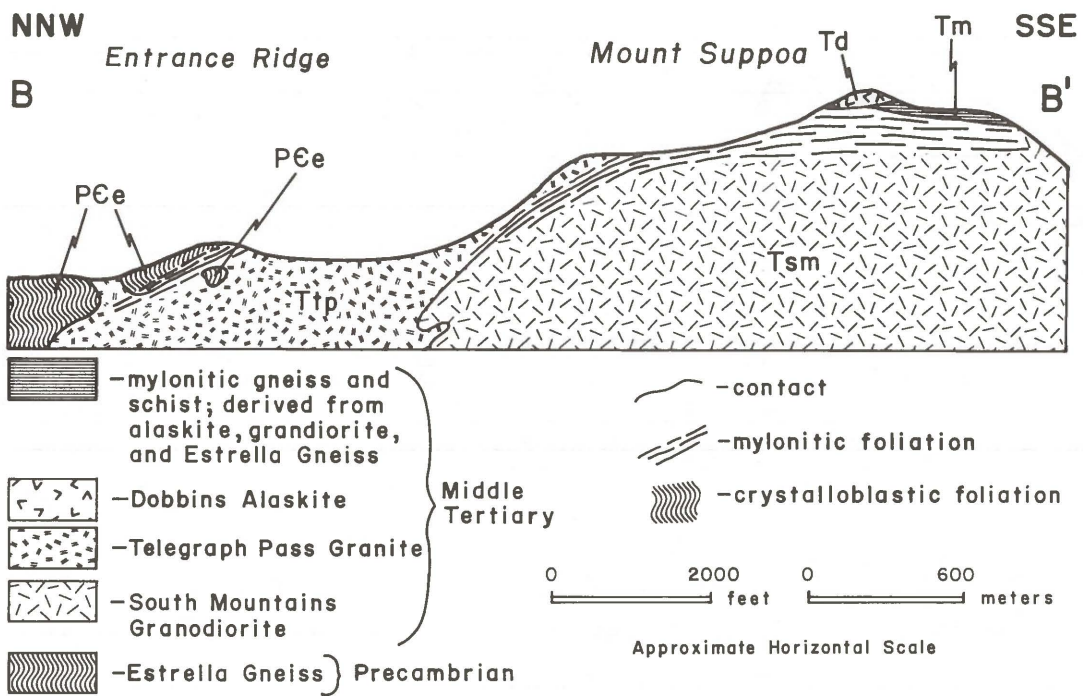


Figure 9. Schematic cross section of Entrance Ridge and adjacent Main Ridge.

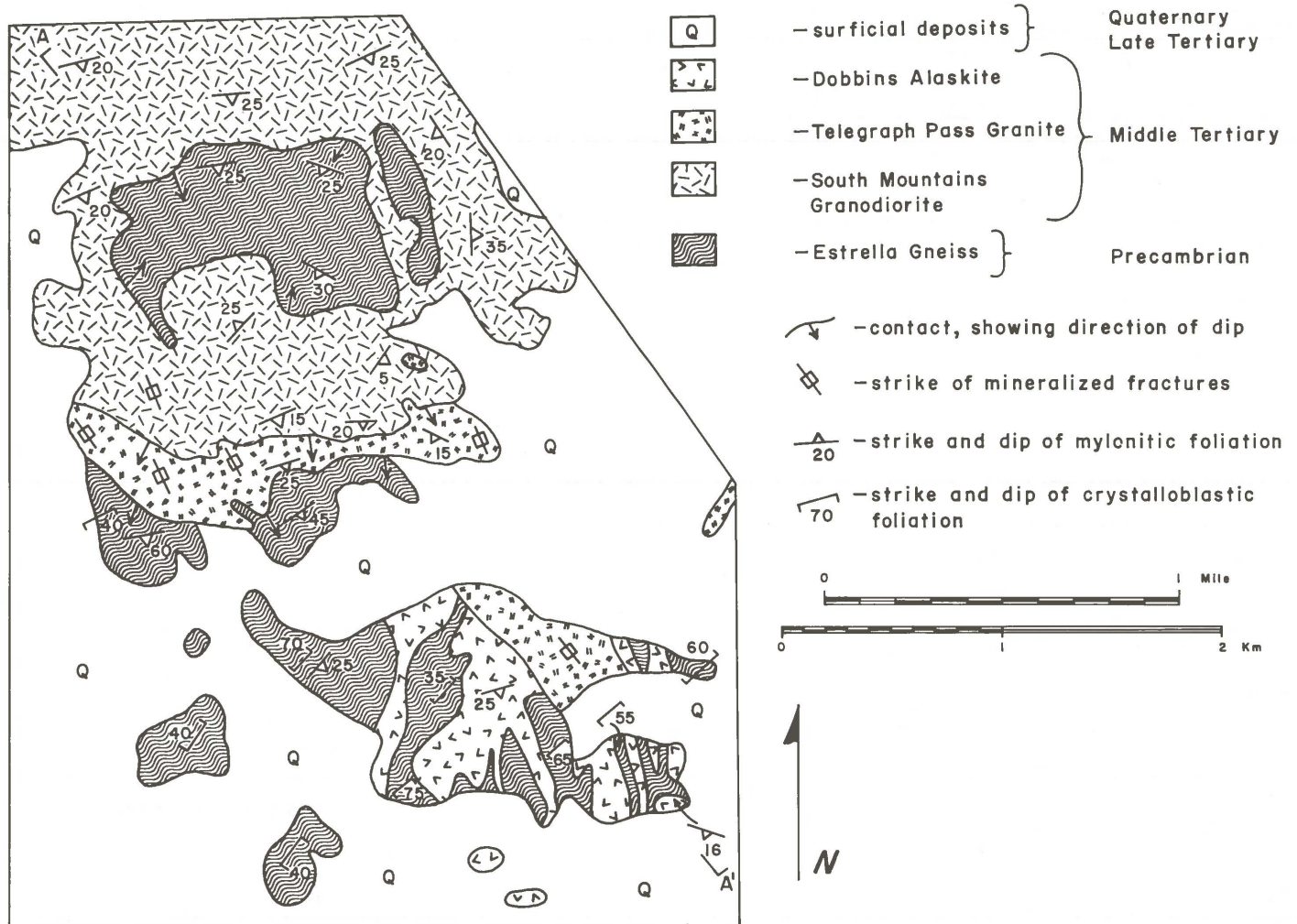


Figure 10. Generalized geologic map of central Southern Foothills and Boundary Hills.

NNW

SSE

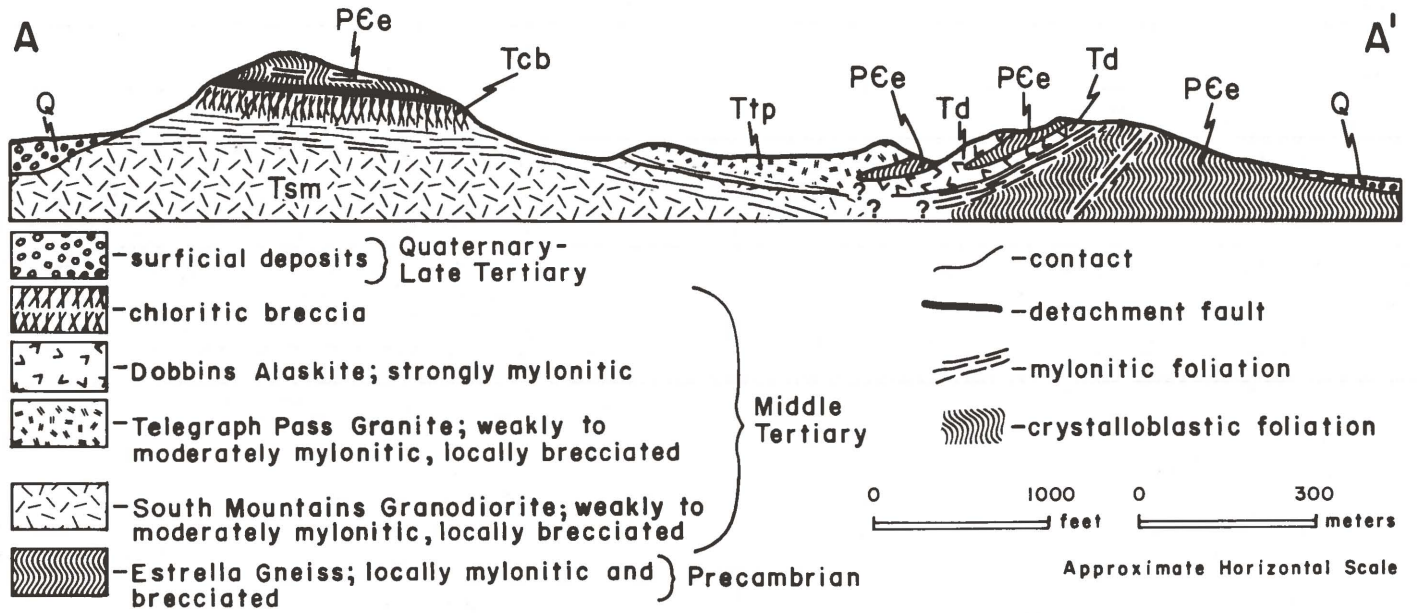


Figure 13. Schematic cross section of Pima and Ahwatukee Ridges.

Precambrian Rocks

The western half of the South Mountains is underlain by a complex terrane of Precambrian metamorphic and granitic rocks (Plate 1 and Figure 6). For the purposes of this study, the Precambrian terrane has been separated into two map units. The older and more widely distributed unit is Estrella Gneiss. The second unit, Komatke Granite, has intruded the gneiss along the western ends of Main and Alta Ridges. Both rock types typically display a steep, crystalloblastic foliation.

Estrella Gneiss

The name Estrella Gneiss is proposed for high-grade gneisses exposed in the western South Mountains and the Sierra Estrella, a rugged mountain range that lies southwest of the South Mountains (Figures 1 and 2). In the central Sierra Estrella, the type locality, the most abundant lithologies are quartzofeldspathic gneiss, biotitic gneiss and schist, amphibolite, granitic gneiss, migmatite, and biotite-muscovite schist. It is suggested that the name Estrella Gneiss be used in a broad sense for many exposures of high-grade metamorphic rocks south and west of Phoenix that are not easily correlated with other named Precambrian formations of Arizona, such as rocks of the Yavapai Series (Anderson and Silver, 1976) or Pinal Schist (Ransome, 1903). The author favors this general usage of the term Estrella Gneiss (Reynolds, 1982; Spencer and others, in preparation), rather than restricting the term to a specific granitic gneiss as suggested by Sommer (1982). Rocks assignable to Estrella Gneiss are pres-

ent in the Sierra Estrella, western South Mountains, Buckeye Hills, and White Tank Mountains.

Within the South Mountains, Estrella Gneiss is widely exposed on Alta Ridge, North Ridge, and the western half of Main Ridge (Plate 1). Additional exposures occur in many parts of the Southern Foothills.

Lithology

Estrella Gneiss generally forms serrated ridges composed of dark-colored, blocky outcrops. The dark color is due to desert varnish and an abundance of dark minerals. Estrella Gneiss is composed of various metamorphic lithologies that are interlayered on a scale of fractions of a centimeter to more than a meter (Figure 14). Rock types include quartzofeldspathic gneiss, amphibolite, biotitic gneiss, granitic gneiss, migmatite, mica schist, and rare quartz-rich rocks.

Quartzofeldspathic gneiss, one of the most abundant lithologies in Estrella Gneiss, is composed of feldspar and quartz with lesser amounts of biotite, hornblende, muscovite, and opaque oxides. It is compositionally banded with the most obvious color change being due to variations in biotite and hornblende content. Feldspar and quartz crystals in gneiss are medium grained and crystalloblastic.

Amphibolite is widely distributed throughout Estrella Gneiss and is composed of varying percentages of hornblende, plagioclase, biotite, and quartz. In addition, diopside, epidote, and magnetite are locally present (Avedisian, 1966). Compositional banding and foliation are less pronounced in amphibolite than in quartzofeldspathic gneiss.

Biotitic gneiss, another common rock type, contains from 10 to 50 percent biotite crystals that are oriented parallel to foliation. Quartz, plagioclase, and potassium feldspar comprise the remainder of the rock.

Granitic gneiss and gneissic granite have a constant lithology over entire outcrops and are not compositionally banded on a large scale. Many exposures are foliated plutonic rocks, such as Komatke Granite.

Migmatite is abundant in many outcrops of Estrella Gneiss and consists of amphibolite, gneiss, and granitoid rocks with numerous lenses and pods of alaskite and pegmatite.

Mica schists in Estrella Gneiss are composed of biotite and muscovite with variable amounts of feldspar and quartz. Sillimanite, cordierite, and pink garnet are also locally present (Avedisian, 1966). Most mica schist occurs as thin lenses interlayered with quartzofeldspathic gneiss and biotitic gneiss.



Figure 14. Photograph of Precambrian Estrella Gneiss below zone of intense mylonitization.

In some areas of the Southern Foothills, muscovite-feldspar-quartz schist is interlayered with amphibolite.

Quartzites and exceptionally quartz-rich gneisses are present, but uncommon. They occur within quartzofeldspathic gneiss and mica schist in the Southern Foothills and Alta Ridge. The interlayered gneisses and schists exhibit pronounced compositional banding on a very fine scale.

Diabasic rocks occur within several areas of Estrella Gneiss. These rocks are commonly only weakly foliated and evidently represent intrusions emplaced after the main Precambrian deformation.

Metamorphic Grade and Protoliths

Mineral assemblages in Estrella Gneiss in the South Mountains and Sierra Estrella are generally indicative of upper amphibolite-facies metamorphism, although the possibility of granulite facies metamorphism has also been suggested, largely to explain the presence of diopside and retrograded pyroxene (Avedisian, 1966; Sommer, 1982). A granulite-facies of metamorphism is inconsistent with the observed abundance of hydrous minerals such as biotite and muscovite.

The gneiss was formed by metamorphism of a wide variety of protoliths. Most of the Estrella Gneiss was probably derived from intermediate to mafic plutonic or volcanic protoliths. For example, some amphibolites must have formed from mafic igneous rocks, such as basalt or gabbro. Quartz-feldspar-muscovite schists that are interlayered with the amphibolites are possibly metarhyolites. A metasedimentary protolith is indicated for some quartzofeldspathic gneiss, biotitic gneiss, mica schist, and quartzite, especially where these rocks display small-scale compositional banding. Most gneissic granite and granitic gneiss are metamorphosed and deformed plutonic rocks that were intruded into other lithologies before or during deformation and metamorphism. Some granitic lenses and pods may represent material that was remobilized during metamorphism, possibly by minor amounts of partial melting or by metasomatism. Diabasic rocks in Estrella Gneiss may be equivalent to diabasic rocks in central and southern Arizona that are 1.1 to 1.2 b.y. old.

Komatke Granite

Komatke Granite occurs primarily along the southwest ends of Alta Ridge and Main Ridge. Additional exposures occur in the Southern Foothills, but are too small to map separately from surrounding Estrella Gneiss. The granite is named after the village of Komatke that lies southwest of the range. The type locality of the granite is at the water tank on the southwest end of Main Ridge in sec. 33, T. 1 S., R. 2 E.

Komatke Granite is exposed on low ridges that are similar in appearance to those formed by Estrella Gneiss. On fresh surfaces, the granite is gray with a pale pinkish tint due to the abundance of potassium feldspar. The granite is generally coarse grained and porphyritic with approximately 10 to 30 percent phenocrysts of potassium feldspar that are as long as 4 cm (Figure 15). Quartz and plagioclase each constitute 20 to 35 percent of the granite, whereas biotite content varies between 5 and 15 percent; hornblende occurs in some exposures. The granite commonly has a well-developed crystalloblastic foliation that is nearly vertical.

Alaskitic and aplitic phases are commonly associated with the granite, especially near its intrusive contacts with Estrella Gneiss. The alaskitic rocks are composed almost entirely of feldspar and quartz, and locally display a graphic texture.

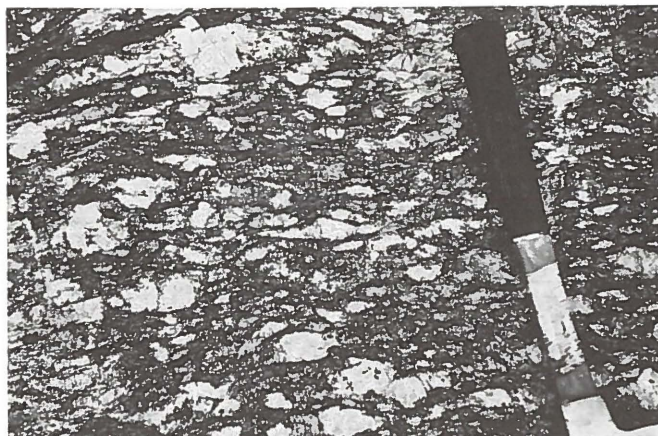


Figure 15. Photograph of strongly deformed Komatke Granite in the Southern Foothills.

Middle Tertiary Rocks

A composite middle Tertiary pluton occupies most of the eastern half of the range. The pluton consists of three closely related phases: South Mountains Granodiorite, Telegraph Pass Granite, and Dobbins Alaskite. South Mountains Granodiorite, the oldest and most widely exposed phase, composes the eastern half of Main Ridge and much of the Southern Foothills. To the west and south, the granodiorite variably grades into or is intruded by Telegraph Pass Granite. The third phase of the pluton, Dobbins Alaskite, generally occurs along border zones of the granite. The youngest middle Tertiary intrusives are numerous, north-northwest-trending dikes and sills.

Intense middle Tertiary deformation accompanied and succeeded plutonism, and formed new rock units from preexisting lithologies. Mylonitic gneiss and schist were formed by pervasive mylonitization of Precambrian and middle Tertiary rocks. Chloritic breccia and middle Tertiary rocks. Chloritic breccia was subsequently formed by intense fracturing, brecciation, and hydrothermal alteration of South Mountains Granodiorite on the east end of the range. Lithologic descriptions given below are summarized from Reynolds (1982). Additional details regarding petrology of Telegraph Pass Granite and middle Tertiary dikes are given in Avedisian (1966).

South Mountains Granodiorite

The South Mountains Granodiorite is so named because it composes most of the eastern half of the range (Plate 1 and Figure 6). The type locality is along Summit Road, approximately 500 m northeast of Telegraph Pass. Accessible reference localities are as follows:

- 1) on the east flank of Dobbins Lookout, 50 m below the top;
- 2) blasted roadcuts in the center of the SW1/4 sec. 16, T. 1 S., R. 3 E.; and
- 3) blasted cuts along the first 100 m of Hidden Valley Trail, SE1/4 NW1/4 sec. 15, T. 1 S., R. 3 E.

The granodiorite has a variably developed mylonitic fabric in most exposures.

Field Relations

The largest exposures of South Mountains Granodiorite occur in the eastern half of Main Ridge and in the Southern Foothills. Along its western contact, the granodiorite both grades into and has been intruded by Telegraph Pass Granite (Figure 8). The contact strikes

north-northwest and is steep near Telegraph Pass, but gradually decreases in dip north of the pass. In a similar manner, the contact progressively decreases in dip as it is followed southeast into the Southern Foothills.

The original roof of the granodioritic pluton is exposed near Mount Suppoa and in the central Southern Foothills (Figures 8 and 11). In both areas, granodiorite has intruded overlying Estrella Gneiss along a subhorizontal contact. The granodiorite is strongly mylonitic along the contacts but becomes less mylonitic downward. A less mylonitized intrusive contact between granodiorite and Estrella Gneiss occurs on the east end of Entrance Ridge.

Lithology

Physical appearances and weathering characteristics of granodiorite depend greatly on its structural condition. Where undeformed, the granodiorite forms bold, spheroidally weathered outcrops. Where mylonitic, it forms ledges and massive outcrops that have rounded tops with serrated edges. The granodiorite has a more subdued physiographic expression northeast of Two Peaks, where it has been brecciated (Figure 4).

Nonmylonitic South Mountains Granodiorite is medium to light gray on fresh surfaces, but most outcrops are stained tan or brown by desert varnish (Figure 16). It is medium-grained and equigranular to slightly porphyritic, with a fairly uniform mineralogy consisting of 35 to 45 percent plagioclase, 15 to 25 percent potassium feldspar, 25 to 35 percent quartz, and 5 percent biotite. These

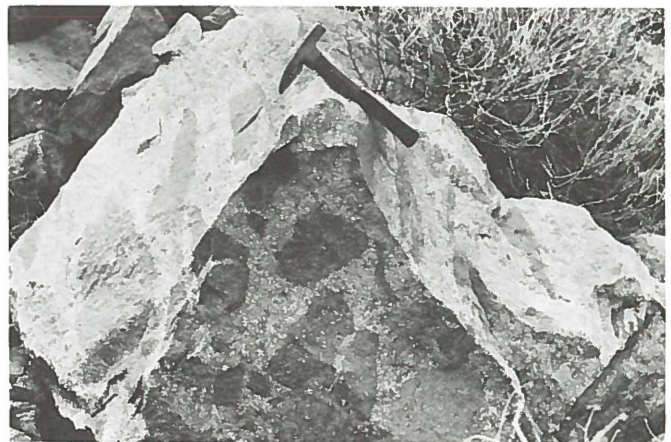


Figure 16. Photograph of inclusion-rich South Mountains Granodiorite along the north edge of Main Ridge.

modal abundances are in the granodiorite field of Streckeisen (1976), very close to the granodiorite-granite boundary. Accessory minerals include magnetite, apatite, zircon, and sphene.

Plagioclase generally occurs as crystals that are 1 to 3 mm in diameter, but is also present as phenocrysts that are between 5 and 10 mm long. Many plagioclase crystals display well-developed twinning and concentric zoning. Most potassium feldspar crystals are generally twinned, somewhat perthitic, subhedral, and interstitial to plagioclase.

Quartz occurs as individual crystals 0.5 to 1 mm in diameter and as irregularly shaped, interlocking aggregates up to 4 mm in diameter. Most quartz crystals display undulatory extinction and have sutured boundaries. Biotite is ubiquitous and occurs both as anhedral, interstitial patches, and as subhedral or euhedral books as large as 1 mm thick and 5 mm in diameter.

A variably developed, mylonitic fabric is present in most exposures of granodiorite. Mylonitic granodiorite is slightly darker in color than undeformed granodiorite, due to smearing out and streaking of biotite and to a general reduction in grain size. Petrography of mylonitic granodiorite is described in detail by Reynolds (1982).

Related Rock Types

Several distinctive lithologies are related to the granodiorite. Mafic granodiorite, quartz diorite, and fine-grained granodiorite occur along contacts between granodiorite and Estrella Gneiss. These phases have been observed on Mount Suppoa, in the central Southern Foothills, and on the north edge of Main Ridge, 1 km east of Entrance Ridge. Mafic granodiorite and quartz diorite contain abundant biotite and, unlike the granodiorite, they contain visible hornblende and sphene in outcrop. Contacts between these rocks and the granodiorite are either gradational or display inconsistent crosscutting relationships.

The granodiorite also locally has a border phase that represents a gradation between granodiorite and Telegraph Pass Granite. Along these gradational contacts, the granodiorite contains less biotite and fewer plagioclase phenocrysts than normal.

The granodiorite contains numerous aplitic dikes that are 1 to 10 cm thick. Most aplites are fine grained and xenomorphic-equigranular (aplitic), with local, medium-grained areas. Quartz and alkali feldspar constitute most of the rock, with plagioclase content varying from 3 to 25 percent.

Field relationships, petrologic considerations, and geochemical arguments indicate that the aplites are comagmatic with the host granodiorite (Reynolds, 1982). The aplites have the same mineralogy as the granodiorite, including small plagioclase phenocrysts identical in size and style of zoning to those in granodiorite. Some aplites have gradational boundaries with the granodiorite, even on a microscopic scale. Aplites occur throughout the granodiorite pluton and are spatially unrelated to younger intrusive bodies. The aplites have not been observed to intrude the post-granodiorite dikes, except in one area

east of Mount Suppoa where several aplite dikes crosscut a microdiorite dike. Finally, all aplites, except for those discussed in the preceding sentence, have undergone the same mylonitic deformation as the granodiorite. This point is important because geochronologic data indicate that the granodiorite was mylonitically deformed soon after its emplacement (see section on geochronology). Therefore, the granodiorite and aplites are essentially the same age.

South Mountains Granodiorite locally contains abundant inclusions of igneous and metamorphic rocks. In undeformed granodiorite, most inclusions are angular, equant, and between 5 and 25 cm in diameter. Igneous inclusions within granodiorite are biotite-rich and largely composed of mafic granodiorite, quartz diorite, and diorite. Metamorphic inclusions are most common where the granodiorite has intruded Precambrian Estrella Gneiss, such as on Entrance Ridge and in the Southern Foothills.

Telegraph Pass Granite

Telegraph Pass Granite is named after Telegraph Pass, the major topographic notch near the center of Main Ridge. The type locality is along Summit Road, approximately 300 m north-northwest of Telegraph Pass. Accessible reference localities are as follows:

- 1) blasted cuts along Summit Road in the NW1/4 sec. 20, T. 1 S., R. 3 E.; and
- 2) numerous outcrops in the center of sec. 17, T. 1 S., R. 3 E.

Field Relations

Telegraph Pass Granite generally inter-venes between Estrella Gneiss and South Mountains Granodiorite. Near Telegraph Pass, the granite has intruded Estrella Gneiss along a contact that strikes north-northwest and dips steeply or moderately to the west (Figures 7 and 8). On Entrance Ridge, the contact dips gently to the north beneath the gneiss and has been locally modified by subsequent mylonitization (Figure 9). Numerous apophyses of granite extend upward into the overlying gneiss.

North and east of Telegraph Pass, the granite both grades into and has been intruded over South Mountains Granodiorite along a contact that dips west at steep to gentle angles. The granite-granodiorite contact nearly projects into Mount Suppoa, where alaskite and associated fine-grained alaskitic granite overlie South Mountains Granodiorite (Figure 9).

In the central Southern Foothills, Telegraph Pass Granite occurs as a south-dipping tabular body that overlies South Mountains Granodiorite and underlies Estrella Gneiss (Figures 10 and 11). The upper and lower contacts of the granite progressively decrease in dip from west to east along strike. The granite extends eastward into the embayment between Pima and Ahwatukee Ridges, where it appears to be a gently dipping sill that overlies granodiorite to the north and Estrella Gneiss to the south (Figures 12 and 13). In the nearby Boundary Hills, the granite is a

steep-sided, north-northwest-trending body that is flanked by an extensively developed border phase of Dobbins Alaskite (Figures 10 and 11).

Lithology

Physical appearance and weathering characteristics of the granite depend on whether or not it is deformed. The granite forms bold, spheroidal outcrops where it is undeformed, but has a more sheeted aspect where it is mylonitic. It is easily eroded and forms a light-colored *grus*, especially where hydrothermally altered, such as near Telegraph Pass. Preferential erosion of altered granite probably formed the topographic embayment south of Entrance Ridge.

Telegraph Pass Granite is light gray on fresh surfaces, but is tan or light brown on weathered surfaces. The granite is lighter in color than South Mountains Granodiorite because it contains less biotite (Figure 17). The granite is medium grained and mostly composed of crystals between 0.5 and 4 mm in diameter. It contains 30 to 40 percent quartz, 30 to 40 percent plagioclase, 20 to 30 percent potassium feldspar, and 2 to 3 percent biotite (see also Avedisian, 1966). These modal abundances plot within the granite field of Streckeisen (1976), very near the granite-granodiorite boundary. Mineralogy of the granite is only slightly different from that of South Mountains Granodiorite, with the granite containing more quartz and potassium feldspar, but less plagioclase and biotite. The granite also contains small amounts of sericite, fine-grained muscovite, magnetite, apatite, and zircon. Limonite and pyrite are present along some altered and mineralized fractures.

Plagioclase occurs as euhedral to subhedral crystals between 0.5 and 5 mm in length and generally does not form obvious phenocrysts. Potassium feldspar is generally present as subhedral and anhedral crystals up to 5 mm in diameter. Orthoclase is the most common potassium feldspar, although perthite and microcline are also present.

Quartz crystals are generally less than 2 mm in diameter, although some are as large as 5 mm. These latter, large crystals commonly weather into conspicuous quartz eyes that are

useful for distinguishing the granite from South Mountains Granodiorite. Most quartz in the granite is anhedral and interstitial to other minerals. Undulatory extinction is prevalent, even in relatively undeformed granite.

Biotite crystals are subhedral and less than 2 mm in diameter. In zones of intense hydrothermal alteration, biotite has been replaced by sericite and muscovite. Minor amounts of sericite and fine-grained muscovite also occur as fine-grained platelets in plagioclase, especially along twin boundaries and in areas where the granite is altered. Avedisian (1966) reported the presence of several generations of muscovite and suggested that the earliest generation occurs as discrete crystals, whereas the later generation occurs as stringers along fracture fillings. Some of the large muscovite crystals have clearly formed by replacement of biotite.

Primary accessory minerals in the granite include magnetite, apatite, and zircon. In addition, limonite and blue-green copper minerals, such as chrysocolla and chalcantite, occur as fracture coatings in hydrothermally altered granite.

The granite commonly possesses a variably developed mylonitic fabric. The gradation from undeformed to strongly mylonitic granite can be extremely abrupt, locally occurring within 10 m. General characteristics of the mylonitic fabric are discussed in a later section on middle Tertiary mylonitization.

Related Rock Types

Aplite dikes, common in many granite exposures, are generally light colored, 1 to 4 cm thick, and composed of quartz, alkali feldspar, plagioclase, and sparse amounts of biotite and muscovite. Quartz veins are also present in the granite. In undeformed granite, the veins generally strike north-northwest, have steep dips, and are associated with zones of hydrothermal alteration. In mylonitically deformed granite, the veins are oriented either parallel to mylonitic foliation or perpendicular to lineation.

The granite contains a variable amount of metamorphic and igneous inclusions. Inclusions of metamorphic rocks are most common near intrusive contacts with Precambrian Estrella Gneiss, whereas inclusions of granodiorite and other igneous rocks are especially abundant near granite-granodiorite contacts.

Dobbins Alaskite

Dobbins Alaskite consists of an assemblage of alaskitic rocks that comprise Dobbins Lookout, Mount Suppoa, and parts of the Southern Foothills. The type locality is on the north flank of Dobbins Lookout. Excellent reference localities occur on Mount Suppoa and in the Boundary Hills. Dobbins Alaskite is interpreted to be a border phase of Telegraph Pass Granite.

Field Relations

At Dobbins Lookout, the alaskite overlies mylonitic South Mountains Granodiorite along a

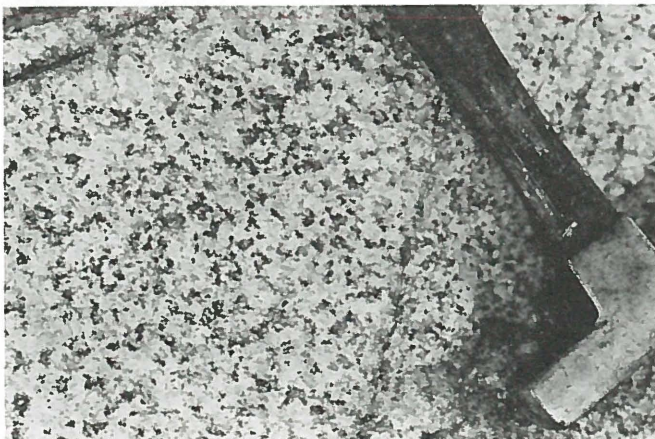


Figure 17. Photograph of undeformed Telegraph Pass Granite near Telegraph Pass.

low-angle contact. The alaskite consists of a series of gently dipping sills that contain a strong mylonitic fabric parallel to their margins. Thin lenses of mylonitic granodiorite and biotite-rich mylonitic schist are interleaved with the sills. Exposures of alaskite at nearby Mount Suppoa have a similar geologic setting.

Dobbins Alaskite is also exposed in several parts of the Southern Foothills. In the Boundary Hills, alaskite occurs as a border phase of Telegraph Pass Granite and as dikes, sills, and irregularly shaped intrusions within Estrella Gneiss. On Pima Ridge, alaskite sills have injected Estrella Gneiss beneath a flat-lying mass of Telegraph Pass Granite (Figures 12 and 13). The alaskite is locally mylonitic in both areas, especially where it occurs as gently dipping sills.

Lithology

Dobbins Alaskite is composed of several related lithologic phases that form distinctive white- or cream-colored outcrops due to a lack of dark minerals (Figure 18). The main phases of the alaskite are fine-grained alaskitic granite, quartz porphyry, and felsite. Contacts between different phases can be either sharp or entirely gradational. Inconsistent crosscutting relationships suggest that the different phases are essentially contemporaneous and comagmatic.



Figure 18. Photograph of mylonitic Dobbins Alaskite near Mount Suppoa. Note the irregularly shaped quartz segregations.

All phases of alaskite are composed of subequal amounts of alkali feldspar, plagioclase, and quartz. In addition, several phases of alaskite contain minor amounts of biotite. Sericite and limonite are present where the alaskite has been hydrothermally altered.

A common phase of Dobbins Alaskite is medium- to fine-grained, alaskitic granite that strongly resembles Telegraph Pass Granite, but is finer grained and biotite-poor. Alaskitic granite forms most of the alaskite at Mount Suppoa and is also present, but less abundant, at Dobbins Lookout. In the Southern Foothills, it is a transitional phase between medium-grained Telegraph Pass Granite and aphanitic felsite. The alaskitic granite usu-

ally contains quartz eyes that are similar to those in Telegraph Pass Granite. Biotite occurs only in trace amounts and has been extensively altered to sericite.

Quartz porphyry, another common phase of Dobbins Alaskite, contains 5 to 10 percent quartz phenocrysts set in an aphanitic or finely crystalline matrix of feldspar and quartz. A light-gray variety of the porphyry with scattered plagioclase and biotite phenocrysts strongly resembles South Mountains Granodiorite.

Felsite is also a major component of alaskite and is a white- or cream-colored, aphanitic rock that lacks visible phenocrysts. The felsite commonly occurs as dikes and sills adjacent to Telegraph Pass Granite.

Every phase of the alaskite possesses a mylonitic fabric in many, if not most, exposures. Quartz segregations, in the form of irregular pods and lenses, are present in most exposures of mylonitic alaskite (Figure 18). Some quartz segregations are mylonitic, but others crosscut mylonitic fabric.

Mylonitic Gneiss and Schist

Extreme mylonitization has formed rocks that are best described as mylonitic gneiss and schist. These rocks are so strongly mylonitic that it is difficult to recognize their protoliths. Mylonitic gneiss and schist are best exposed at Mount Suppoa and Dobbins Lookout, where they overlie and grade downward into mylonitic South Mountains Granodiorite. Small, unmapped outcrops are also present in the central Southern Foothills along the contact between South Mountains Granodiorite and an overlying roof pennant of Estrella Gneiss.

Lithology

The characteristics of mylonitic gneiss and schist are variable due to differences in protolith and in degree of deformation. All exposures contain a pervasive mylonitic fabric. Many outcrops, including those at Mount Suppoa, are dark colored when viewed from a distance, primarily because of the



Figure 19. Photograph of mylonitic gneiss and schist south of Mount Suppoa. Protolith of this outcrop is probably South Mountains Granodiorite.

fine-grained nature of the rocks and the abundance of dark minerals such as biotite, amphibole, chlorite, and epidote. Some exposures are lighter in color because they contain significant amounts of aplite, alaskite, and fine-grained granite. Most outcrops are banded due to interlayering of these light- and dark-colored lithologies (Figure 19). Mylonitic equivalents of Estrella Gneiss, South Mountains Granodiorite, Telegraph Pass Granite, and Dobbins Alaskite are all present in mylonitic gneiss and schist (see descriptions in Reynolds, 1982).

As might be expected, mylonitic gneiss and schist display much variation in thin section. They are very fine-grained rocks with small-scale compositional banding or lamination defined by alternating light- and dark-colored lenses (Figure 20). Light-colored lenses are principally composed of quartz with lesser amounts of muscovite, plagioclase, and potassium feldspar. Dark-colored lenses contain a high proportion of epidote, biotite, amphibole, plagioclase, and fine-grained minerals.



Figure 20. Photomicrograph of mylonitic gneiss under crossed nicols. Width of photograph represents approximately 50 mm. This and all subsequent photomicrographs were taken with a 35-mm camera attached to a bellows and macrolens system. Polarizing glass and a polarizing lens were used to cross the nicols. All thin sections were cut parallel to lineation and perpendicular to foliation.

Quartz usually occurs as lenticular aggregates that are composed of numerous, small crystals or subgrains of quartz. The lenticular aggregates have length-to-thickness ratios of approximately 10:1 as viewed parallel to foliation, but perpendicular to lineation. Some quartz is also present as ribbons that have undulatory extinction.

Plagioclase is abundant and occurs as discrete porphyroclasts and as a major component of the finer grained fractions. Most plagioclase in the mylonitic rocks has been extensively replaced by sericite and epidote.

Amphibole is abundant in outcrops of mylonitic gneiss and schist that represent deformed amphibolite. Amphibole commonly occurs as fractured crystals that are aligned parallel to foliation and lineation.

Muscovite, biotite, and chlorite are usually present within strongly mylonitic

rocks. Muscovite is more common in mylonitic gneiss and schist than in the nonmylonitic protoliths, and is partly responsible for the schistose appearance of many mylonitic rocks. Biotite is present both as polycrystalline aggregates that exhibit undulatory extinction and as recrystallized platelets that contain no obvious cleavage or deformational fabric. Chlorite occurs in fine-grained, dark-colored layers, in quartz-filled tension gashes, and in pressure shadows next to plagioclase porphyroclasts. Some chlorite has formed at the expense of biotite and amphibole.

Epidote is an important mineralogic component in nearly all lithologies and occurs as a replacement of plagioclase and in quartz-filled tension gashes. Other minerals, including alkali feldspar, apatite, and zircon, are sparsely present in mylonitic gneiss and schist. Alkali feldspar appears to reside mostly in fine-grained layers, whereas apatite occurs as undeformed crystals that are widely disseminated throughout the rock. Zircon crystals are rounded and display internal fracturing and breakage.

Dikes and Sills

Intermediate to felsic dikes and sills are common in most parts of the South Mountains, but are particularly abundant in the center of the range (Plate 1, Figure 21). They are concentrated into two north-northwest-trending swarms. The western swarm has intruded Estrella Gneiss in the western Southern Foothills and on Main Ridge, west of Telegraph Pass (Avedisian, 1966). The eastern dike swarm cuts South Mountains Granodiorite and Estrella Gneiss east of Telegraph Pass and in the central Southern Foothills.

There is great variability in the lithology of dikes and sills because they were emplaced at slightly different times and from a parent magma that was probably evolving in composition. Many dikes and sills have a bimodal grain size that reflects a multistage crystallization history (Figure 22). Dikes and sills that were emplaced early in the intrusive sequence are somewhat coarser grained than those that were emplaced later. Also, early dikes and sills are mylonitic, whereas the youngest dikes are not. The dikes and sills can be grouped into the following six suites: rhyodacite and dacite, fine-grained granodiorite, andesite, felsite, mafic granodiorite, and microdiorite. Although the lithology of each suite is described separately below, there is much gradation and overlap among the suites, except for the microdiorite dikes, which are distinctive in both lithology and age.

Porphyritic rhyodacite and dacite are perhaps the most common dikes and sills in both dike swarms. They are light to medium gray and contain 10 to 30 percent phenocrysts of quartz, plagioclase, alkali feldspar, and biotite. Quartz and alkali feldspar are the dominant phenocrysts in rhyodacite, whereas plagioclase and biotite are most common in dacite. The phenocrysts are generally between 2 and 5 mm in length and are encased in an extremely fine-grained matrix.

Fine-grained granodiorite dikes occur



Figure 21. Photograph of middle Tertiary microdiorite dikes intruding South Mountains Granodiorite north of Telegraph Pass.

throughout both dike swarms and are coarser in grain size than the rhyodacites and dacites. They are medium gray and commonly resemble South Mountains Granodiorite, except for their finer grain size. Crystals in fine-grained granodiorite are approximately 1 mm in diameter, with plagioclase being the most abundant mineral, followed by quartz, orthoclase, and biotite. Zoned plagioclase and biotite are common as phenocrysts and as components of the fine-grained matrix, whereas quartz and alkali feldspar are restricted to the matrix.

Andesitic sills up to several meters thick are common in the eastern swarm and in parts of the Southern Foothills. They usually dip gently, although short, steep segments are also present. The sills form distinctive outcrops that are dark gray and green with tan desert varnish. Most have a well-developed mylonitic fabric and some are more deformed than their country rocks. Andesite is composed of approximately 15 to 25 percent zoned plagioclase phenocrysts in a dark-colored matrix of plagioclase, biotite, hornblende, quartz, alkali feldspar, and chlorite.

Light-colored felsite dikes and sills are a major component of both dike swarms. Some dikes are very resistant to erosion and form linear walls more than 10 m high and 5 m thick. Most felsite dikes and sills are very

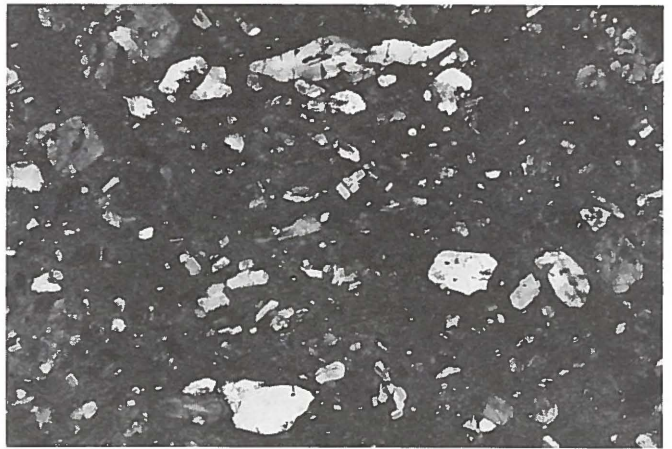
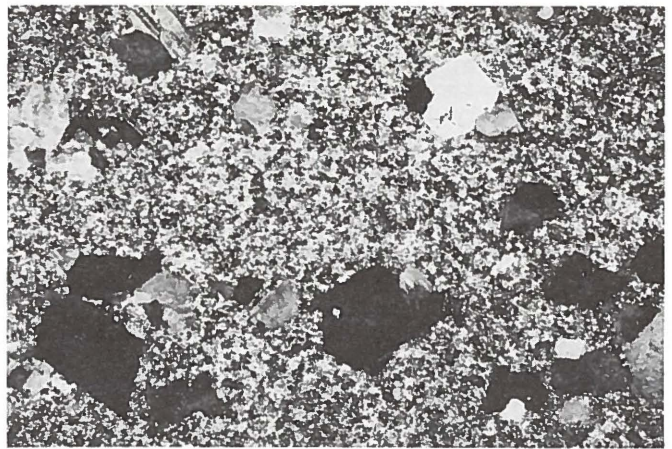


Figure 22. Photomicrographs of dikes under crossed nicols: (a, top) fine-grained, porphyritic, intermediate dike; and (b, bottom) porphyritic, intermediate dike with aphanitic matrix. Note lenticular, deformed quartz phenocryst at top of photograph. Widths of photographs represent approximately 1 cm.

fine grained, except for sparse phenocrysts of plagioclase, quartz, and alkali feldspar.

Mafic granodiorite dikes contain a higher proportion of mafic minerals than most granodiorite dikes in the range. Mafic granodiorite dikes are present in both dike swarms, but are probably most abundant in the Southern Foothills. They form bold, linear ridges that have a heavy coat of tan and brown desert varnish. Mafic granodiorite is medium gray and contains 15 to 30 percent plagioclase phenocrysts and less than 5 percent biotite phenocrysts.

Microdiorite dikes, which constitute a distinctive suite of igneous rocks, are younger than all other dikes in the range. They are most common in the eastern half of the range where they have intruded South Mountains Granodiorite. Some dikes form dark, linear troughs that extend across the entire 5-km width of the range. They range in thickness from several centimeters to more than 20 m. The thickest dikes have coarse- to medium-grained, dioritic to quartz dioritic centers, whereas thin dikes are fine grained throughout. The microdiorite dikes are not mylonitically deformed, except possibly in one area on Mount Suppa.

Microdiorite is composed of nearly equal amounts of plagioclase and hornblende, which together compose approximately 90 percent of

the rock. The hornblende occurs as prismatic and acicular crystals that form an interlocking network through the plagioclase matrix. The remaining 10 percent of the rock is composed of biotite and quartz, with lesser amounts of magnetite, epidote, sphene, and apatite.

Chloritic Breccia and Microbreccia

Chloritic breccia is a mappable rock unit on the eastern ends of Main and Ahwatukee Ridges (Figures 6, 12, and 13). It was formed by extreme brecciation, fracturing, faulting, and hydrothermal alteration of South Mountains Granodiorite or, less commonly, of other middle Tertiary intrusive rocks.

Chloritic breccia underlies and is related to a low-angle detachment fault. In most exposures, the breccia grades downward through a transitional zone of nonpervasive brecciation into unbrecciated South Mountains Granodiorite. It is composed of two distinct lithologies: chloritic breccia and microbreccia. These two rock types occur together in most outcrops and were formed by similar processes. Each type is lithologically distinct and is described separately below.

Chloritic Breccia

Chloritic breccia is a very distinctive rock unit that forms dark-colored cliffs where it is protected by an overlying cap of erosion-resistant microbreccia. The breccia is dissected by numerous fractures that impart a jagged aspect to most outcrops (Figure 23). The outcrops have a definite green coloration due to a high content of chlorite and epidote.

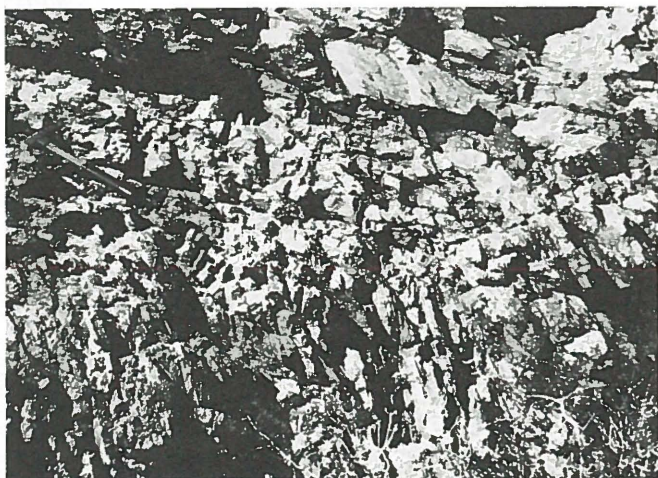


Figure 23. Photograph of chloritic breccia on Two Peaks. Protolith of breccia is mylonitic South Mountains Granodiorite.

The breccia is composed of countless angular fragments in a finely granulated matrix. Although the fragments vary in diameter from fractions of a millimeter to several meters, most are microscopic. There are two varieties of chloritic breccia. The first variety is more chaotic: fragments have been rotated and

totally detached from one another. In the second variety, the rocks are highly fractured, but adjacent fragments have not been rotated with respect to one another. Although these two varieties of breccia are widely intermixed, the more chaotic variety is most common in structurally high exposures.

Chloritic breccia is dissected by numerous fractures and small faults. The fractures vary from planar to curvilinear and commonly intersect one another at relatively low angles. Some fractures are striated, whereas others are purely dilational features devoid of striations.

In thin section, the breccia appears as a collage of angular fragments that are intermixed in a random arrangement (Figure 24). The largest fragments are approximately 5 mm in diameter, whereas the smallest fragments are too small to be resolved with a conventional petrographic microscope. Most fragments are monocrystalline, but some are polycrystalline or polymineralic.



Figure 24. Photomicrograph of chloritic breccia under crossed nicols. Width of photograph represents approximately 1.7 cm.

Microscopic textures in the breccia differ markedly from those in mylonitic rocks from which the breccia was derived. For example, almost all minerals in the breccia, including quartz, display evidence of brittle deformation. Most mineral fragments are brecciated, granulated, and shattered by numerous fractures and microfaults. Some fragments have textures, such as ribbon quartz, that are relicts of mylonitic fabrics that existed in the rocks before brecciation.

Brecciation was accompanied by extreme alteration of unstable mineral phases. Biotite is notably absent in chloritic breccia, although it is abundant in rocks from which the breccia was derived. Plagioclase fragments in breccia are extensively altered to sericite, epidote, and calcite. Some crystals of magnetite are rimmed by hematite, whereas others are unaltered. Sphene has been largely replaced by opaque oxides and hematite.

Crystals of chlorite, epidote, calcite, hematite, and magnetite were formed both during and after brecciation. Chlorite is ubiquitous and occurs as irregularly shaped masses in the interstices between fragments, in veins, as fracture coatings within fragments, and as mineral replacements. In addition,

chlorite is a major component of the fine-grained matrix that encloses the larger fragments. Many chlorite crystals lack fractures or other deformational features, which indicates that chlorite deposition accompanied and outlasted brecciation. The same is true of sericite, epidote, calcite, hematite, and magnetite, which accompany chlorite in the fine-grained matrix of the breccia. Calcite also occurs in veins, irregular void fillings, and disseminated replacements.

Some exposures of chloritic breccia contain well-developed foliation and striation-style lineation. These features were formed during brecciation and are not relicts inherited from the underlying mylonitic granodiorite. They are most common near the top of the breccia, slightly below the microbreccia ledge. The fabrics have a mylonitic aspect, but contain more evidence for brittle behavior than most mylonitic fabrics in the range; they appear to represent deformation intermediate in style between mylonitization and brecciation.

Microbreccia

Mesoscopic characteristics of microbreccia are distinct from those of chloritic breccia. Microbreccia forms erosion-resistant outcrops due to its compact character and lack of mesoscopic fractures. It is fine grained and has a gray color and a distinctive resinous or flinty luster on fresh surfaces (Figure 25). Weathered outcrops are normally shades of beige, tan, or brown. Some discrete fragments of chloritic breccia occur within the microbreccia.

Microbreccia, like chloritic breccia, is composed of a mosaic of angular fragments. The fragments vary markedly in size, but most are extremely small. Microbreccia consists of approximately 90-percent fine-grained matrix, in which fragments are less than 0.01 mm in diameter (Figure 26). The remainder of the rock is composed of larger fragments scattered throughout the matrix. Mineralogy of matrix material, although difficult to resolve with a conventional petrographic microscope, probably includes chlorite, epidote, hematite, and



Figure 25. Photograph of microbreccia on the northeast end of Main Ridge.



Figure 26. Photomicrograph of microbreccia under crossed nicols. Width of photograph represents approximately 1.7 cm.

sericite. Microbreccia differs from chloritic breccia in that it contains fragments of chlorite, but generally lacks chloritic void-fillings and veins.

Late Tertiary-Quaternary Surficial Deposits

Bedrock exposures of the South Mountains are surrounded by several types of surficial deposits. These deposits underlie low-relief plains adjacent to the range and are also widely exposed in topographic embayments of the Southern Foothills and in San Juan Valley. Additional unmapped patches occur in most drainages.

The most common surficial deposits are unconsolidated sand, gravel, and talus. Coarse-grained material is most abundant near mountain fronts, whereas fine-grained material occurs in more distal areas. Aprons of coarse talus cover many slopes, especially those around outcrops of Precambrian Estrella

Gneiss.

A second type of surficial deposit occurs in several locations along the northern flank of the range. These deposits are composed of well-bedded sand and gravel that were probably deposited by the Salt River.

Well-consolidated gravels occur in several areas, most notably in embayments of the Southern Foothills and in San Juan Valley. These gravels are the oldest exposed surficial deposits and usually form terraces that are being exhumed by modern drainages. The gravels are poorly sorted and well cemented by caliche. Bedding in the gravels is subhorizontal or gently dips away from the mountain range.

Geochronology

Introduction

A relative chronology of plutonic, metamorphic, and deformational events can be reconstructed using contact relationships, but an absolute chronology must be determined by isotopic geochemistry or by comparing undated rocks of the South Mountains to rocks of known age elsewhere in Arizona. As part of this study, Rb-Sr whole-rock isotopic analyses were used to evaluate the ages of Estrella Gneiss, South Mountains Granodiorite, Telegraph Pass Granite, and several dikes. In addition, U-Pb isotopic analyses have been performed on two size fractions of zircon from South Mountains Granodiorite. Cooling histories of the Tertiary plutonic rocks were constrained by K-Ar isotopic analyses on biotite. Additional K-Ar ages were determined on hornblende from mylonitic Estrella Gneiss and from a microdiorite dike that is one of the youngest intrusions in the range. All Rb-Sr and K-Ar isotopic analyses were done in cooperation with Muhammed Shafiqullah and Paul E. Damon of the Laboratory of Isotope Geochemistry, University of Arizona. The U-Pb isotopic study of the South Mountains Granodiorite is being carried out by Ed DeWitt of the USGS.

Geologic Constraints

Field relationships indicate that Estrella Gneiss is the oldest rock unit in the range (Figure 27). Igneous and sedimentary protoliths of the gneiss were metamorphosed and deformed prior to emplacement of all other rock types, except for Komatke Granite, which is probably synkinematic.

The next major event was the intrusion of South Mountains Granodiorite, Telegraph Pass Granite, Dobbins Alaskite, and numerous dikes and sills. Intense mylonitization accompanied and outlasted emplacement of the plutonic rocks. Microdiorite dikes, the youngest dikes in the range, are postmylonitic. Chloritic breccia and microbreccia formed after, but probably close to the same time as, the microdiorite dikes. Deposition of surficial deposits and erosion of the range were the last recorded geologic events.

Absolute ages of this relative chronology can be inferred by comparing rocks in the South Mountains to rocks of known age elsewhere in Arizona. Estrella Gneiss and Komatke Granite are lithologically and structurally similar to many Precambrian terranes in central, western, and northern Arizona (Giletti

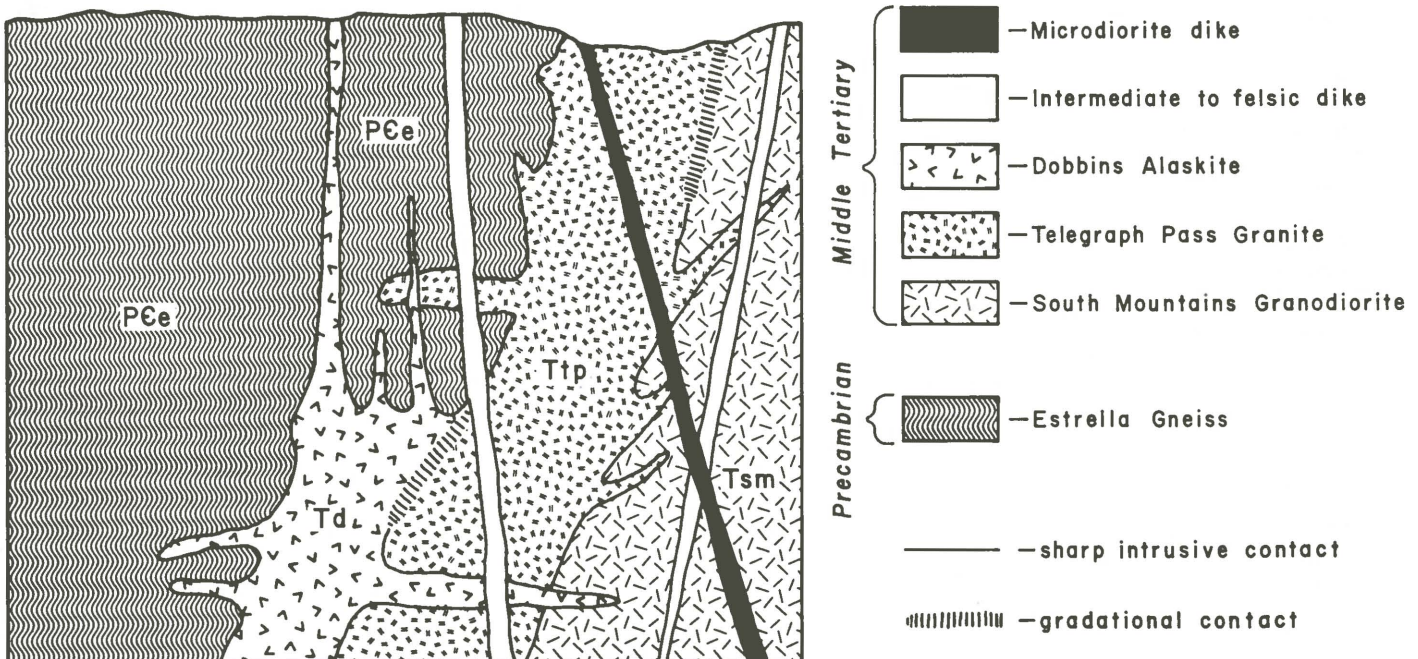


Figure 27. Schematic cross section illustrating contact relationships.

and Damon, 1961; Wasserburg and Lanphere, 1965; Damon, 1968; Livingston and Damon, 1968; Livingston, 1969; Pushkar and Damon, 1974; Anderson and Silver, 1976; Christenson and others, 1978; Shafiqullah and others, 1980). The steep crystalloblastic foliation in the gneiss and granite is characteristic of Precambrian terranes throughout Arizona.

South Mountains Granodiorite, Telegraph Pass Granite, and Dobbins Alaskite resemble both Laramide and middle Tertiary plutons, but are lithologically and structurally most similar to upper Oligocene granites of the Tortolita and Picacho Mountains north of Tucson (Keith and others, 1980; Banks, 1980). The numerous north-northwest-trending dikes of the South Mountains are similar in lithology and trend to dated middle Tertiary dikes of the Harquahala, Vulture, and Tortolita Mountains (Rehrig and Reynolds, 1980; Rehrig and others, 1980; Keith and others, 1980; Banks, 1980). Finally, chloritic breccia in the South Mountains is similar to chloritic breccia zones in western Arizona that are associated with low-angle detachment faults of Oligocene to middle Miocene age (Rehrig and Reynolds, 1980; G. A. Davis and others, 1980, 1982).

Rb-Sr Geochronology

Rb-Sr whole-rock analyses were determined on samples of Estrella Gneiss, South Mountains Granodiorite, Telegraph Pass Granite, and several types of dikes (Table 1; Appendix). All isotopic analyses were performed by the author and M. Shafiqullah. The analyses yield definitive emplacement ages for the granodiorite,

granite, and some dikes, but not the age of Estrella Gneiss.

Estrella Gneiss

Rb-Sr analyses were performed on a single sample of Estrella Gneiss that was collected for a K-Ar determination on hornblende. This sample is an amphibolite that has been overprinted by mylonitization. The amphibolite has a very low Rb content (14 ppm) and $^{87}\text{Rb}/^{86}\text{Sr}$ ratio (0.1918; Table 1). The measured $^{87}\text{Sr}/^{86}\text{Sr}$ ratio of the sample (0.706) is also relatively low. The low Rb/Sr ratio of the sample prohibits a unique model age. Model ages of 1.8, 1.6, and 1.1 b.y. B.P. are calculated by assuming initial $^{87}\text{Sr}/^{86}\text{Sr}$ ratios of 0.701, 0.7015, and 0.703, respectively. Younger model ages result from assuming higher initial ratios. No interpretation of the data is unique, but a reasonable hypothesis is that the amphibolite is Precambrian in age, possibly 1.6 to 1.8 b.y. old, as suggested by correlation of Estrella Gneiss with isotopically dated Precambrian rocks in the Sierra Estrella (Pushkar and Damon, 1974) and elsewhere in Arizona. The South Mountains amphibolite would have originally been a Rb-poor mafic igneous rock, and, therefore, would have evolved ^{87}Sr very slowly. The low initial $^{87}\text{Sr}/^{86}\text{Sr}$ ratio calculated for the Estrella Gneiss amphibolite, if valid, indicates a primitive mantle source for the original mafic igneous rock.

South Mountains Granodiorite

Four whole-rock samples of South Mountains Granodiorite and three samples of aplite-

SAMPLE NUMBER	ROCK TYPE	Rb (ppm)	Sr (ppm)	$^{87}\text{Rb}/^{86}\text{Sr}$	$^{87}\text{Sr}/^{86}\text{Sr}$	NUMBER OF RUNS
Estrella Gneiss						
EG-1	amphibolite	14	211	0.192	0.70597 ± 0.00017	16
South Mountains Granodiorite						
SMG-1	granodiorite (mylonitic)	54	589	0.266	0.70559 ± 0.00036	13
SMG-2	granodiorite	66	462	0.414	0.70556 ± 0.00035	11
SMG-3	granodiorite	71	443	0.464	0.70558 ± 0.00037	4
SMG-4	granodiorite	79	476	0.480	0.70591 ± 0.00023	13
SMG-5	aplite in granodiorite	99	101	2.83	0.70695 ± 0.00040	17
SMG-6	aplite in granodiorite	130	60.0	6.27	0.70846 ± 0.00015	5
SMG-7	aplite in granodiorite	189	20.0	27.4	0.71517 ± 0.00074	23
Telegraph Pass Granite						
TPG-1	granite	80	231	1.00	0.70659 ± 0.00034	6
TPG-2	granite	113	202	1.62	0.70661 ± 0.00036	20
TPG-3	granitic dike	110	180	1.77	0.70721 ± 0.00031	10
TPG-4	aplite in granite	139	24.0	16.8	0.71280 ± 0.00121	10

Table 1. Rb-Sr analyses. Sample locations, field numbers, and decay constants are listed in Appendix A.

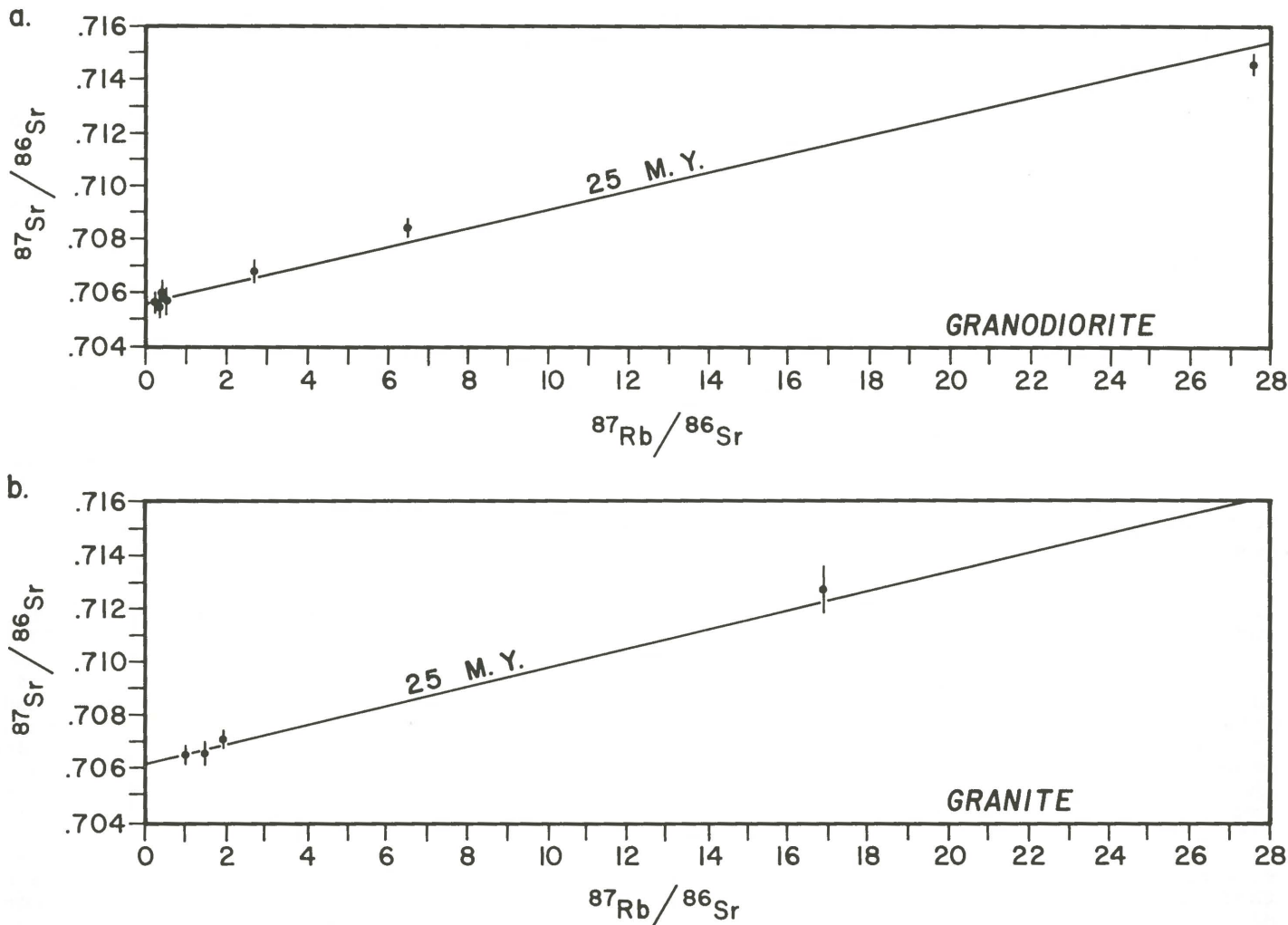


Figure 28. Rb-Sr whole-rock isochrons for South Mountains Granodiorite and Telegraph Pass Granite: (a) 25-m.y. reference isochron for South Mountains Granodiorite;

(b) 25-m.y. reference isochron for Telegraph Pass Granite.

ic phases of the granodiorite were collected and analyzed for Rb and Sr. The spread in $^{87}\text{Rb}/^{86}\text{Sr}$ ratios for the four granodiorite samples is too limited to permit construction of a tightly constrained isochron, but inclusion of the three aplite samples enables the age of the granodiorite to be determined using a standard isochron plot (Figure 28a). All data points plot near a 25-m.y. isochron. An emplacement age of $24.6 \text{ m.y.} \pm 0.4 \text{ m.y.}$ with

an initial $^{87}\text{Sr}/^{86}\text{Sr}$ ratio of 0.7056 results from a least-squares regression on all seven data points.

The $^{87}\text{Rb}/^{86}\text{Sr}$ ratios of the aplites permit a relatively precise determination of the age and initial $^{87}\text{Sr}/^{86}\text{Sr}$ ratio of granodiorite. Representative model ages at different assumed $^{87}\text{Sr}/^{86}\text{Sr}$ initial ratios are given for the most radiogenic aplite in Table 2. The model ages are middle Tertiary, regardless of what reasonable initial $^{87}\text{Sr}/^{86}\text{Sr}$ ratio is assumed. Evidence that the aplites and granodiorite are comagmatic was previously presented in this report.

ASSUMED INITIAL RATIO	MODEL AGES OF APLITES (m.y.)	
	SOUTH MOUNTAINS GRANODIORITE	TELEGRAPH PASS GRANITE
0.709	15.9	16.0
0.708	18.5	20.2
0.707	21.0	24.4
0.706	23.6	28.5
0.705	26.2	32.7
0.704	28.7	36.9
0.703	31.3	41.1

Table 2. Rb-Sr model ages for aplites in South Mountains Granodiorite and Telegraph Pass Granite.

Telegraph Pass Granite

Rubidium and strontium analyses were performed on two samples of main-phase Telegraph Pass Granite, one sample of an aplite within the granite, and one sample from a granitic dike. All data points plot near a 25-m.y. reference isochron (Figure 28b), and a least-squares regression on the data yields an age of $27.7 \text{ m.y.} \pm 0.7 \text{ m.y.}$, with an initial $^{87}\text{Sr}/^{86}\text{Sr}$ ratio of 0.7062. Model ages calculated for the aplite sample are middle Tertiary, re-

SAMPLE NUMBER	MINERAL/LITHOLOGY	K (%)	RADIOGENIC $^{40}\text{Ar} \times 10^{-12} \text{m/g}$	PERCENT	
				ATMOSPHERIC ^{40}Ar	AGE (m.y.)
UAKA 78-27	hornblende/ mylonitic amphibolite	0.586	49.81	19.3	48.3 ± 1.0
UAKA 78-80	biotite/South Mountains Granodiorite, slightly mylonitic	7.308	261.2	18.6	20.5 ± 0.4
UAKA 78-81	biotite/South Mountains Granodiorite	7.300	256.9	17.6	20.2 ± 0.4
UAKA 73-110	biotite/Telegraph Pass Granite	7.203	241.2	28.0	19.2 ± 0.4
UAKA 79-133	hornblende/microdiorite dike	1.148	56.90	27.6	28.4 ± 0.5

Table 3. K-Ar analyses. Sample locations, field numbers, and decay constants are listed in Appendix A.

ardless of what reasonable initial $^{87}\text{Sr}/^{86}\text{Sr}$ ratio is assumed (Table 2).

The 0.7062 initial $^{87}\text{Sr}/^{86}\text{Sr}$ ratio determined for the granite is very close to, but slightly higher than, the 0.7056 initial ratio determined for the granodiorite. Similar initial ratios for the two rock types support a comagmatic origin. The slightly higher initial ratio of the granite might be due to its proximity to radiogenic micaceous and feldspathic lithologies in Precambrian Estrella Gneiss.

Adherence of both granite and granodiorite data to 28- to 25-m.y. isochrons verifies that the two rock types are phases of a single pluton. A least-squares regression on all granodiorite and granite samples gives an age of 25.5 m.y. ± 1.5 m.y. Field relationships and isotopic geochemistry are mutually supportive and unambiguous; the granite and granodiorite are both late Oligocene (approximately 25 m.y.) in age. By analogy, Dobbins Alaskite is also 25 m.y. old because it is a border phase of Telegraph Pass Granite.

K-Ar Geochronology

K-Ar mineral ages were determined for five rocks from the South Mountains (Table 3; Appendix). Biotite was dated from two samples of South Mountains Granodiorite and one sample of Telegraph Pass Granite. Hornblende was dated from mylonitically deformed Estrella Gneiss and from an undeformed microdiorite dike. All ages were determined by Muhammed Shafiqullah and Paul E. Damon of the Laboratory of Isotope Geochemistry, University of Arizona.

Estrella Gneiss

A K-Ar age of 48.3 m.y. ± 1.0 m.y. was determined on hornblende from a mylonitic amphibolite within Estrella Gneiss. This age can be interpreted in several ways. One possible interpretation is that the date is a

simple cooling age, which implies that the amphibolite cooled below approximately 450°C 48 m.y. ago. Such an interpretation would be most plausible if the amphibolite had experienced a simple, single-stage metamorphic and deformational history. However, hornblende in the sample is a relict of Precambrian metamorphism that has survived subsequent mylonitization; therefore, the cooling history of the sample might be extremely complex.

A second interpretation is that the 48-m.y. age reflects both the original Precambrian metamorphism and subsequent middle Tertiary mylonitization. The 48-m.y. age determination is much closer to the age of mylonitization than to the age of original Precambrian metamorphism, which suggests that the hornblende age is mostly recording thermal events that accompanied Tertiary mylonitization. In this interpretation, Tertiary heating at 25 m.y. B.P. was sufficient to expel nearly 99 percent of the argon that had accumulated in the hornblende since its formation during the Precambrian.

South Mountains Granodiorite and Telegraph Pass Granite

Biotite was dated from two separate localities of South Mountains Granodiorite and from one exposure of Telegraph Pass Granite. The K-Ar ages on the two samples of granodiorite are 20.5 m.y. ± 0.4 m.y. and 20.2 m.y. ± 0.4 m.y. The K-Ar age on the biotite from the granite is slightly younger at 19.2 m.y. ± 0.4 m.y. The ages indicate that both rock types cooled below approximately 250°C (the temperature at which biotite retains argon) 20 m.y. ago. The similarity of biotite ages from three different locations suggests that the plutons experienced a relatively uniform cooling history. It is significant that the K-Ar cooling ages are approximately 5 m.y. younger than the 25-m.y. emplacement age indicated by Rb-Sr whole-rock analyses. The disparity between the emplacement and cooling ages indicates that the plutons had a somewhat protracted cooling history.

Microdiorite Dike

A single K-Ar age was determined on hornblende from a microdiorite dike in the Southern Foothills. The dike is a constituent of a north-northwest-trending swarm of microdiorite dikes that traverse the entire width of the range. They crosscut mylonitic foliation in the country rocks, but have been extensively overprinted by brittle deformation associated with the chloritic breccia. The sampled dike is coarse grained, fresh, and unbrecciated.

The K-Ar hornblende age on the microdiorite dike is 28.4 m.y. \pm 0.5 m.y., approximately the same age as emplacement of the South Mountains Granodiorite and Telegraph Pass Granite. Field relationships demonstrate that the microdiorite dikes are younger than both the granodiorite and granite. The 28-m.y. hornblende age may indicate that the emplacement ages of the granodiorite and granite are closer to 28 m.y. than to 25 m.y. Alternatively, the hornblende age is anomalously old due to extraneous argon that was incorporated into the hornblende during crystallization. If this is the case, the microdiorite dikes would be between 20 and 25 m.y. old.

U-Pb Geochronology

Subsequent to completion of the Rb-Sr and K-Ar geochronologic studies discussed above, Ed DeWitt has determined the U-Pb isotopic composition of two size fractions of zircons from South Mountains Granodiorite. Both size fractions are discordant, but define a chord that has a lower intercept of 22 m.y. \pm 1 m.y. and an upper intercept of 1617 m.y. \pm 26 m.y. (Ed DeWitt, 1984, written communication). The finer size fraction yields younger U-Pb ages than the coarse fraction. Based on the existing data, DeWitt concludes that the emplacement age of the South Mountains Granodiorite

is approximately 22 m.y. B.P., and that the discordance of the zircon data reflects inheritance of radiogenic Pb from the regional Proterozoic basement. The significance of the slight discrepancy between the 22-m.y. age and the 25-m.y. age determined by Rb-Sr methods cannot be fully evaluated until a third, finer grained size fraction of zircon has been analyzed.

Geochronologic Summary

Geochronologic studies have conclusively dated the emplacement of most intrusive rocks in the range. Estrella Gneiss and Komatke Granite are isotopically undated, but both rocks are probably Precambrian in age (approximately 1.6-1.7 b.y.). South Mountains Granodiorite, Telegraph Pass Granite, and Dobbins Alaskite were emplaced approximately 25 m.y. ago as phases of a composite middle Tertiary pluton. All dikes in the range were intruded approximately 25 to 20 m.y. ago, with the youngest dikes being microdiorites. The actual time of dike emplacement may have been within a much more restricted age range. K-Ar biotite ages indicate that the middle Tertiary plutonic rocks had cooled below approximately 250°C by 19 to 20 m.y. B.P.

The isotopic ages, in conjunction with field relationships, constrain the ages of the major deformational events. Deformation and metamorphism that formed the Estrella Gneiss are almost certainly Precambrian, although they are isotopically undated in the South Mountains. Intense mylonitization occurred synchronously with plutonism at approximately 25 m.y. B.P. and may have continued until 20 m.y. B.P. Development of chloritic breccia largely postdates the microdiorite dikes, although the dikes and breccia may overlap in age. Most of the breccia was probably formed by 19 to 20 m.y. B.P., when the plutonic rocks were cooling below 250°C. The microbreccia may be slightly younger.

Structural Geology

Field relationships, isotopic geochemistry, and regional considerations indicate that at least six deformational episodes are represented by structures of the South Mountains and vicinity. From oldest to youngest, they are:

- 1) Precambrian deformation;
- 2) Middle Tertiary dilation associated with plutonism;
- 3) Middle Tertiary mylonitization;
- 4) Middle Tertiary fracturing, brecciation, and detachment faulting;
- 5) Middle (?) Tertiary arching; and
- 6) Late Tertiary Basin and Range deformation.

There was probably considerable overlap among some episodes of deformation. The character, orientation, kinematic significance, and age of structures formed during each episode of deformation are discussed in the following sections.

Precambrian Deformation

Precambrian Estrella Gneiss and Komatke Granite have undergone a major episode of Precambrian deformation. This deformation produced a well-developed crystalloblastic foliation that generally strikes northeast and dips steeply or moderately to the southeast. Deformation was accompanied by amphibolite-facies metamorphism.

Character and Orientation

Crystalloblastic foliation in Estrella Gneiss and Komatke Granite is defined by compositional banding and by preferred orientation of minerals (Figure 14). Estrella Gneiss is compositionally banded on a wide variety of scales, whereas Komatke Granite is compositionally banded only on the scale of several millimeters. In both rock types, oriented mineral grains, such as biotite and muscovite, help to define the foliation, but generally do not form an obvious lineation.

The orientation of Precambrian crystalloblastic foliation is variable when viewed over the entire South Mountains, but is more systematic within smaller areas or domains (Figure 29, Table 4). Most crystalloblastic foliation strikes northeast to east-west and dips steeply or moderately to the southeast or south (Figure 30). The overall strike is northeast in the eastern parts of Main Ridge, Alta Ridge, and the Southern Foothills, but gradually changes to east-west or west-

northwest toward the west end of the range. Crystalloblastic foliation has more variable strikes and more gentle dips in the areas that have been overprinted by Tertiary mylonitization (Figure 31).

Age and Kinematics

The age of deformation and metamorphism that produced the crystalloblastic foliation in Estrella Gneiss and Komatke Granite cannot be directly established in the South Mountains. Some deformation probably took place during emplacement of the Komatke Granite, because the granite discordantly intrudes some crystalloblastic foliation, yet is itself foliated. Development of foliation in both rock units predated emplacement of all middle Tertiary intrusions. Crystalloblastic foliation in the South Mountains is similar in character, structural style, and orientation to dated, middle Proterozoic (1.6 - 1.7 b.y. B.P.) fabrics in central and western Arizona (Anderson and Silver, 1976).

The kinematic significance of crystalloblastic foliation in Precambrian terranes of Arizona is not well known, and data from the South Mountains provide little insight into this problem. Crystalloblastic foliation in the range is probably a transposition foliation that has disrupted any original sedimentary and igneous layering in the rocks. It is likely that the steep northeast-striking foliation was formed by northwest-southeast flattening in response to northwest-southeast-directed compression. A second, less likely possibility is that the foliation was formed by layer-parallel shear along the northeast-striking foliation.

Middle Tertiary Dilation Associated With Plutonism

Emplacement of middle Tertiary intrusions was accompanied by formation of a variety of dilational structures. The largest structures are those reflected by the overall form of South Mountains Granodiorite and Telegraph Pass Granite. Smaller dilational structures include systematically oriented aplite dikes and fractures in granite and granodiorite. Emplacement of the main pluton was followed by intrusion of numerous middle Tertiary dikes and sills. The consistent north-northwest trend of the dike, aplites, and fractures (Table 5) reflects a consistent orientation of stress and strain during the entire episode of middle Tertiary plutonism.

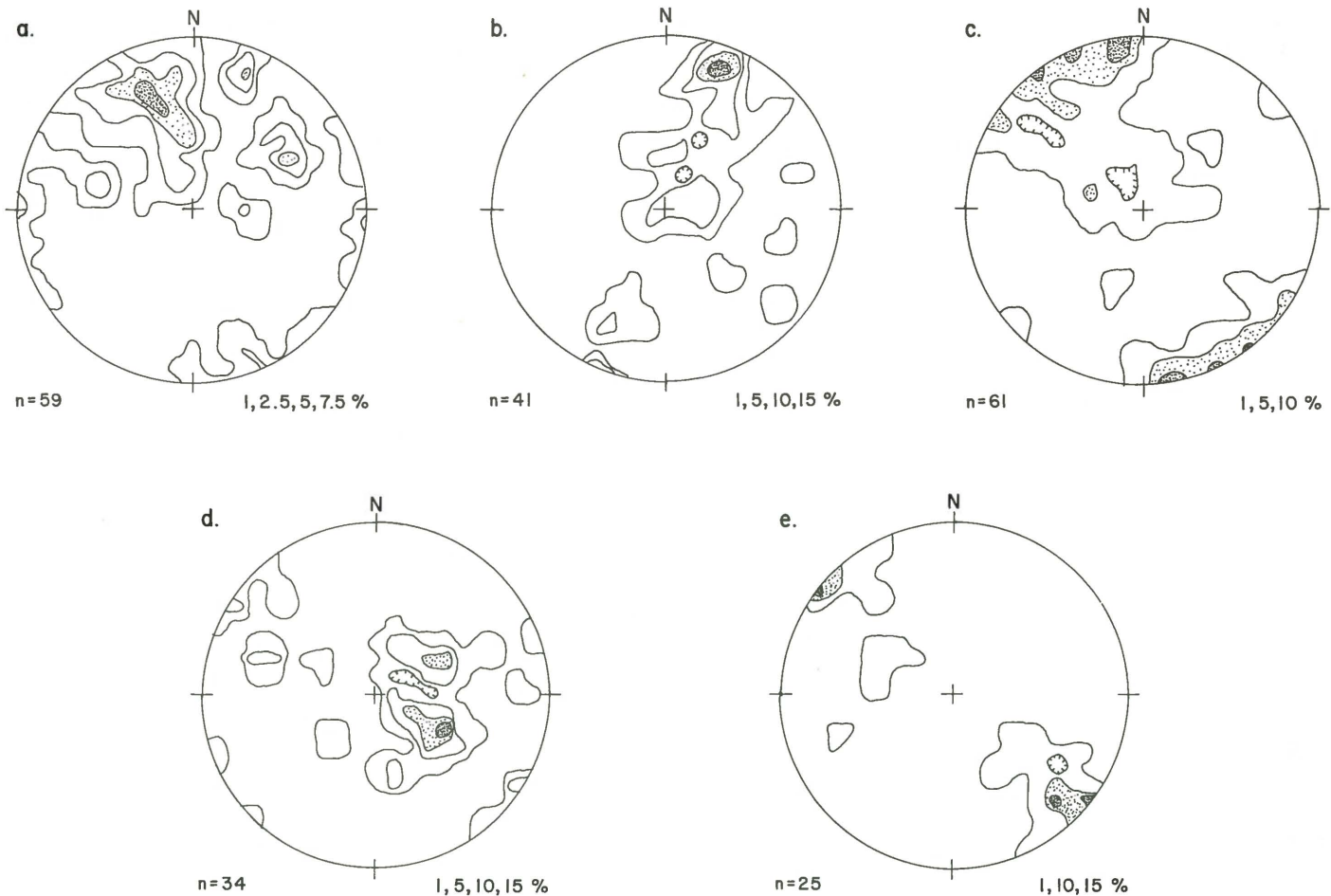


Figure 29. Contoured equal-area plots of poles to crystalloblastic foliation in Precambrian rocks: (a) Domain 1 - eastern Alta Ridge and North Ridge; (b)

Domain 2 - western Alta Ridge; (c) Domain 3 - Main Ridge; (d) Domain 4 - western Southern Foothills; and (e) Domain 5 - Boundary Hills and Pima Ridge.

FIGURE NUMBER	PRECAMBRIAN DOMAIN	MODAL FOLIATION	NUMBER OF READINGS
29a	1	N 66° E, 66°SE	59
29b	2	N 70° W, 74°S	41
29c	3	N 85° E, 90°	61
29d	4	N 28° E, 35°W	34
29e	5	N 37° E, 90° N 45° E, 75°NW	25

Table 4. Modal orientation of crystalloblastic foliation in Precambrian domains.

South Mountains Granodiorite and Telegraph Pass Granite

Emplacement of South Mountains Granodiorite and Telegraph Pass Granite was accommodated by east-northeast directed dilation of the preexisting basement. The granite is a north-northwest-trending, dikelike body, whose upper parts flatten out to the east over South Mountains Granodiorite. Geometry of the contact, in conjunction with field observations, indicates that the granite was emplaced along a north-northwest-trending zone of dilation that is more than 6 km long (Figures 6-8). On a smaller scale, north-northwest-trending

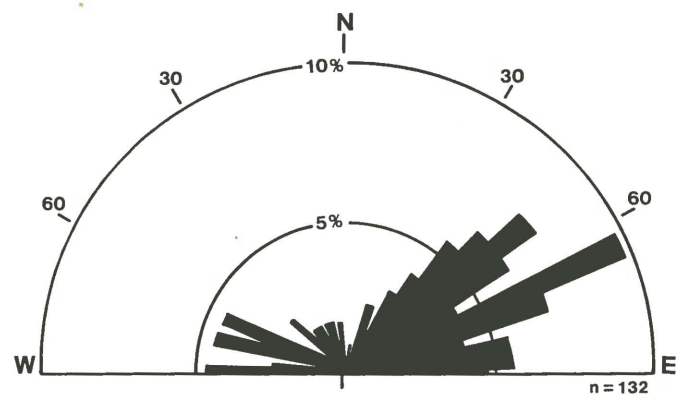
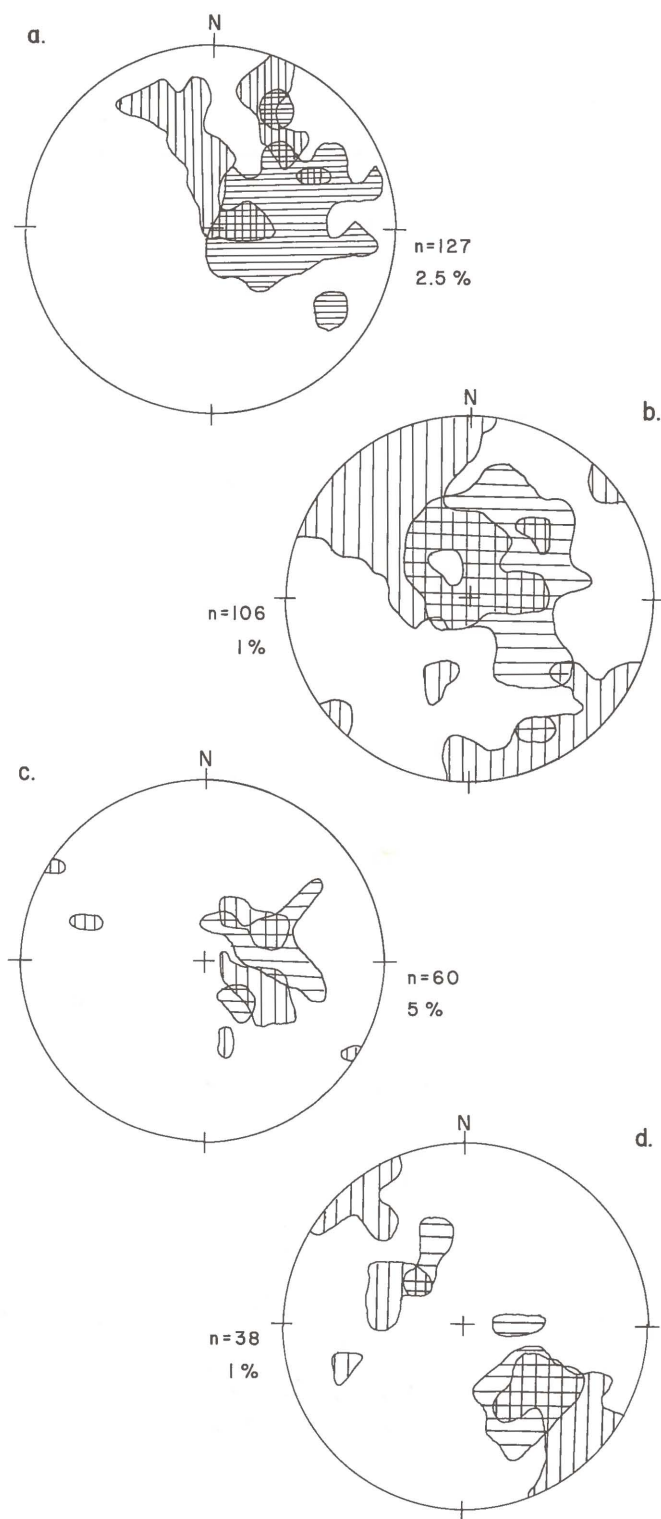


Figure 30. Strike-frequency diagram of crystalloblastic foliation that dips 60° or more.

apophyses of granite and granodiorite extend outward from the main plutons.

Aplite dikes are common in both granodiorite and granite. Models for the origin of aplites indicate that aplites form in fractures that develop during the late stages of magmatic crystallization (Jahns and Burnham, 1969). The aplites, therefore, provide a means for evaluating the late magmatic deformational history and state of stress of the plutonic host rock.



Most aplites in South Mountains Granodiorite strike north-northwest and dip steeply (Figure 32). Nearly 90 percent of all measured aplites have strikes between N. 10° W. and N. 40° W. The systematic orientation of aplites demonstrates that north-northwest-striking fractures opened during late-stage crystallization of the 25-m.y.-old granodiorite. Aplite orientations in adjacent Telegraph Pass Granite have not been studied in detail but appear to be similar.

Figure 31. Contoured equal-area plots of poles to crystalloblastic and mylonitic foliations in Precambrian rocks. Crystalloblastic and mylonitic foliations are represented by vertically and horizontally lined areas, respectively. (a) Domains 1 and 2 - Alta and North Ridges; (b) Domain 3 - Main Ridge; (c) Domain 4 - western Southern Foothills; and (d) Domain 5 - Boundary Hills and Pima Ridge.

FIGURE NUMBER	TYPE OF STRUCTURE	MEAN	MODE	NUMBER OF READINGS
32	Strike of aplites in South Mountains Granodiorite	N 26° W	N 30° W	68
33a	Strike of mineralized fractures in Telegraph Pass Granite	N 25° W	N 20° W	125
33b	Strike of mineralized fractures in granodiorite and granite in Southern Foothills	N 29° W	N 30° W	20
33c	Strike of mineralized fractures in Dobbins Alaskite	N 35° W	N 40° W	13
34a	Trend of dikes in western dike swarm	N 30° W	N $30-35^{\circ}$ W	94
34b	Trend of dikes in eastern dike swarm	N 32° W	N $30-35^{\circ}$ W	164
34c	Trend of dikes in both dike swarms	N 31° W	N $30-35^{\circ}$ W	258
36	Trend of microdiorite dikes	N 33° W	N 30° W	60

Table 5. Modal and mean orientations of middle Tertiary igneous structures.

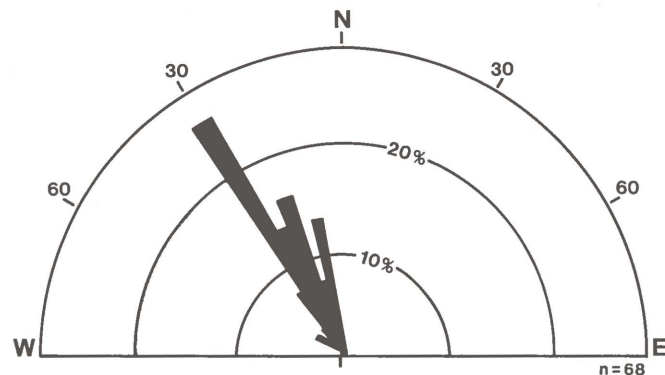


Figure 32. Strike-frequency diagram of aplite dikes in South Mountains Granodiorite.

South Mountains Granodiorite and Telegraph Pass Granite are dissected by numerous hydrothermally altered and mineralized fractures. Most fractures are quite planar and are accompanied by limonite, pyrite, minor amounts of copper minerals, and locally intense, argillic and sericitic alteration. These characteristics distinguish this suite of fractures from the more curvilinear, anastomosing fractures that are associated with chloritic breccia. Hydrothermally altered and mineralized fractures are most abundant near the contact between the granite and granodiorite. Most mineralized fractures in the granite, granodiorite, and alaskite strike north-northwest and dip steeply (Figure 33). The fractures were also noted by Avedisian (1966), who reported that "primary jointing" in the granite strikes N. 28° W. and dips vertically.

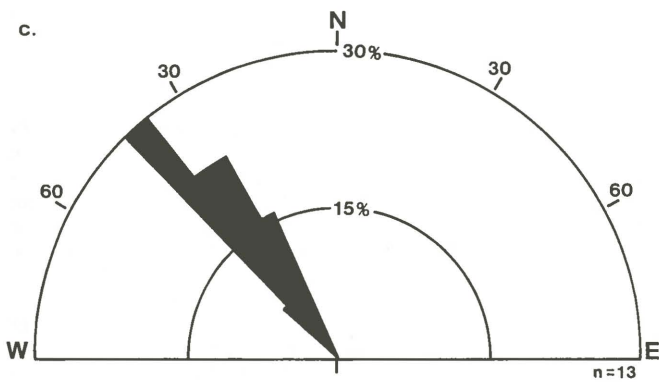
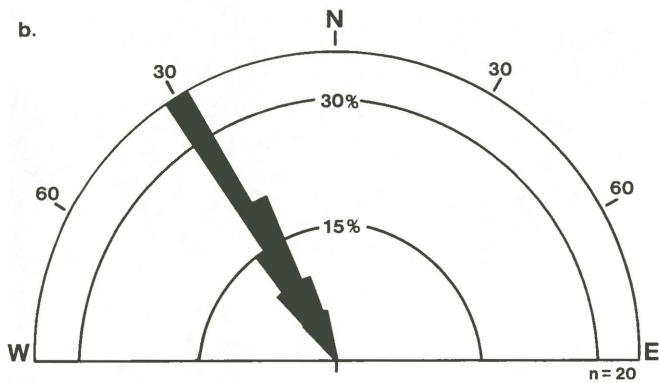
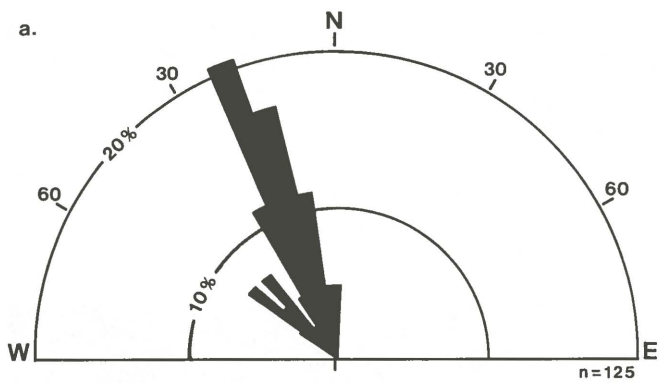


Figure 33. Strike-frequency diagrams of mineralized fractures in Telegraph Pass Granite, South Mountains Granodiorite, and Dobbins Alaskite: (a) Telegraph Pass Granite near Telegraph Pass; (b) South Mountains Granodiorite and Telegraph Pass Granite in Southern Foothills; and (c) Dobbins Alaskite.

Dikes and Sills

Telegraph Pass Granite, Dobbins Alaskite, South Mountains Granodiorite, and Estrella Gneiss have been intruded by numerous intermediate to felsic dikes and sills. The dikes maintain a remarkably consistent north-northwest trend throughout the range. Trend-rosette diagrams for the dikes have been constructed by measuring the overall trend of 1,000-foot segments of each dike. These diagrams document a predominance of north-northwest trends for both the western and eastern dike swarms (Fig-

ures 34a and 34b). A composite trend-rosette diagram for both dike swarms, representing a combined trend length of nearly 80 km, further emphasizes the uniformity in trend (Figure 34c). A conventional histogram of the same data displays a symmetrical distribution around the N. 31° W. mean trend (Figure 35). Microdiorite dikes, not included on earlier plots, have a similar N. 30° W. modal trend (Figure 36).

Kinematics

All dilational structures related to plutonism have a systematic north-northwest trend. The granite and granodiorite were

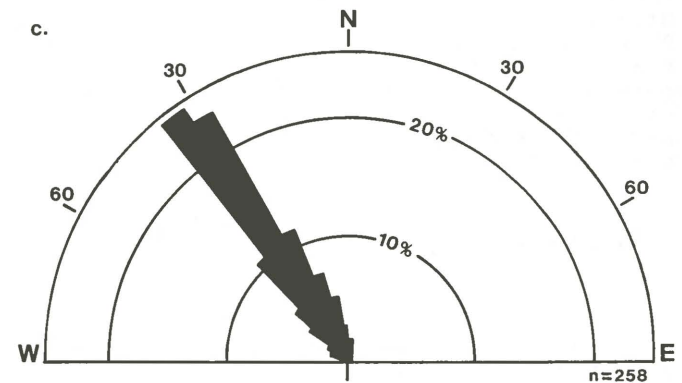
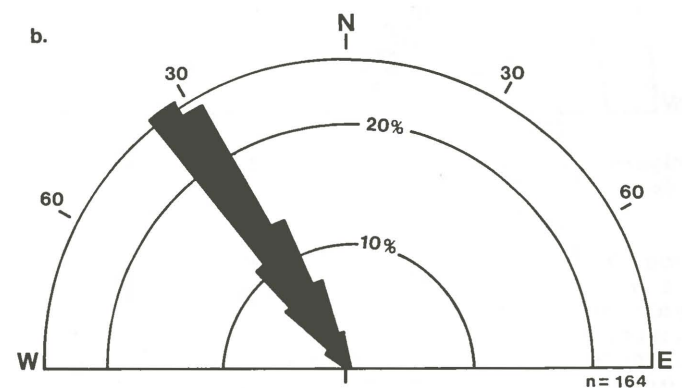
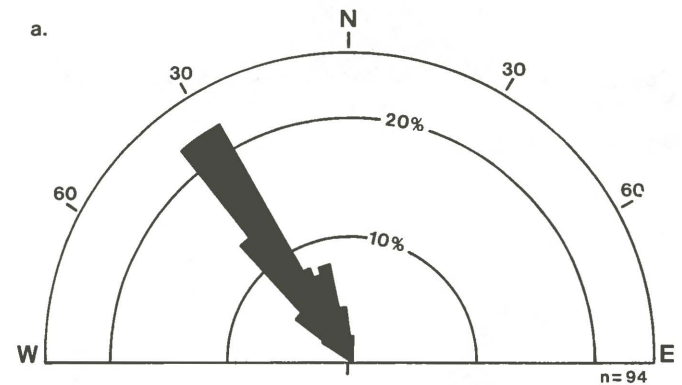


Figure 34. Trend-frequency diagrams of dikes in western and eastern dike swarms: (a) western dike swarm; (b) eastern dike swarm; and (c) both dike swarms.

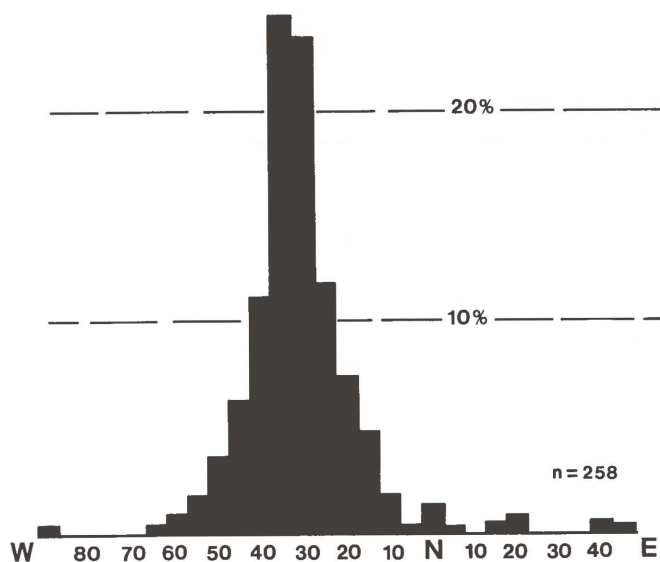


Figure 35. Histogram of dike trends in both swarms.

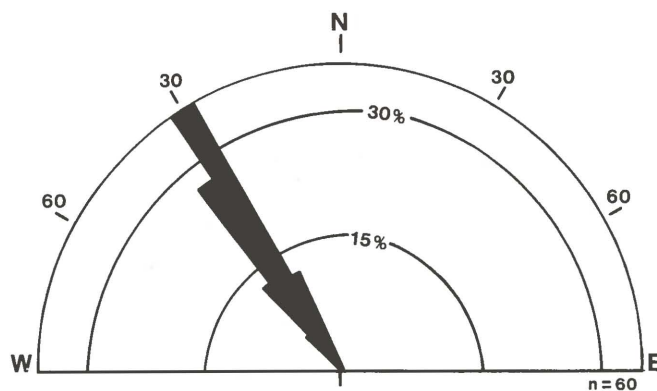


Figure 36. Trend-frequency diagram of microdiorite dikes.

emplaced along a north-northwest-trending zone of dilation. Intrusion of aplites and dikes was accommodated by dilation of north-northwest-striking fractures that formed soon after emplacement of the main pluton. North-northwest-striking, altered and mineralized fractures in the granite and granodiorite appear to be simple dilational features. The fractures, dikes, and aplites are most readily interpreted as being formed by N. 60° E.-S. 60° W. extensional strain. Such an extensional origin is compatible with evidence from elsewhere in Arizona for east-northeast extension during the middle Tertiary (Rehrig and Heidrick, 1976; Banks, 1980; Davis, G. H., 1980).

Middle Tertiary Mylonitic Deformation

Rocks throughout much of the range have been subjected to variable amounts of Tertiary mylonitic deformation (Figure 37). Mylonitic fabrics occur in nearly all areas of the eastern half of the range, but are less abundant in the western half. Mylonitization has variably affected all rock types, except the

microdiorite dikes. Complete gradations can be observed from undeformed to highly mylonitized rocks. Tertiary plutonic rocks are undeformed in structurally low exposures, but are progressively more mylonitic upward. Mylonitic fabric cuts through Estrella Gneiss as a broad, diffuse zone that dips 30° to the west. Gneiss above and below the zone is less mylonitic and largely retains its original steep crystalloblastic foliation.



Figure 37. Photograph of mylonitic South Mountains Granodiorite with foliated quartz veins and aplite dikes.

Mylonitization produced a gently to moderately dipping foliation and a conspicuous lineation that consistently trends east-northeast. Mylonitic fabrics cut preexisting Precambrian crystalloblastic foliation and Tertiary igneous structures discussed in the preceding section. Mylonitization was locally accompanied by the formation of tension gashes, pinch-and-swell structures, normal shear zones, and several types of folds. Microscopic characteristics of mylonitic fabrics are discussed in more detail by Reynolds (1982) and Champine (1982).

Mylonitic Fabrics

Mylonitization has produced distinctive fabrics that are equally apparent at mesoscopic and microscopic scales of observation. The most dominant fabric elements are foliation, lineation, and small-scale extensional features such as tension gashes. Mylonitization was usually accompanied by a decrease in overall grain size via comminution, recrystallization, and neomineralization (these terms are discussed by Higgins, 1971). Much variation in mesoscopic and microscopic appearances is due to differences in original mineralogy of the protolith. Specifically, quartz content of the protolith had a profound influence on the degree to which mylonitic fabric was developed. Mylonitic fabric is most easily recognized in quartz-rich rocks, and is less

obvious in quartz-poor amphibolite and mica schist.

Mylonitic rocks display a distinctive, lenticular foliation that is primarily defined by lenticular or blade-like mineral aggregates (Figures 38 and 39). Color banding, where present, is due to an interlayering of light-colored lenses of quartz and alkali feldspar with darker lenses of epidote, plagioclase, and biotite. Some lenticular mineral aggregates are draped around feldspar porphyroclasts, producing flaser structure. In addition, many porphyroclasts of biotite and feldspar have become lenticular through comminution and strain-induced recrystallization.

Foliation is also partly defined by the parallel orientation of platy minerals such as biotite, muscovite, and chlorite, and by small-scale variations in grain size or porphyroclast content. Medium-grained, moderately deformed rocks usually contain thin bands of fine-grained, intensely deformed rock. In many cases, these differences in grain size reflect differences in degree of deformation.

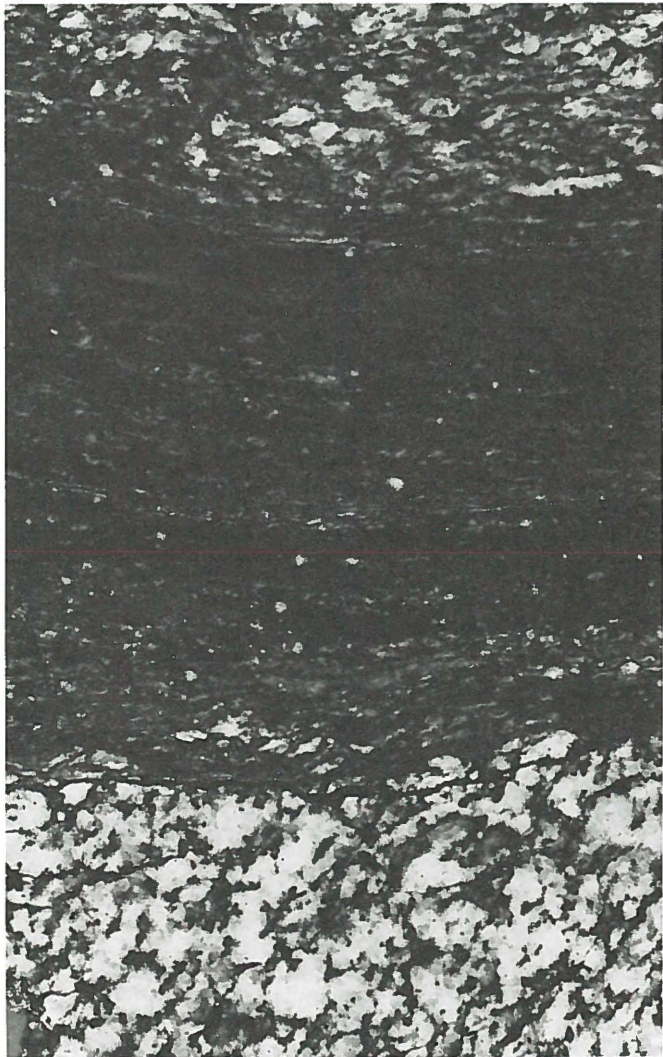
A well-defined lineation accompanies foliation in virtually all mylonitic rocks of the South Mountains (Figure 40). Lineation is

largely defined by rod- or blade-like aggregates of quartz and feldspar. These aggregates have a distinctive "smeared-out" appearance that imparts a streaky aspect to foliation surfaces. Individual quartz and feldspar aggregates commonly display delicate lineations that resemble small-scale striations. Lineation is also defined by discontinuous trains of feldspar, biotite, and hornblende porphyroclasts. Larger porphyroclasts are flanked by crush trails of small angular fragments that are "strung out" in the direction of lineation. Lineation is also defined by aligned prismatic minerals such as epidote and hornblende. Some of the prismatic crystals have grown during mylonitization, whereas others were rotated into the lineation direction.

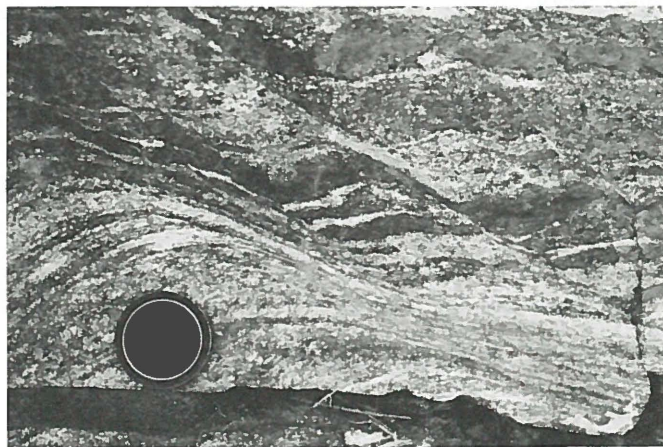
Mineralogic Response to Mylonitization

Different minerals have responded to mylonitization in different ways. For example, quartz in mylonitic rocks commonly occurs in thin section as lenticular or irregular aggregates that are composed of small quartz crystals with varying crystallographic orien-

Figure 38. Photographs of mylonitic fabric: (a, left) thin mylonitic zone in cut slab of South Mountains



Granodiorite; zone is approximately 5 cm thick; (b, top right) mylonitic foliation and northeast-directed S-C fabric in slab of South Mountains Granodiorite cut parallel to lineation and perpendicular to foliation; width of photograph represents approximately 4 cm; and (c, bottom right) west-directed, mylonitic shear zones in Estrella Gneiss west of Telegraph Pass.



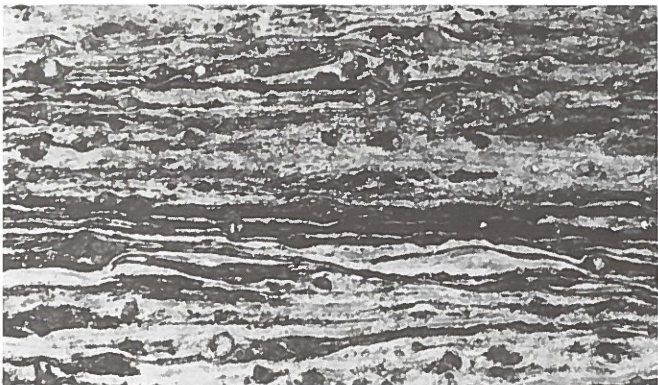


Figure 39. Photomicrographs of mylonitic fabric: (a, top) moderately mylonitic South Mountains Granodiorite under crossed nicols; width of photograph represents approximately 2 cm; (b, middle) thin ultramylonitic zone in Dobbins Alaskite from Dobbins Lookout; zone is approximately 2 mm wide; and (c, bottom) mylonitic Komatke Granite; width of photograph represents approximately 2 cm.

tations. Some of the small individual crystals display undulatory extinction and most have sutured boundaries. Many aggregates are draped over brittlely deformed porphyroclasts of plagioclase and potassium feldspar. Some quartz aggregates bifurcate laterally toward their margins and interfinger with adjacent rock in a fashion reminiscent of fiamme or flame structures in welded ash-flow tuffs. Quartz also occurs as greatly elongated ribbons that have undulatory extinction. Adjoining ribbons are commonly separated by thin zones of small equant crystals of quartz.

Plagioclase and orthoclase occur in



Figure 40. Photograph of mylonitic lineation in South Mountains Granodiorite.

mylonitic rocks as porphyroclasts that are strongly fractured into discrete fragments and that are separated from one another by fine-grained matrix or by microscopic fractures and faults. Many porphyroclasts display rounded corners, brecciated concentric zoning, and bent twin lamellae. Some individual crystals have been pulled apart in the direction of lineation, leaving voids and fissures that were filled with quartz, biotite, and other constituents of the fine-grained matrix. These fissure fillings were not formed by the replacement of the porphyroclasts, but represent either matrix material that was physically forced into the opening voids or crystals that were precipitated by fluids circulating within the voids. Most plagioclase crystals in mylonitic rocks have been extensively replaced by sericite and epidote. In addition, some porphyroclasts are flanked by pressure shadows of chlorite, biotite, and sericite.

Biotite has accommodated mylonitization by brittle deformation and recrystallization. Some biotite grains have been pulverized, flattened, and drawn out in the direction of lineation; other grains occur as fissure fillings with quartz and as constituents of the fine-grained matrix. A variable amount of biotite has been replaced by muscovite and fine-grained sericite, with the percentage of biotite replaced being proportional to the intensity of mylonitization. For example, muscovite is common in mylonitic South Mountains Granodiorite, but is absent in the undeformed equivalent.

Amphibole occurs in multicrystal aggregates that are aligned parallel to foliation and lineation. Some crystals are highly fractured, whereas others probably recrystallized during mylonitization.

Chlorite occurs in fine-grained, dark-colored layers, quartz-filled tension gashes, and pressure shadows next to plagioclase porphyroclasts. Some chlorite has formed at the expense of biotite and amphibole.

Epidote is an important mineralogic component in nearly all mylonitic lithologies, especially those that were originally rich in plagioclase, biotite, or amphibole. It has replaced plagioclase in porphyroclasts and in the fine-grained matrix. Epidote replacement has occurred preferentially along the tops and bottoms of many porphyroclasts. Epidote also occurs in quartz-filled gash fractures as acicular crystals aligned parallel to lineation.

Minor Structures

Gash Fractures. Lenticular gash fractures or veins are common in most mylonitic rocks. Individual gash fractures are usually less than several centimeters long, and nearly all are oriented perpendicular to lineation. The fractures are predominantly filled with quartz, although epidote, chlorite, and other minerals are also common. In some gash fractures there is a clear relationship between mineralogy of the vein and mineralogy of the adjacent wall-rock layers. For example, a single vein may contain only quartz where the vein is enclosed within quartz-rich layers, but may contain epidote in addition to quartz where it is enclosed in plagioclase-rich layers. Other gash fractures contain both chlorite and quartz where they cut biotite- or amphibole-rich layers. Such dependence of gash-fracture mineralogy on host-rock lithology indicates some local derivation of vein material. Also, some minerals in the vein are actually fragments of the adjacent wall rocks. Some sphene fragments are aligned in ghostlike layers that provide a discontinuous link between sphene-rich layers on opposite sides of the vein. The alignment of these ghostlike layers with their wall-rock sources implies a purely extensional origin for the gash fractures and suggests that mineral growth occurred during fracture opening. An extensional origin is further suggested by the observation that individual layers on either side of the vein are generally not offset; where offsets are present, they have a normal sense of displacement.

Pinch-and-Swell Structures. Many mylonitic rocks contain pinch-and-swell structures expressed by small-scale, gentle warps in the mylonitic foliation. The axes of the warps generally trend north-northwest, perpendicular to the trend of lineation. Pinch-and-swell structures are most common in mylonitic rocks derived from heterogeneous lithologies, such as Estrella Gneiss. The margins of the "swells" are low-angle, ductile shear zones or faults with normal separation. These shear zones are slightly discordant to the overall orientation of mylonitic foliation in adjacent rocks. As a consequence, foliation near the

shear zones is dragged into subparallelism with the orientation of the zones, with the resulting drag folds indicating normal slip (Figure 38).

Microscopic drape features are essentially small-scale analogs of mesoscopic pinch-and-swell structures. These are characterized by draping of lenticular mineral aggregates around brittlely deformed porphyroclasts of plagioclase and other minerals. Wedge-shaped pressure shadows of quartz, chlorite, and epidote occur beside some plagioclase porphyroclasts. Many pressure shadows are symmetrical with respect to the porphyroclasts, whereas others are somewhat asymmetrical. The presence of both asymmetrical and symmetrical pressure shadows implies that some porphyroclasts have been rotated, but others have not.

Folds. Mylonitic rocks of the South Mountains contain few folds. Except for gentle warps, not a single fold has been observed in either mylonitic South Mountains Granodiorite or Telegraph Pass Granite. The few tight folds observed in mylonitic Estrella Gneiss have amplitudes of less than 10 cm and are asymmetrical with their axes aligned parallel to lineation. It is uncertain whether the folds have a uniform direction of overturning, such as has been observed for analogous folds in the Whipple Mountains of southeastern California (G. A. Davis, 1981, personal communication).



Figure 41. Photograph of low-angle, mylonitic fabric cutting steep, crystalloblastic foliation in Precambrian Estrella Gneiss. Photograph taken looking south.

Other folds occur where the preexisting steep foliation in Estrella Gneiss has been cut by discrete zones of younger mylonitic fabric (Figure 41). In these areas, crystalloblastic foliation in the gneiss defines folds that have interlimb angles between 60° and 150° . Axial surfaces of the folds are subconcordant to gently dipping mylonitic foliation, and fold axes are aligned subparallel to mylonitic lineation. Mylonitic lineation is well developed on the hinges of some folds.

Another variety of fold is present in

areas where steep crystalloblastic foliation in Estrella Gneiss has been concordantly overprinted by steep mylonitic foliation. This relationship is most common on Entrance Ridge and in the Southern Foothills. Outcrops in these areas contain a steep, composite foliation and numerous passive-flow folds with complex geometries. This unusual style of folding was produced because mylonitization utilized the preexisting crystalloblastic foliation instead of forming a new discordant foliation.

Orientation

Mylonitic lineation consistently trends east-northeast, but mylonitic foliation varies in orientation from one area to another. Overall, the attitude of foliation defines the large, doubly plunging South Mountains antiform that trends N. 60° E.-S. 60° W., parallel to the topographic axis of the range (Plate 1 and Figures 6 and 64). The antiform is accompanied by several smaller-amplitude synforms and structural terraces. Mylonitic foliation generally has dips of 30° or less, except along the southwestern nose of the South Mountains antiform. The orientation of mylonitic fabric is discussed separately for Precambrian and middle Tertiary rocks (see Table 6).

Precambrian Rocks. The orientation of mylonitic fabric in Precambrian rocks varies among different areas or domains. The attitudes of mylonitic foliation define a nose of the South Mountains antiform that plunges approximately 30° to the west-southwest. A pole-density diagram of mylonitic foliation in all Precambrian rocks indicates that foliations have gentle to moderate dips, but highly variable strikes (Figure 42). A weakly developed, northwest-trending girdle on the diagram reflects the geometry of the plunging antiform. The modal attitude of foliation (N. 22° W., 30° SW.) represents the southwest-plunging nose of the fold. Pole-density diagrams for mylonitic foliation in each Precambrian domain are given in Figure 43 (see also Table 6). The plots are similar to one another in displaying a predominance of southwest-dipping foliation. An exception to this pattern occurs on Pima Ridge, where mylonitic foliation dips moderately to the northwest (Figure 43d). This orientation is roughly concordant to the attitude of middle Tertiary sills that intrude the Precambrian rocks and to mylonitic foliation within the sills.

The orientation of mylonitic lineation is more consistent. A trend-frequency diagram for lineation in all Precambrian domains exhibits a prominent N. 60° E.-S. 60° W. trend (Figure 44). A stereoplot of the same data yields a modal lineation direction of 28°, S. 60° W. (Figure 45). There is, however, some variation between different domains (Figures 43 and 46). East-west-trending lineation is common on Alta and Main Ridges, but not in the Southern Foothills (Figure 46). The relative abundance of east-west trends in the northern domains may have been caused by east-west strikes of Precambrian crystalloblastic foliation that were present prior to mylonitization. In other words, east-west-trending lineation formed because the rocks had a preexisting fabric in this direction. Folds in

mylonitic Estrella Gneiss generally have their axes parallel to lineation (Figure 47).

Middle Tertiary Rocks. The orientation of mylonitic fabric is more systematic in middle Tertiary rocks (Table 6). Mylonitic foliation generally dips less than 30°, except in some deformed dikes and sills. The overall attitude of mylonitic foliation defines the east-northeast-trending South Mountains antiform and several low-amplitude warps. A stereoplot of foliation in the central part of the range displays a strong maximum that represents a northwest strike and 12° dip to the northeast (Figure 48a). This orientation of foliation approximates the overall plunge of the northeast nose of the main antiform. In contrast, mylonitic foliation in brecciated and chloritic granodiorite along the northeast end of the range dips to the southwest because of rotation that accompanied formation of the chloritic breccia (Figure 48b).

Mylonitic lineation in all middle Tertiary rocks is generally subhorizontal and trends within several degrees of N. 60° E. (Figures 49-51). The trend of lineation is especially consistent in Dobbins Alaskite and in the dikes and sills, presumably reflecting the synkinematic nature of these intrusions. Trends are slightly more scattered in mylonitic gneiss and schist and in brecciated and rotated granodiorite. It is significant that the trend of mylonitic lineation is independent of the orientation of the associated foliation, and, in the case of dikes and sills, independent of the attitude of the dike or sill.

Inclusions are locally abundant in South Mountains Granodiorite and Telegraph Pass Granite. Within undeformed rocks, they are more or less equant but highly angular. In strongly deformed rocks, they are elongated parallel to lineation and are flattened perpendicular to foliation. Long axes of the inclusions are aligned N. 60° E.-S. 60° W. (Figure 52). The average axial ratios of 20 inclusions are approximately 9:3:1. If the inclusions started as spheres of unit radius, the axial ratios for deformed inclusions would be 3:1:0.33. These axial ratios indicate that the long axes have been elongated an average of three times their original length, and that the short axes have been correspondingly flattened to one-third of their original lengths. The length of the intermediate axis appears to have been unchanged by mylonitization.

Relationship to Preexisting Features

Mylonitization has been superimposed on a variety of preexisting features. Mylonitic fabric commonly cuts discordantly across crystalloblastic foliation in Estrella Gneiss (Figure 41). In many exposures, steep crystalloblastic foliation is truncated at right angles by gently dipping mylonitic fabric. The boundary between the two fabrics is locally knife-sharp, without any deflection of either fabric. In other areas, crystalloblastic foliation has been rotated into parallelism with mylonitic foliation. On Entrance and Pima Ridges, mylonitic fabric has been overprinted concordantly onto steep, crystalloblastic foliation.

FIGURE NUMBER	ROCK TYPE AND AREA	MODAL FOLIATION	MODAL LINEATION	MEAN LINEATION	NUMBER OF READINGS
42	All Precambrian domains	N 22° W, 32° SW			111
43a	Precambrian domains 1 and 2	N 28° W, 40° SW	40°, S 85° W		27
43b	Precambrian domain 3	N 84° W, 26° S	25°, S 63° W		45
43c	Precambrian domain 4	N 20° W, 30° W	35°, S 60° W		26
43d	Precambrian domain 5	N 25-70° E, 35-45° NW	0°, S 60° W		13
43e	Precambrian rocks of central Southern Foothills	N 45° W, 25° SW	25°, S 60° W		13
44*	All Precambrian domains		N 60° E	N 66° E	133
45	All Precambrian domains		28°, S 60° W		124
46a*	Precambrian rocks in Alta Ridge		N 60° E	N 71° E	38
46b*	Precambrian rocks in Main Ridge		N 70° E	N 61° E	43
46c*	Precambrian rocks in Southern Foothills		N 60° E	N 64° E	52
48a	South Mountains Granodiorite	N 53° W, 12° NE			92
48b	Brecciated South Mountains Granodiorite	N 16° W, 14° SW			27
49a*	South Mountains Granodiorite in Main and Alta Ridges		N 60° E	N 60° E	137
49b*	South Mountains Granodiorite in Southern Foothills		N 60° E	N 60° E	44
49c*	Brecciated South Mountains Granodiorite		N 60° E	N 61° E	26
49d*	Telegraph Pass Granite		N 60° E	N 58° E	36
49e*	Dobbins Alaskite		N 60° E	N 61° E	25
49f*	All dikes and sills		N 60° E	N 61° E	60
49g*	Mylonitic gneiss and schist		N 60-65° E	N 60° E	11
50a	South Mountains Granodiorite		10°, N 62° E		28
50b	Brecciated South Mountains Granodiorite		15°, S 55° W		26
50c	Telegraph Pass Granite and Dobbins Alaskite	N 35° E, 20° NW	6°, S 60° W		22
51a	All dikes and sills	N 20° W, 25° W	0-10°, N 60° E 0-30°, S 60° W		58
51b	North-northwest-trending dikes	N 20° W, 25° W	7°, N 61° E 25°, S 60° W		36
51c	Sills and dikes with trends other than north-northwest	subhorizontal	10-15°, S 60° W		22
52*	Deformed inclusions		N 60° E	N 61° E	17

*Indicates trend-frequency diagram. All other figures are equal-area plots.

Table 6. Modal and mean orientations of mylonitic fabric.

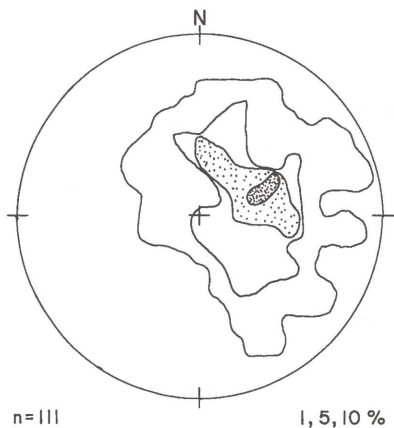


Figure 42. Contoured equal-area plot of poles to mylonitic foliation in all Precambrian domains.

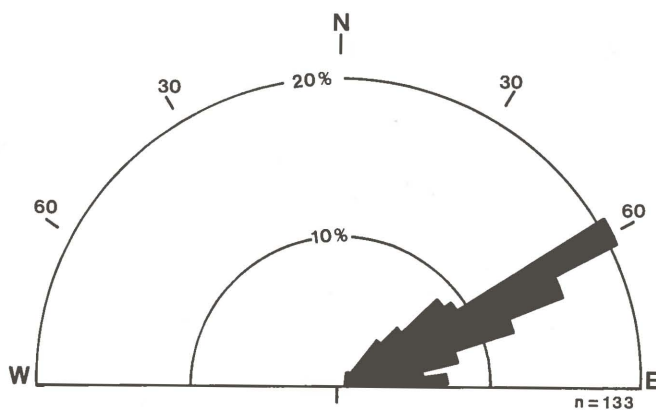


Figure 44. Trend-frequency diagram of mylonitic lineation in all Precambrian domains.

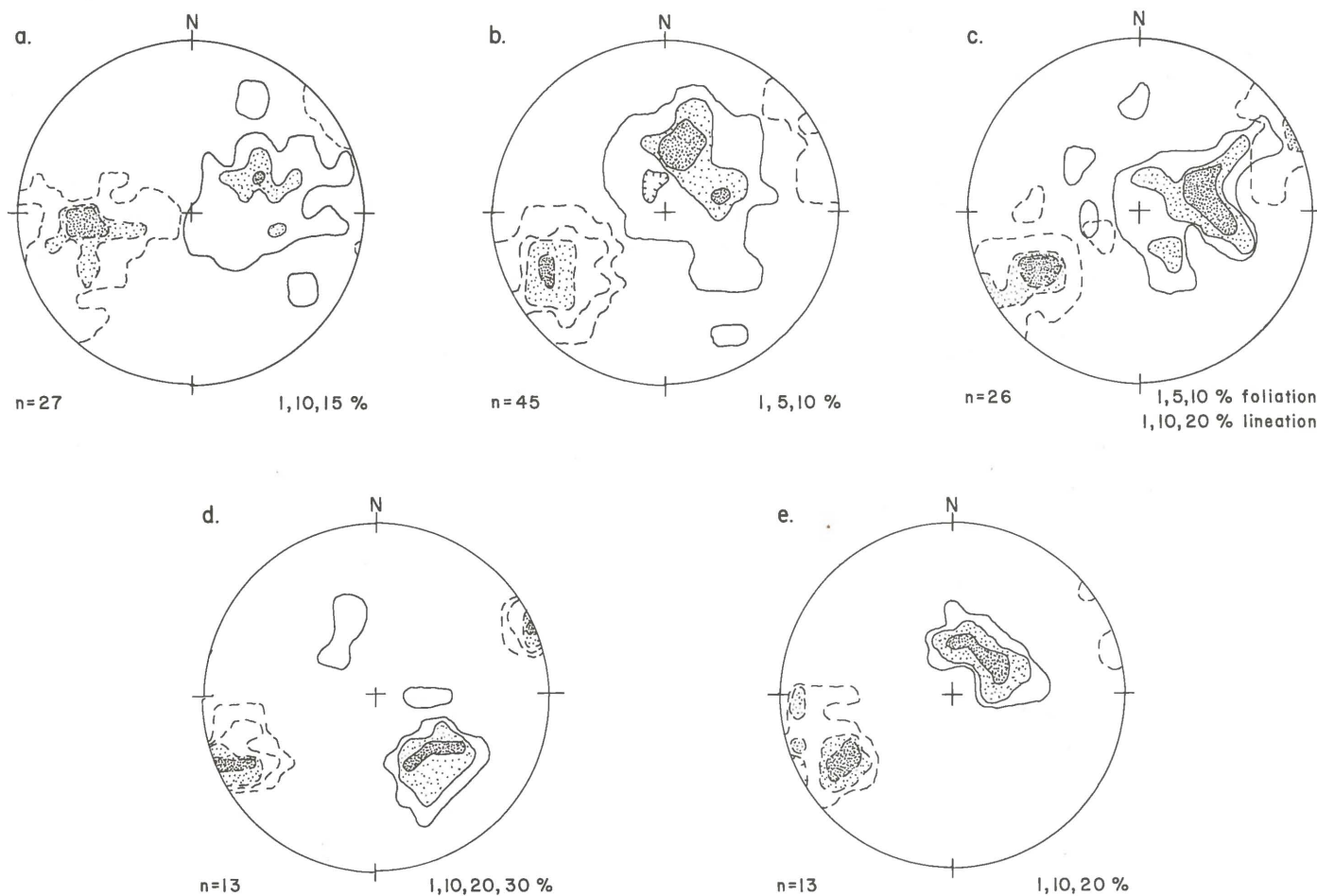


Figure 43. Contoured equal-area plots of mylonitic fabric in individual Precambrian domains: (a) Domains 1 and 2 - Alta and North Ridges; (b) Domain 3 - Main

Ridge; (c) Domain 4 - western Southern Foothills; (d) Domain 5 - Boundary Hills and Pima Ridge; and (e) central Southern Foothills.

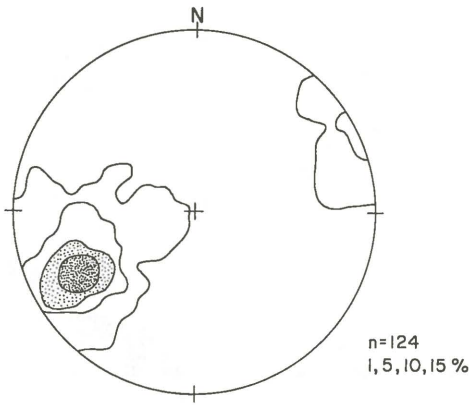


Figure 45. Contoured equal-area plot of mylonitic lineation in all Precambrian domains.

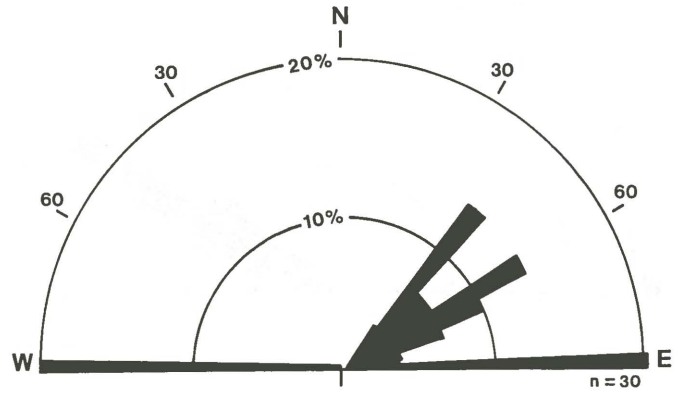


Figure 47. Trend-frequency diagram of fold axes in mylonitically deformed, Precambrian rocks.

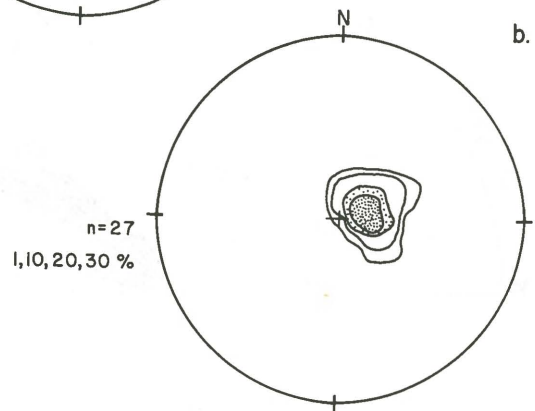
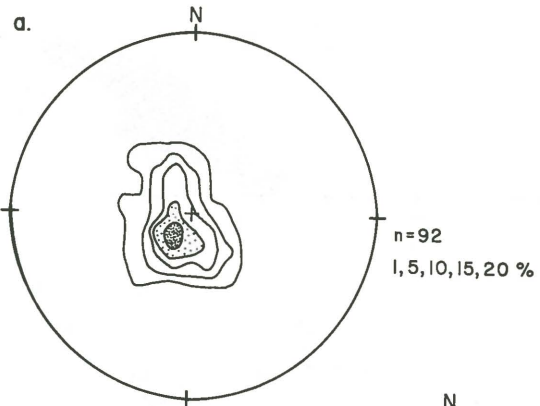
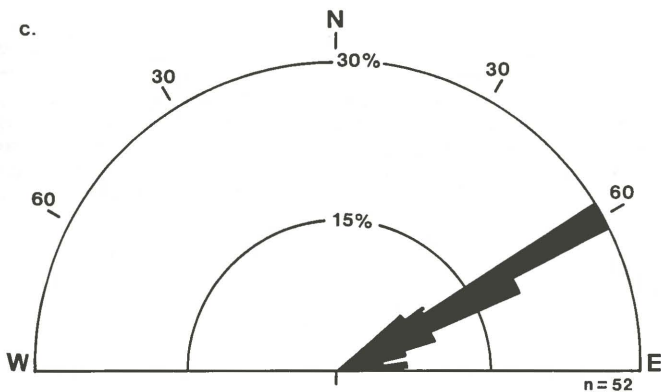
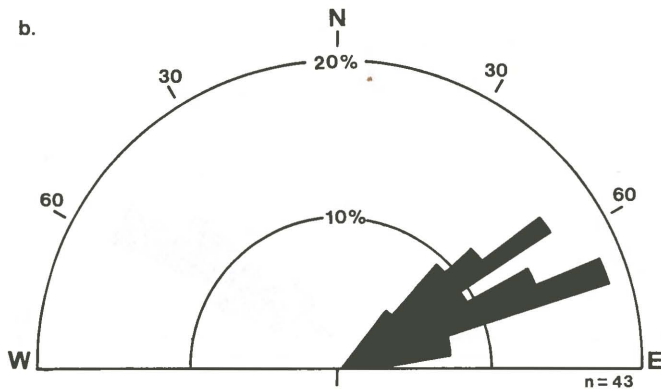
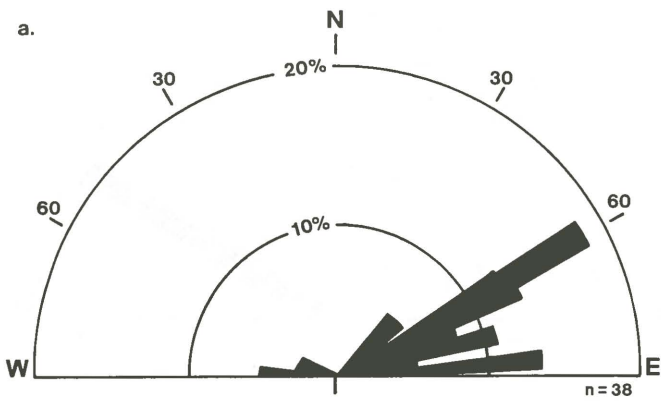


Figure 48. Contoured equal-area plots of poles to mylonitic foliation in South Mountains Granodiorite: (a) central part of Main Ridge; and (b) brecciated granodiorite on eastern end of Main Ridge.

Figure 46. Trend-frequency diagrams of mylonitic lineation in Precambrian rocks: (a) Alta Ridge; (b) Main Ridge; and (c) Southern Foothills.

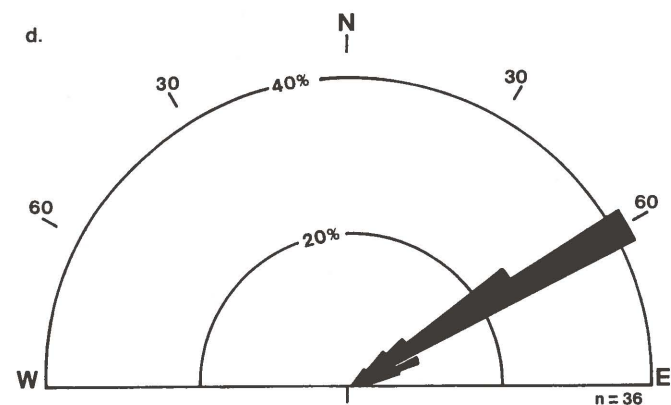
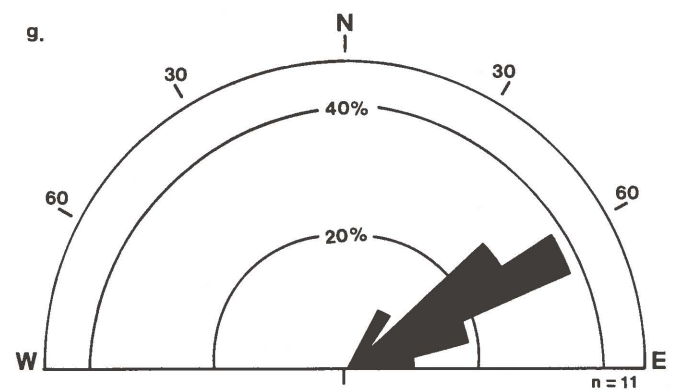
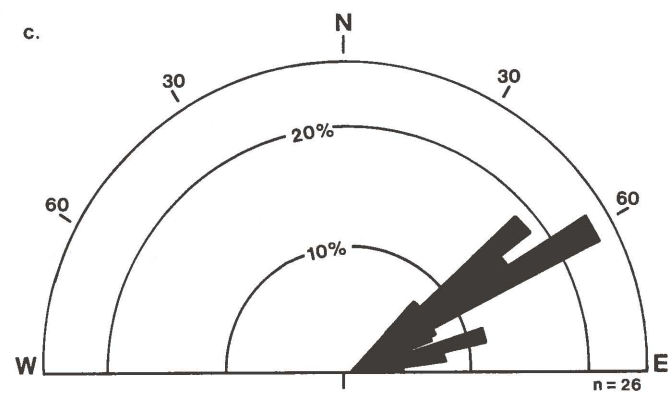
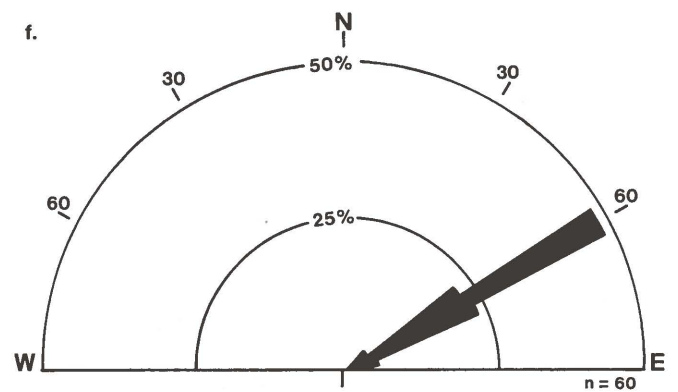
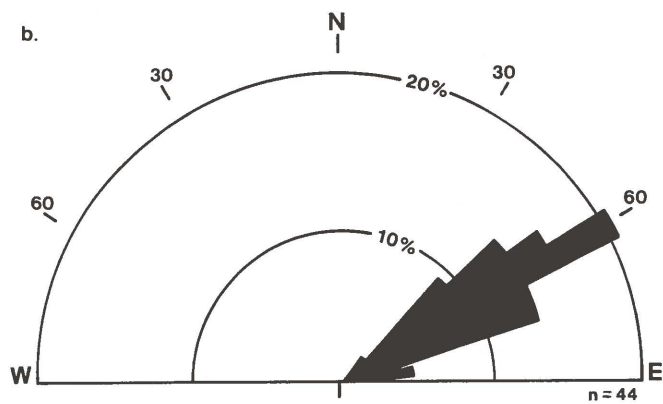
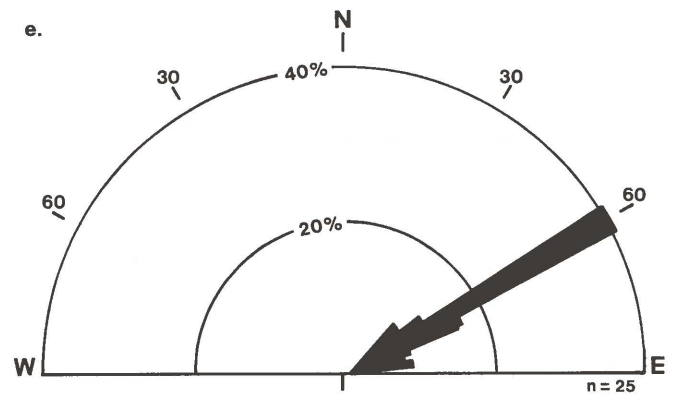
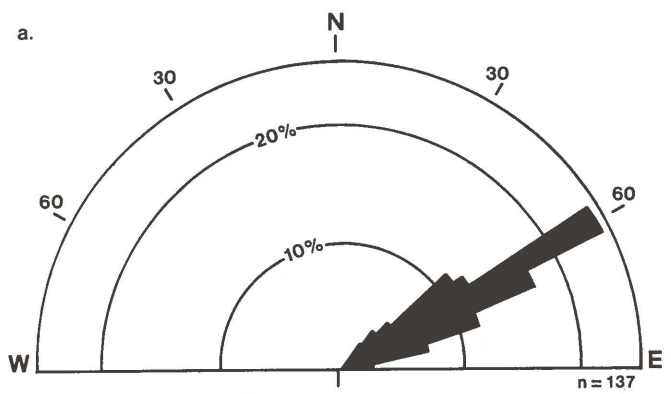


Figure 49. Trend-frequency diagrams of mylonitic lineation in middle Tertiary rocks: (a) South Mountains Granodiorite on Main and Entrance Ridges; (b) South Mountains Granodiorite in Southern Foothills; (c) brecciated South Mountains Granodiorite on eastern end of Main Ridge; (d) Telegraph Pass Granite; (e) Dobbins Alaskite; (f) dikes and sills; and (g) mylonitic gneiss and schist.

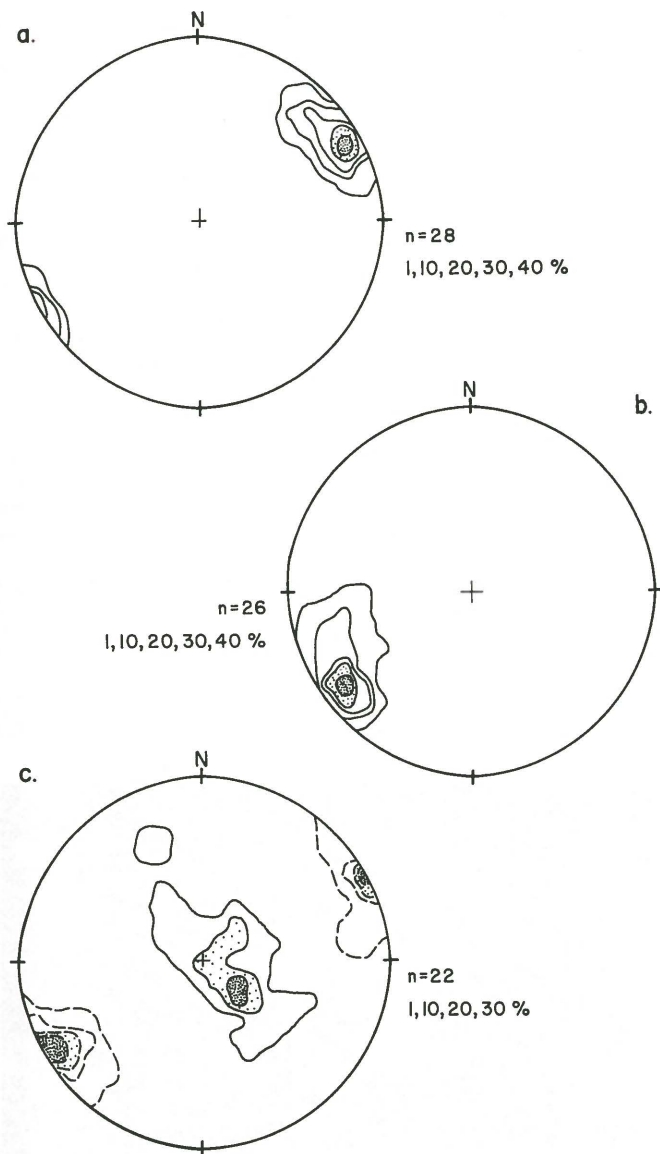


Figure 50. Contoured equal-area plots of mylonitic fabric in middle Tertiary rocks. Solid contours represent poles to foliation; dashed contours represent lineation. (a) South Mountains Granodiorite in central part of Main Ridge; (b) brecciated South Mountains Granodiorite on eastern end of Main Ridge; and (c) Telegraph Pass Granite and Dobbins Alaskite.

Mylonitic fabrics are also superimposed over various middle Tertiary igneous features. For example, the contact between South Mountains Granodiorite and Telegraph Pass Granite is commonly mylonitized. North of Telegraph Pass, the contact decreases in dip and becomes more mylonitic toward higher structural levels, which suggests that the contact was flattened during mylonitization or that mylonitization occurred preferentially along flat-lying segments of the contact. At least some changes in dip reflect the original geometry of emplacement because they occur where the contact is undeformed.

North-northwest-striking aplite dikes within South Mountains Granodiorite and Telegraph Pass Granite have generally undergone the same amount of mylonitization as their

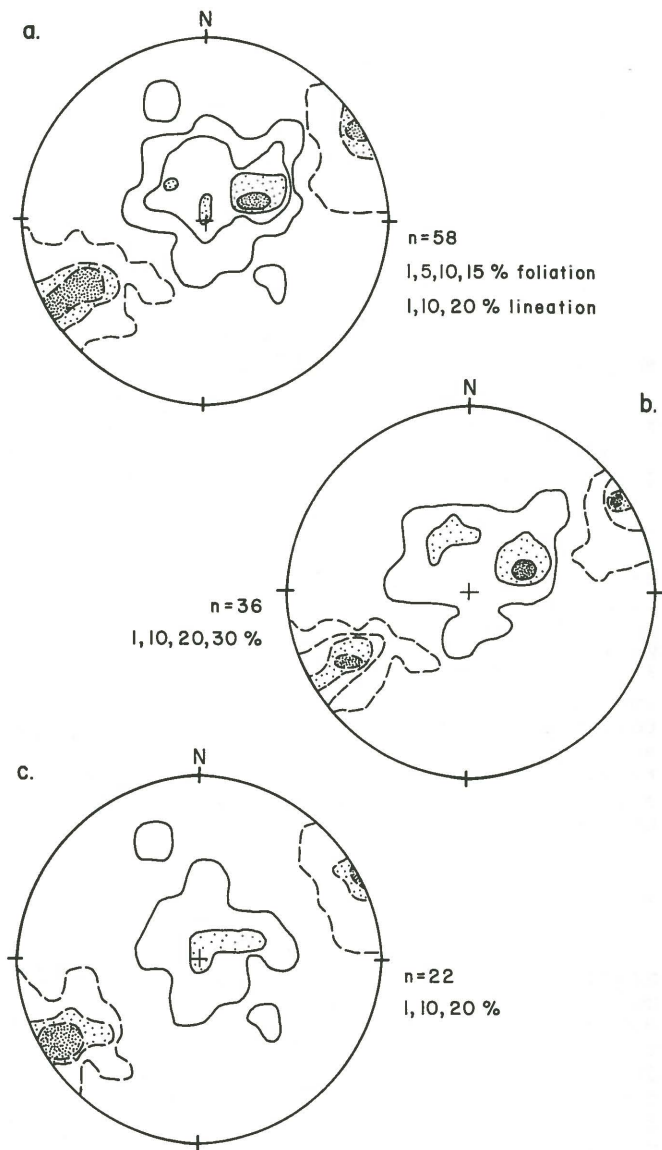


Figure 51. Contoured equal-area plot of mylonitic fabric in dikes and sills. Solid contours represent poles to foliation; dashed contours represent lineation. (a) All dikes and sills; (b) north-northwest-trending dikes; and (c) sills and dikes with trends other than north-northwest.

plutonic host rock. Many steep aplite dikes have a well-developed mylonitic fabric, but are not offset in a systematic direction. In strongly deformed rocks, aplites tend to dip more gently, presumably as a result of extreme flattening and shear. They do not dip consistently either southwest or northwest.

Mylonitization has also affected many north-northwest-striking dikes and sills. Mylonitic foliation is variably discordant or concordant to margins of the dikes and sills. The margins are generally not offset, even where horizontal mylonitic fabric cuts a vertical dike. Some dikes decrease in dip as they become more mylonitic. As with the aplites, flattened dikes do not dip preferentially either southwest or northeast (Figure 51). In fact, adjacent deformed dikes commonly dip in opposite directions.

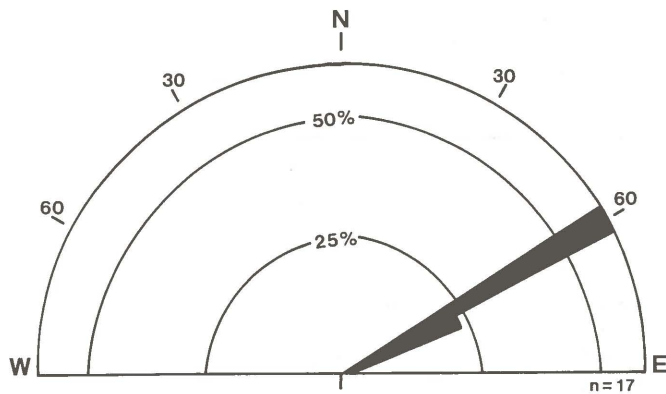


Figure 52. Trend-frequency diagram of long axes of deformed inclusions in South Mountains Granodiorite and Telegraph Pass Granite.

In several cases, strongly mylonitic dikes and sills occur within less mylonitic or nonmylonitic country rocks. This is especially true of gently dipping andesitic sills that have intruded South Mountains Granodiorite. East of Mount Suppoa, one such sill branches upward into a nearly vertical dike. Mylonitic foliations in the dike and sill are concordant and subhorizontal. The steep dike can be traced vertically for more than 50 m without any offset of its margins or any change in orientation.

Age

The age of most mylonitization is tightly bracketed by crosscutting relationships and by geochronology of middle Tertiary intrusions. Mylonitization began before final consolidation of the 25-m.y.-old South Mountains Granodiorite, because the granodiorite discordantly intrudes some mylonitic fabric in Estrella Gneiss. Most mylonitization, however, occurred during or after emplacement of the granodiorite. In some areas, mylonitic granodiorite is crosscut by less deformed Telegraph Pass Granite, which indicates that the fabric in the granodiorite began to form before emplacement of the granite. Younger mylonitization is represented by fabric that occurs in Telegraph Pass Granite. In some areas, mylonitic fabric in the granite is discordantly intruded by Dobbins Alaskite, a relationship that strongly suggests that mylonitic fabric was developing during final consolidation of the granite. Many sills of alaskite are strongly mylonitic, more so than the adjacent country rocks, which indicates that significant amounts of mylonitization accompanied intrusion of alaskite. Mylonitic fabric in alaskite is commonly intruded by north-northwest-trending dikes and sills. Many of the dikes and sills are undeformed, but others contain a well-developed mylonitic fabric that is discordant to that in the wall rocks. Such mylonitic fabric formed contemporaneously with intrusion of the dikes and sills. Most, if not all, mylonitization had ceased by the time the microdiorite dikes were intruded. Mylonitization, therefore, took place at approximately 25 m.y. B.P. and was closely related to the various middle Tertiary intrusions. If the K-

Ar hornblende age of the microdiorite dike is too old due to excess argon, mylonitization could be as young as the 20-m.y.-old, K-Ar biotite ages of the granite and granodiorite.

Conditions of Mylonitization

The close spatial and temporal association of mylonitization and plutonism indicates that mylonitization occurred under conditions of elevated temperatures but relatively low confining pressures. High temperatures, probably approaching those of a granitic melt, are indicated by evidence that mylonitization occurred during the main episode of plutonism. Textures in the synkinematic plutons indicate that mylonitization took place under conditions of relatively low confining pressures. South Mountains Granodiorite and Telegraph Pass Granite have characteristics that suggest intrusion at only moderate depth. Both plutons locally have fine-grained border phases that imply chilling upon contact with cooler wall rocks. Dobbins Alaskite contains fine-grained lithologies, such as felsite and quartz porphyry, which indicates that the granitic magma rapidly cooled at relatively shallow depths. Synkinematic dikes and sills are extremely fine grained, almost to the point of being

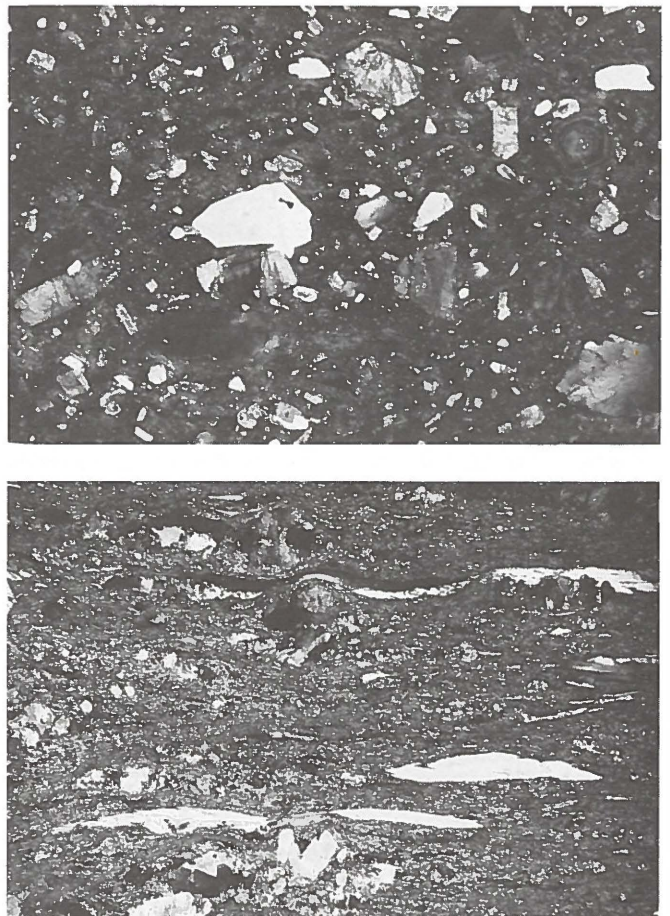


Figure 53. Photomicrographs of undeformed and deformed dikes: (a, top) undeformed dike quartz porphyry; (b, bottom) mylonitic equivalent of (a); note draping of quartz lenses over brittlely deformed feldspars. Widths of both photographs represent approximately 1.5 cm.

glassy, which requires that they were intruded at depths shallow enough to allow them to be rapidly chilled by their wall rocks (Figure 53).

Mineral assemblages within mylonitic rocks can also be used to infer the temperatures and pressures of mylonitization. Most minerals within mylonitic rocks are relicts of original mineralogy of the protoliths. For example, most biotite has survived moderate degrees of mylonitization with little or no replacement or alteration. Such biotite is genuinely stable or is a metastable relict of the original protolith. In strongly deformed rocks, however, biotite has been extensively replaced by muscovite or chlorite. Chlorite also occurs in pressure shadows adjacent to plagioclase porphyroclasts and in association with epidote and quartz in tension gashes. Plagioclase was unstable during mylonitization and was replaced by sericite and epidote. Some amphibole is present as porphyroclasts that were only slightly altered by mylonitization, but other amphibole crystals probably recrystallized during deformation. This relationship suggests that mylonitization occurred under conditions that were near the stability limits of amphibole.

The various mineralogic reactions suggest that deformation occurred under metamorphic conditions of upper greenschist to lower amphibolite facies (Reynolds, 1982; Champine, 1982). This inferred metamorphic grade is supported by the relationship between plutonism and mylonitization, which suggests that deformation took place at high temperatures but relatively low confining pressure.

Kinematics

The systematic orientation of mylonitic fabrics implies that such fabrics are the result of a single main episode of mylonitization. The excellent geometric coordination between different fabric elements permits use of a broad array of large- and small-scale structures for interpreting the kinematics of mylonitization.

Most mylonitic foliation is gently dipping and probably formed with an original, low-dipping attitude. The present dip of mylonitic foliation is largely due to formation of the South Mountains antiform, which is probably late- or postmylonitic. A simple unfolding of the flanks of the antiform would leave most mylonitic foliation dipping gently to the northeast, except for the moderately southwest-dipping mylonitic zone within Estrella Gneiss. The southwest dip of this latter zone is probably not entirely due to postmylonitic folding, because dikes and mineralized fractures in the adjacent plutonic rocks are nearly vertical, and probably formed with this orientation. This westerly mylonitic zone, therefore, may have formed with an original southwest dip. Mylonitic lineation trends N. 60° E., irrespective of the rock type or orientation of mylonitic foliation.

Small-scale structures associated with the foliation and lineation provide information on the bulk strain of deformation. The shapes of individual mineral grains indicate that the bulk strain accompanying mylonitization consisted of stretching parallel to

lineation and flattening perpendicular to foliation. For example, quartz ribbons aligned parallel to lineation reflect extreme vertical attenuation and N. 60° E.-directed stretching of favorably oriented, single crystals. East-northeast stretching is also indicated by north-northwest-striking, synmylonitic gash fractures, normal shear zones, dikes, and other extensional features. Subvertical flattening is suggested by subhorizontal pinch-and-swell structures, microscopic drape structures, pressure shadows that flank porphyroclasts, and folds formed by vertical buckling of preexisting crystalloblastic foliation in Estrella Gneiss. Also, the selective replacement of the tops and bottoms of plagioclase porphyroclasts suggests that compressive strain was concentrated in these areas. The shapes of deformed inclusions indicate that during mylonitization the rocks were stretched to three times their original length parallel to lineation, and flattened to one-third their original diameter perpendicular to foliation.

Mylonitization was accompanied by coaxial and noncoaxial strain (Reynolds, 1982, 1983; Champine, 1982). The strongest evidence for localized coaxial strain is the relationship between mylonitic fabric and various dikes. Some dikes and quartz-filled tension gashes have a mylonitic fabric perpendicular to their margins, yet their margins are not systematically offset (Figure 54). This is especially true of aplitic dikes within weakly to moderately mylonitic South Mountains Granodiorite. Coaxial strain is also indicated by the presence of symmetrical pressure shadows around some porphyroclasts. Coaxial strain has also been suggested to explain quartz c-axis fabrics that have axial symmetry (Champine, 1982).

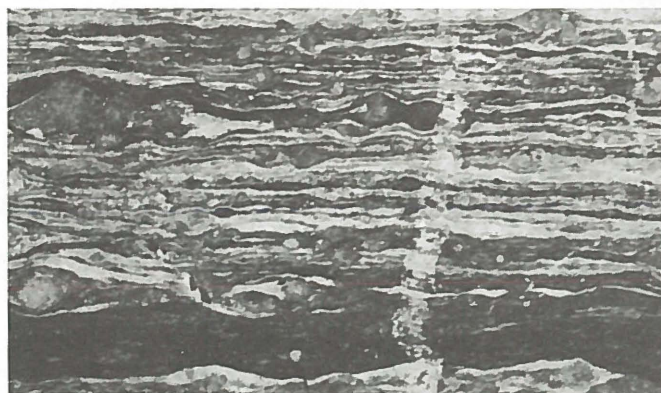


Figure 54. Photograph of tension gash in mylonitic Estrella Gneiss.

In contrast, there is also much evidence for a noncoaxial, rotational deformation (i.e., simple shear). Some mylonitic plutonic rocks contain asymmetric pressure shadows and mica "fish," which suggests noncoaxial strain. The author and G. S. Lister have observed numerous examples of penetratively developed, mesoscopic and microscopic shear bands (C-surfaces of Berthe and others, 1979) transecting mylonitic foliation (S-surfaces). S-C fabrics are currently interpreted as an indication of noncoaxial strain (Berthe and

others, 1979; Simpson and Schmid, 1983). Other evidence for noncoaxial strain includes oblique foliations in dynamically recrystallized quartz aggregates (Champine, 1982) and asymmetric quartz c-axis fabrics (S. J. Reynolds and G. S. Lister, in preparation). Finally, a noncoaxial origin for the mylonitic fabric explains why the mylonitic fabric dies out downward, yet is not supplanted by some other form of extension, as is required by a coaxial origin for the mylonites (see Rehrig and Reynolds, 1980).

Although there is clearly evidence for both coaxial and noncoaxial strain, most of the mylonitic fabrics were probably formed by noncoaxial, laminar flow, with a significant component of simple shear (S. J. Reynolds and G. S. Lister, in preparation). The dominant sense of shear is N. 60° E., parallel to mylonitic lineation and the direction of bulk stretching. S-C fabrics in South Mountains Granodiorite and Dobbins Alaskite on Main Ridge have a uniform, northeast sense of shear (Figure 55). Microstructures and quartz fabrics from oriented samples of these same rocks are strongly asymmetric, with a consistent northeast sense of shear (G. S. Lister, 1983, written communication). A northeast sense of shear is also displayed by asymmetric mica "fish" in mylonitic sills of Dobbins Alaskite on Pima Ridge in the Southern Foothills. An opposing, southwest sense of shear is revealed by asymmetric mica "fish" in southwest-dipping, mylonitic dikes northeast of Dobbins Lookout. This opposite sense of shear is most easily interpreted as being due to localized antithetic shear between adjacent synthetically rotating blocks (i.e., domino-type rotation).

The sense of shear is less clear in the southwest-dipping mylonitic zone within Estrella Gneiss, largely because of a general lack of S-C fabrics, asymmetric mica fish, and other kinematic indicators. There are, however, a number of mesoscopic shear bands that dip more steeply southwest than the main mylonitic zone. These shear bands have a southwest, or normal, sense of shear, and may be an

indication that the entire southwest-dipping mylonitic zone has an overall southwest sense of shear. Alternatively, they may be the result of late-stage shear that is antithetic to a predominantly northeast sense of shear. A third, attractive possibility is that the kinematic ambiguity of this zone indicates that coaxial strain, or pure shear, was the dominant deformational mechanism. In this last interpretation, the southwest-dipping mylonitic zone represents the downward-projecting "feather edge" of a northeast-directed shear zone, in the manner suggested by G. H. Davis (1983) for metamorphic core complexes near Tucson.

Middle Tertiary Fracturing, Brecciation, and Detachment Faulting

Subsequent to mylonitization, rocks of the South Mountains were affected by an episode of fracturing, brecciation, and detachment faulting. This brittle deformation disrupted mylonitic fabrics, produced a variety of new structures, and was accompanied by intense chloritization. It formed numerous zones of closely spaced fractures that dissect South Mountains Granodiorite. The fracture zones are widely spaced and sporadically developed in the center of the range, but are more abundant on the eastern margin of the range. The area of extensive fracturing, as delineated on the geologic map (Plate 1), represents a zone of gradation between underlying, nonbrecciated granodiorite and overlying, chloritic breccia. Chloritic breccia and microbreccia represent the most extreme development of this episode of brittle deformation. In the Southern Foothills, chloritic breccia and accompanying microbreccia occupy the footwall of a low-angle detachment fault whose upper plate consists of highly fractured and brecciated Estrella Gneiss.

The character and orientation of brittle structures is discussed separately for the

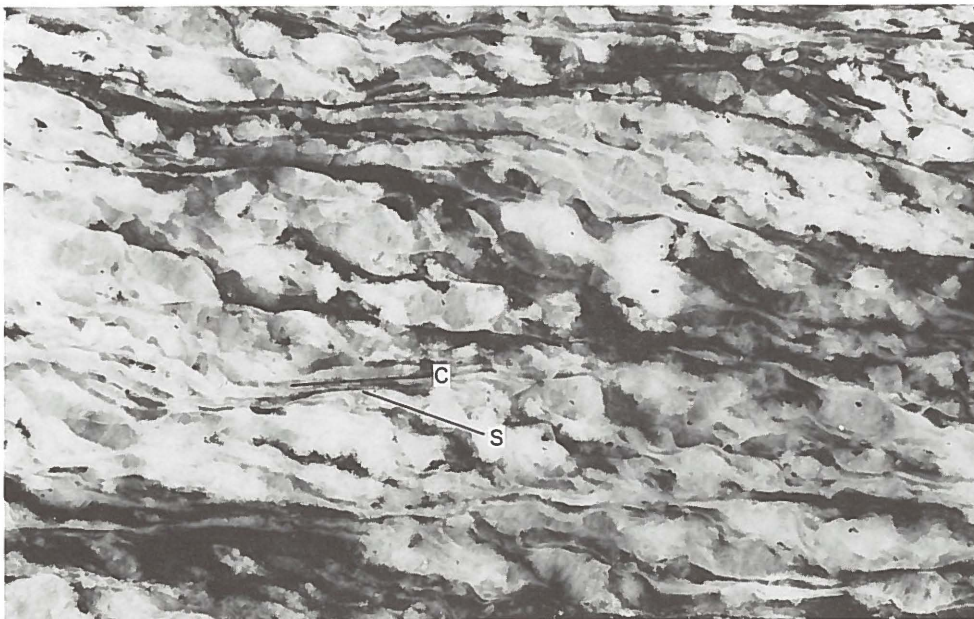


Figure 55. Photograph of S-C relationships in a cut slab of South Mountains Granodiorite. The sample displays a sinistral, or northeast, sense of shear (see also Figure 38).

FIGURE NUMBER	ROCK TYPE AND AREA	STRIKE OF CHLORITIC FRACTURE ZONES		TREND OF STRIATIONS		NUMBER OF READINGS
		MEAN	MODE	MEAN	MODE	
56a	South Mountains Granodiorite west of Dobbins Lookout	N 26° W	N 30° W			44
56b	South Mountains Granodiorite east of Mount Suppoa	N 48° W	N 40-50° W			32
59a, 60a	Chloritic breccia on east end of Main Ridge	N 32° W	N 20-30° W	N 59° E	N 60° E	85, 158
59b, 60b	Chloritic breccia on east end of Ahwatukee Ridge	N 33° W	N 35° W	N 62° E	N 60° E	118, 113
59c, 60c	All areas	N 33° W	N 30° W	N 60° E	N 60° E	296, 271

Table 7. Modal and mean orientations of chloritic fracture zones and striations in chloritic breccia.

following four structural settings (see also Table 7):

- 1) chloritic fracture zones within South Mountains Granodiorite;
- 2) transitional zone between unfractured granodiorite and chloritic breccia;
- 3) chloritic breccia and microbreccia; and
- 4) detachment fault.

Chloritic Fracture Zones Within South Mountains Granodiorite

The structurally lowest manifestation of brittle deformation is a series of chloritic fracture zones that dissect mylonitic granodiorite. The fracture zones occur sporadically throughout the granodiorite, but are most numerous in structurally high exposures. They consist of steeply dipping, quasi-planar zones of intense fracturing, jointing, and brecciation. Most fracture zones are less than 100 m long and several meters thick. Individual joint and fracture surfaces within the zones are closely spaced and vary from planar to curvilinear. They have an overall orientation parallel to that of the entire fracture zone, but intersect one another at small angles, producing a braided or anastomosing aspect. Chloritization is ubiquitous along fracture zones, but extends only a small distance outward into unfractured granodiorite. Some fracture zones increase in width upward and ultimately merge with the overlying chloritic breccia.

The chloritic fracture zones have a characteristic north-northwest strike (Figure 56a). An anomalous, more northwesterly strike is revealed by a strike-frequency diagram for chloritic fractures in an area east of Mount Suppoa (Figure 56b). Significantly, the mean strike of these fractures (N. 48° W.) is similar to the mean strike of dikes in the same area (N. 47° W.). In addition, mylonitic lineation trends almost due northeast, perpendicular to the strikes of the dikes and fracture zones. Field relationships in this area suggest that the dikes and mylonitization are semicontemporaneous. Also, there is a clear spatial and geometric association between the dikes and the chloritic fracture zones: many

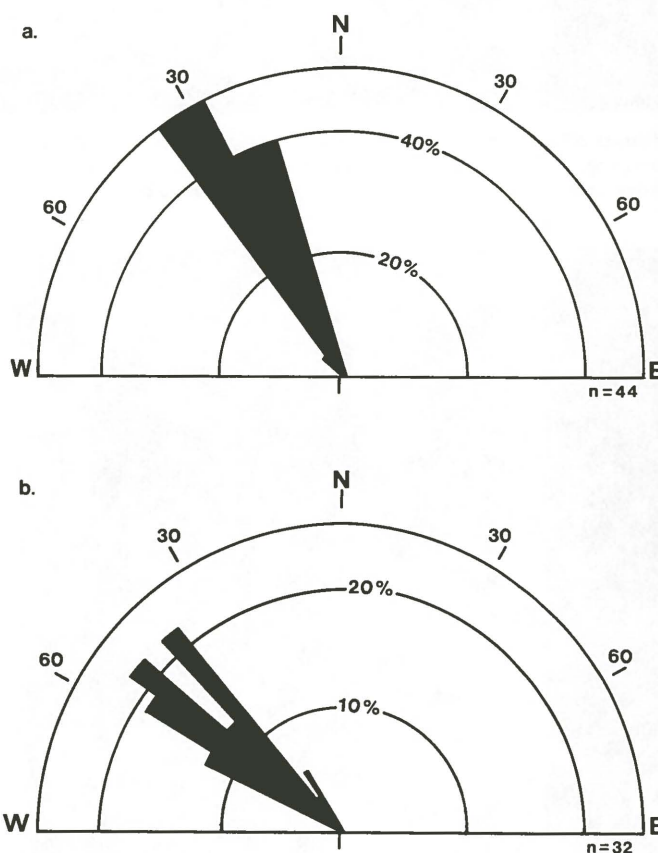


Figure 56. Strike-frequency diagram of chloritic fracture zones in South Mountains Granodiorite: (a) west of Dobbins Lookout; and (b) east of Mount Suppoa.

dikes thin out along strike and are supplanted by chloritic fractures. These observations suggest that mylonitization, the dikes, and chloritic fracture zones are closely related.

Transitional Zone Between Unfractured Granodiorite and Chloritic Breccia

Along the northeastern end of the range, the granodiorite has been extensively brecciated

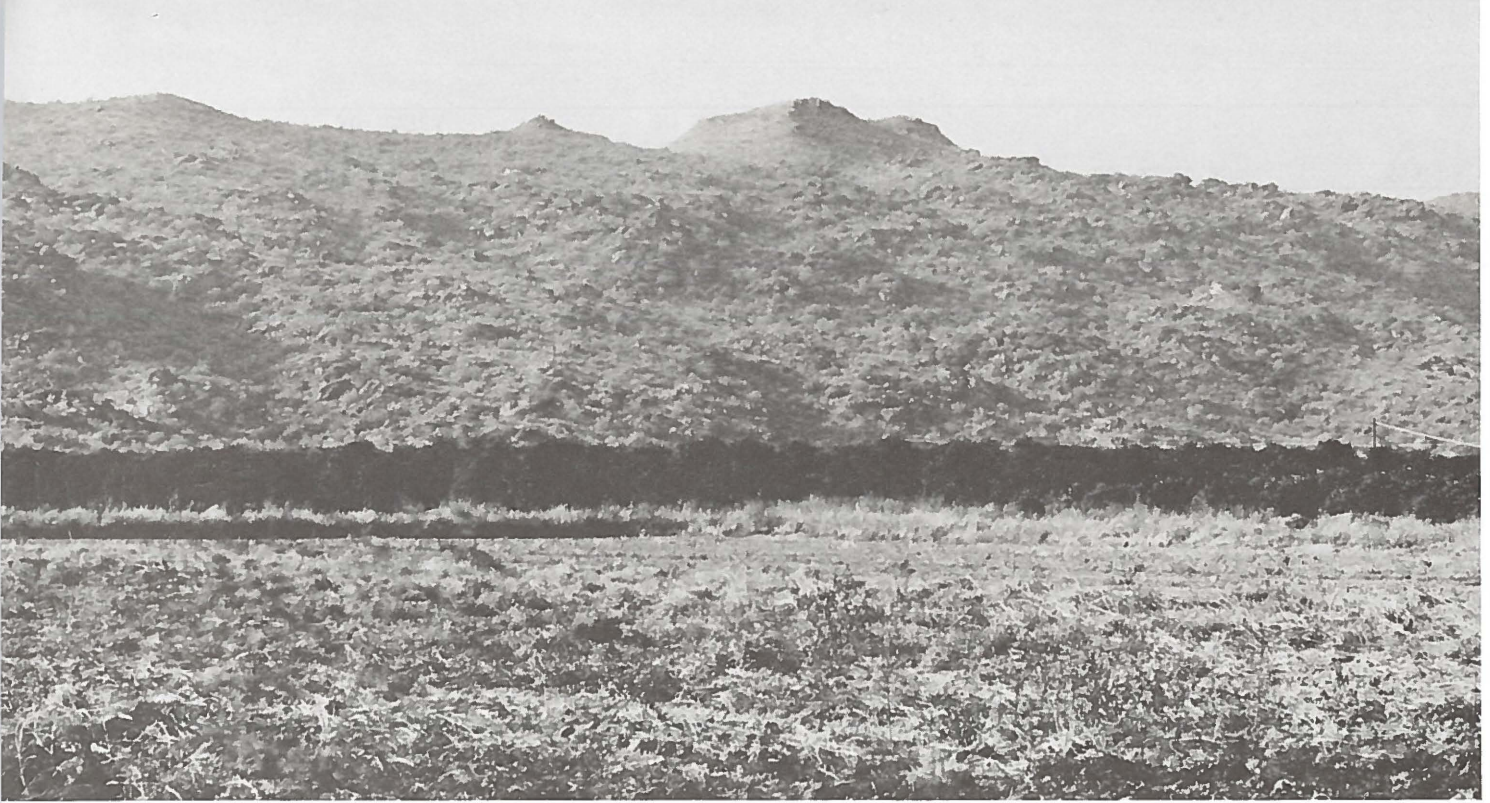


Figure 57. Photograph of Main Ridge near Two Peaks, looking southwest. All outcrops in this picture are composed of mylonitic South Mountains Granodiorite

except for Two Peaks, which are composed of chloritic breccia derived from the underlying granodiorite.



Figure 58. Photographs of structure in chloritic breccia: (a, left) anastomosing fractures in chloritic breccia on Ahwatukee Ridge; and (b, right) thin zones of microbreccia in a cut slab of Dobbins Alaskite from Dobbins Lookout.

ated and chloritized. This zone of structurally disrupted granodiorite is 30 to 50 m thick and has a gently dipping, archlike morphology when viewed over the entire range. The zone grades upward into chloritic breccia associated with the detachment fault and grades downward into less fractured and less jointed granodiorite (Figure 57). Although they are not shown on the geologic map, small exposures of jointed and chloritic granodiorite also occur along the northern margin of the range as far west as Entrance Ridge. These exposures may represent the transition between underlying granodiorite and structurally overlying, but unexposed, chloritic breccia.

Brittle structures within this zone have a predominant north-northwest strike. Discrete zones of steep, closely spaced fractures generally strike north-northwest. Small faults within the transitional zone dip gently to the northeast; drag folding of mylonitic foliation in the granodiorite indicates normal displacement of the hanging wall down to the northeast. Striations associated with the faults have east-northeast trends.

Chloritic Breccia and Microbreccia

Chloritic breccia and accompanying microbreccia represent the most intense manifesta-

tion of brittle deformation. The chloritic breccia is characterized by closely spaced fractures, joints, and faults. Most fractures have steep to moderate dips and intersect one another at small angles, producing a distinctive anastomosing pattern (Figure 58). Most fractures strike north-northwest, as revealed by strike-frequency diagrams for fracture zones in the breccia (Figure 59, Table 7). Each measurement on the diagrams is an outcrop average of numerous subparallel fractures. The mean strike of all measured chloritic fractures is N. 33° W. The mean trend of striations on small-scale faults within the breccia is N. 60° E. (Figures 60 and 61, Table 7).

Microbreccia generally occurs as a thin,

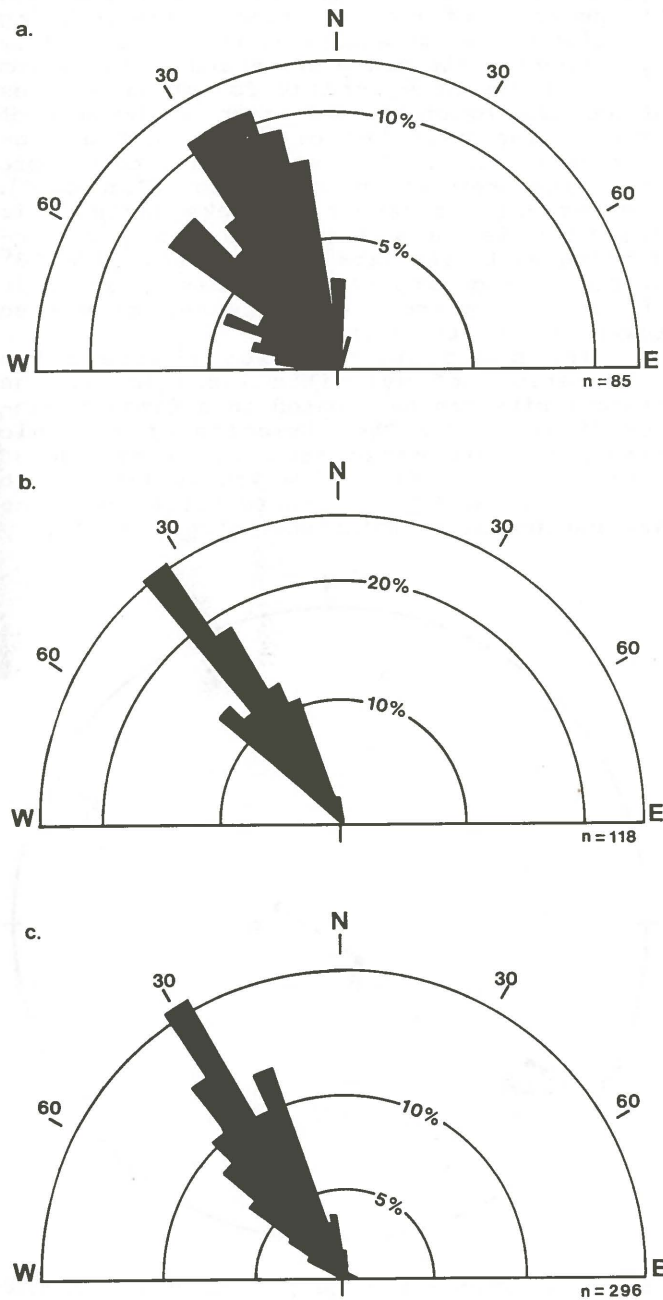


Figure 59. Strike-frequency diagrams of fracture zones in chloritic breccia: (a) eastern end of Main Ridge; (b) eastern end of Ahwatukee Ridge; and (c) all chloritic fracture zones.

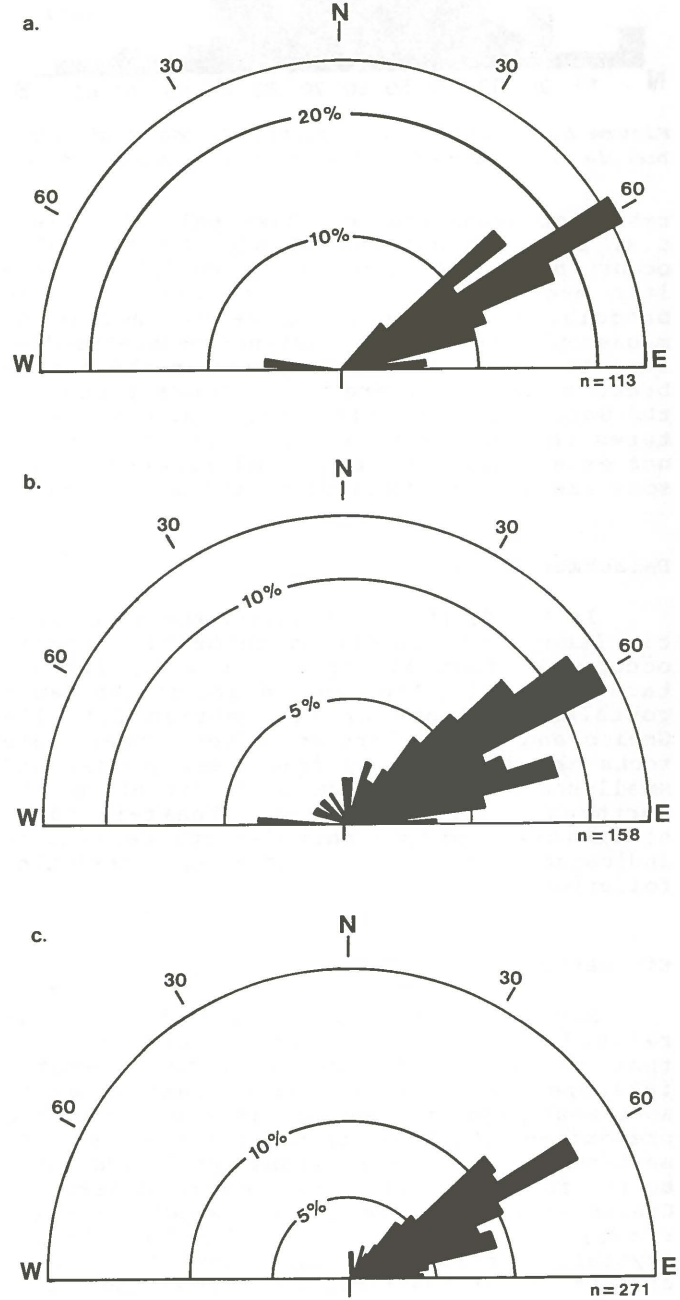


Figure 60. Trend-frequency diagram of striations in chloritic breccia: (a) eastern end of Main Ridge; (b) eastern end of Ahwatukee Ridge; and (c) combination of (a) and (b).

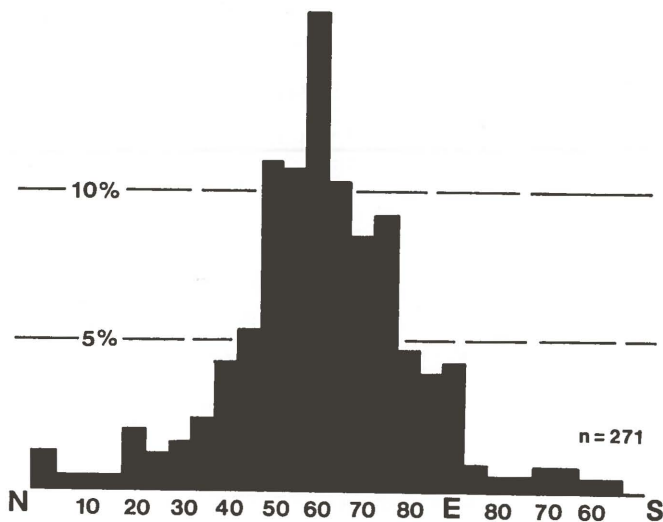


Figure 61. Histogram of striation trends in chloritic breccia on eastern ends of Main and Ahwatukee Ridges.

resistant ledge that overlies chloritic breccia, although patches of microbreccia also occur intermixed within the underlying chloritic breccia. In contrast to the chloritic breccia, microbreccia is nearly devoid of megascopic fractures. East-northeast-trending striations are locally present in the microbreccia, but they are less abundant than in the underlying chloritic breccia. Most fractures that dissect the chloritic breccia do not extend upward into the microbreccia, and some are clearly crosscut by the microbreccia.

Detachment Fault

In the Southern Foothills, the microbreccia ledge and underlying chloritic breccia occupy the footwall of a gently dipping detachment fault. The upper plate of the fault contains a klippe of Precambrian Estrella Gneiss and middle Tertiary dikes. Upper-plate rocks are dissected by fractures, joints, and small-scale faults. Several faults dip to the northeast, contain east-northeast-trending striations, and have normal displacement, as indicated by minor drag folding of preexisting foliations in gneiss.

Kinematics

Structures within chloritic breccia and related rocks have systematic orientations that readily lend themselves to kinematic interpretation. An east-northeast or west-southwest line of transport is required by the predominant N. 60° E. trend of striations. An east-northeast sense of transport is indicated by the following: (1) displacement of Estrella Gneiss over South Mountains Granodiorite; (2) rotation and drag folding of mylonitic and crystalloblastic foliations; and (3) observed offsets on northeast-dipping normal faults.

Fractures associated with this episode of brittle deformation have a pronounced north-northwest strike that is perpendicular to the trend of striations and the inferred direction of tectonic transport. Many fractures are

dilational features that formed in response to east-northeast-directed extension. Such a strain environment is compatible with observed offsets on east-northeast-dipping faults that cut chloritic breccia, the underlying granodiorite, and Estrella Gneiss. East-northeast extensional strain is also indicated by the N. 30° W. strike of microdiorite dikes that are inferred to overlap in age with the fracturing.

Brittle deformation was accompanied by rotation of preexisting mylonitic fabrics in South Mountains Granodiorite. Mylonitic foliation preserved in the chloritic breccia and underlying zone of brecciation dips to the southwest, rather than to the northeast as is typical for rocks unaffected by brecciation. The geometry of this rotational strain during brecciation may be evaluated stereographically by comparing the prerotation and postrotation orientations of mylonitic foliation (Figures 48 and 62). Mylonitic foliation in the zone of brecciation must be rotated around a sub-horizontal, N. 32° W.-trending axis to restore it to its prerotation orientation (Figure 62). The tectonic transport of rocks during this rotation is in a direction that is perpendicular to the axis of rotation, or N. 58° E. The average amount of angular rotation is 26° in a counterclockwise sense, as viewed toward the north-northwest.

The prerotation versus postrotation orientations of mylonitic lineation in the granodiorite can be treated in a similar manner (Figure 62). The direction of tectonic transport determined from the rotation of lineation is N. 60° E., which is similar to that determined from rotated foliation. The average amount of rotational strain is 25°.

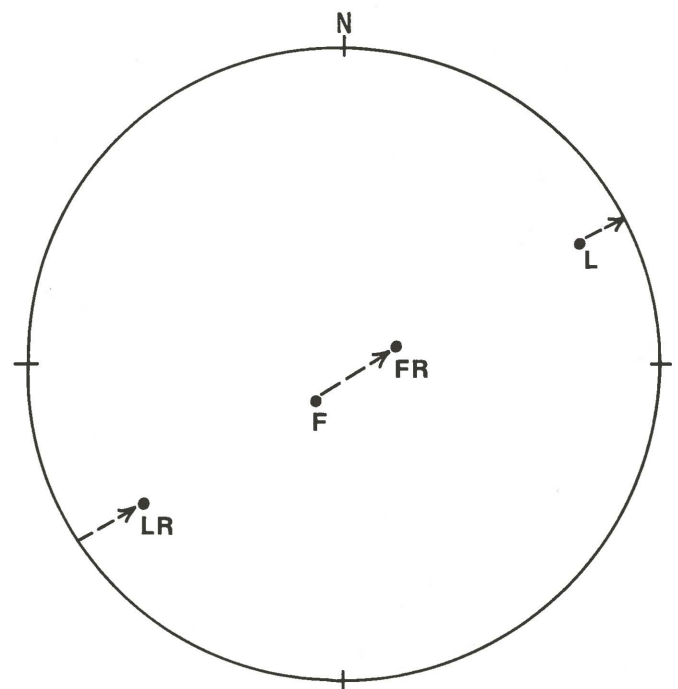


Figure 62. Stereographic projection showing rotation of mylonitic foliation and lineation by brecciation. Symbols are as follows: F - pole to nonrotated foliation; FR - pole to rotated foliation; L - nonrotated lineation; LR - rotated lineation. Arrows indicate sense of rotation.

The amount of transport on the exposed detachment fault can be estimated by comparing rocks within the klippe in the Southern Foothills with those in the footwall. The upper-plate rocks can be closely matched to lower-plate rocks located 2 to 5 km to the southwest, based on similarities in the following: (1) lithology of Estrella Gneiss, especially the presence of graphic-textured pegmatites; (2) percentages of mylonitic versus original crystalloblastic foliations; (3) the abundance and lithologies of middle Tertiary dikes; and (4) the style of brittle deformation.

In summary, tectonic transport during brittle deformation was in a N. 60° E. direction. Transport of 2 to 5 km took place on the exposed detachment fault. Relatively minor displacements on subsidiary faults resulted in antithetic rotation of preexisting mylonitic fabric. North-northwest-striking fracture zones accommodated differential rotational strain and east-northeast extension. North-northwest-striking microdiorite dikes may have been emplaced during the initial phases of brittle deformation.

It is important to note that in several exposures on Main Ridge, the microbreccia ledge is overlain by small outcrops (less than 2 m in diameter) of brecciated South Mountains Granodiorite. It is possible that these outcrops represent the same "upper plate" as the klippe of Estrella Gneiss in the Southern Foothills. However, these small knobs of granodiorite and the klippe of Estrella Gneiss are probably not the structurally highest plates. It is likely that a major low-angle fault overlies all rocks exposed in the South Mountains. This fault would dip to the northeast and would separate plutonic and meta-

morphic rocks of the South Mountains from highly tilted, Tertiary supracrustal rocks and their crystalline basement near Tempe (Figure 1). The amount of transport on this hypothetical low-angle fault might be substantially greater than the observed offset on the lower fault exposed in the South Mountains. Large amounts of northeast-directed, normal displacement on this postulated fault might explain the following: (1) the proximity of ductilely deformed, middle Tertiary plutonic rocks to essentially contemporaneous, brittlely deformed, and unmetamorphosed Tertiary volcanic and sedimentary rocks; (2) the moderate southwest dip of these Tertiary supracrustal rocks; and (3) the apparent contrast in metamorphic grade between Estrella Gneiss and equivalent, but lower grade, Precambrian rocks to the northeast in the Phoenix and McDowell Mountains (Figure 1). Total transport on this hypothetical fault could easily be 20 km or more.

The South Mountains detachment fault projects in the air to the southwest over the western South Mountains. The fault would probably project over, rather than under, the Sierra Estrella. The Sierra Estrella is either in the lower plate of the fault, or else displacement on the fault dies out before the Sierra Estrella. It is also possible that the steep, northeast-facing escarpment of the Sierra Estrella represents the original breakaway of the detachment fault.

Age

Detachment faulting and associated fracturing and brecciation occurred in the middle Tertiary. Detachment faulting postdates



Figure 63. Aerial photograph of South Mountains, looking southwest.

emplacement of the 25-m.y.-old composite pluton and most, if not all, dikes, including the youngest, microdiorite dikes. The 20- and 19-m.y. cooling ages on the plutonic rocks probably reflect uplift caused by tectonic denudation during detachment faulting. Some faulting is probably younger than 17-m.y.-old volcanic rocks near Tempe that dip to the southwest and are probably in the upper plate of the South Mountains detachment fault. A 25- to 17-m.y. age of detachment faulting is consistent with the age of detachment faulting elsewhere in Arizona and southeastern California (Crittenden and others, 1980).

Middle(?) Tertiary Arching

The orientation of mylonitic foliation within Main Ridge defines the east-northeast-trending South Mountains antiform that strongly controls the overall physiography of the range (Plate 1 and Figures 6, 63, and 64). The axis of the antiform is parallel to and coincident with the topographic crest of Main Ridge. The antiform is doubly plunging, but asymmetrical. Its northeastern nose plunges 10° to 15° to the northeast, whereas its southwestern nose plunges approximately 30° to the southwest. The antiform is a fairly open structure, with an exposed width of 3 to 4 km and a visible amplitude of nearly 0.5 km.

Dips on the flanks of the fold rarely exceed 30° . In the northeastern half of the range, the simple antiformal profile is complicated by a small structural terrace. The terrace occurs slightly north of the crest of the main antiform and has a gentle east-northeast plunge. A similar structural terrace or synform may extend southwest down San Juan Valley. Antiforms and synforms are also present in the Southern Foothills, but their recognition is made difficult by widespread rotation of mylonitic fabric during fault-related brecciation and by complex geometries of middle Tertiary intrusions.

The origin of the South Mountains antiform is problematical. It is uncertain whether the present attitudes of mylonitic foliation are indeed the result of postmylonitization arching. There is abundant evidence that the orientation of mylonitic foliation can be greatly influenced, at least on a small scale, by preexisting fabrics, contacts between rock units, and geometries of synkinematic intrusions. These influencing factors may also control the orientation of mylonitic fabric on a large scale. Mylonitic fabric on the relatively steeper, southwestern nose of the antiform is nearly concordant with the tabular form of Telegraph Pass Granite. It is possible that the southwest plunge of the antiform reflects an original orientation of mylonitic fabric influenced by intrusive geometry of the granite, and is not due to later folding.

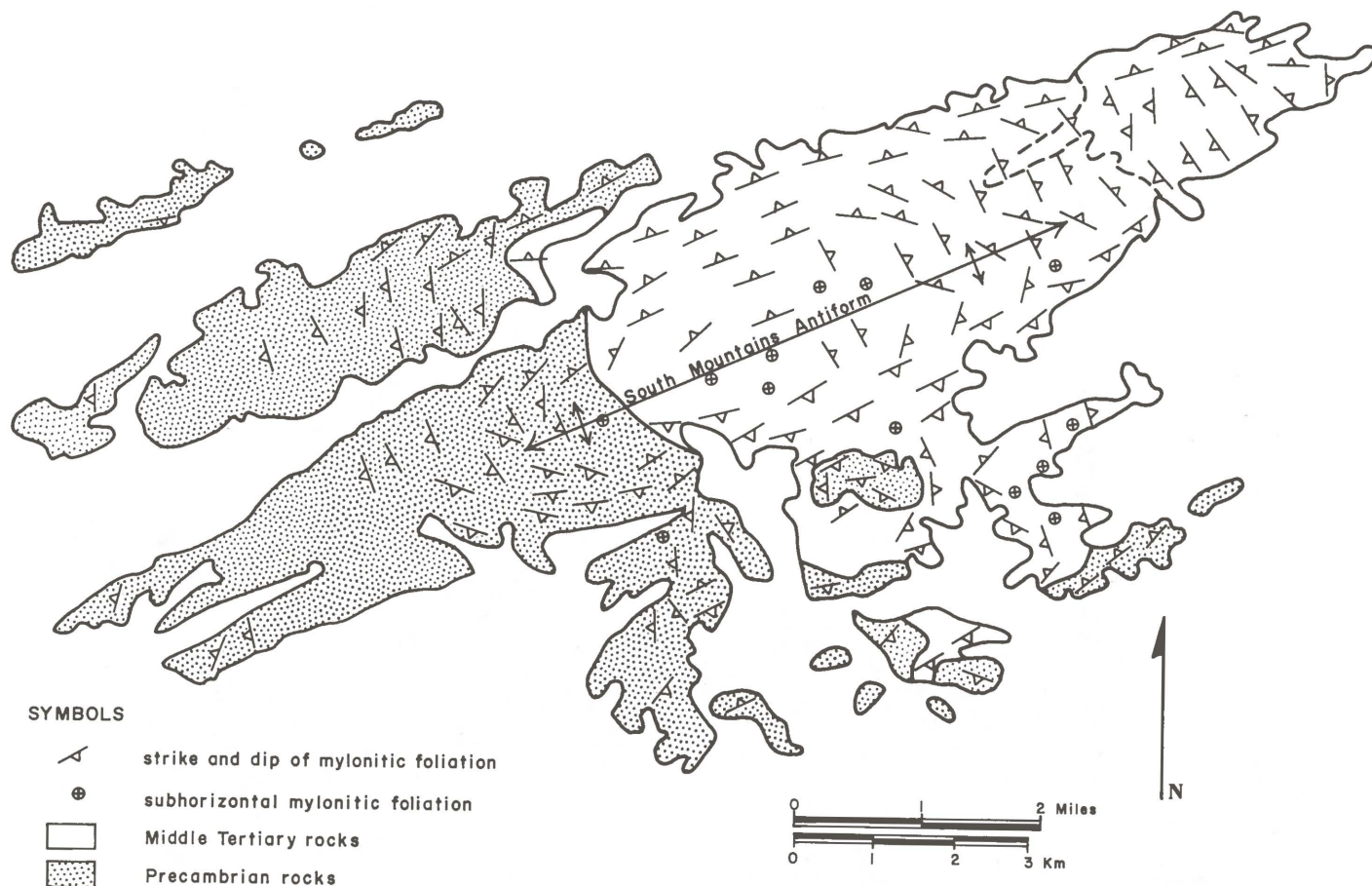


Figure 64. Map showing attitude of mylonitic foliation in the South Mountains. Precambrian rocks are shown with stippled pattern.

Another possibility, mentioned previously in the section on mylonitization, is that the southwest-dipping mylonitic fabric is due to original distributions of strain in a megascopic shear zone (Davis, G. H., 1983). This latter explanation would be consistent with the overall, northeast sense of shear inferred for the mylonitic rocks.

The above explanations do not resolve the origin of the east-northeast-trending antiform itself. Unfortunately, relationships in the range do not provide much insight on the timing of arching relative to other middle Tertiary events, such as mylonitization and brecciation. The mylonitic foliation and chloritic breccia either formed with an arch-like morphology or were arched after their formation. It is important to note that the axis of the antiform is parallel to the trend of mylonitic lineation and to the direction of tectonic transport during brittle deformation. This geometric coordination suggests that the fold may be related to mylonitization and detachment faulting. Direction of tectonic transport for detachment faulting is consistent over the entire arch, which indicates that the chloritic breccia was not formed by radial movement off the antiform. The antiform may have developed during formation of the breccia and associated detachment faulting, as suggested by Frost (1981) for antiforms and synforms along the Colorado River trough.

Late Tertiary Basin and Range Deformation

Basin and Range tectonism was largely responsible for outlining the major distribution of valleys and mountain ranges in the region around the South Mountains. There is clear evidence that Basin and Range block faulting formed the Luke and Higley basins that lie northwest and east, respectively, of the South Mountains (Peirce, 1976b; Eberly and Stanley, 1978). Most Basin and Range faulting

in this region evidently occurred between 14 and 8 m.y. ago.

There is little evidence of Basin and Range tectonism within the South Mountains. Near Telegraph Pass, there are a number of north-northwest-trending fracture zones that bear oblique-slip striations and evidence of combined normal and right-lateral movement. These fractures, which are not kinematically coordinated with middle Tertiary mylonitization, cut the mylonitic fabric. They could be a minor manifestation of Basin and Range faulting.

There is no known evidence for recent faulting around the periphery of the South Mountains. The interface between bedrock and surrounding late Tertiary-Quaternary surficial deposits is highly irregular and devoid of obvious recent faults. The Southern Foothills, in particular, are deeply embayed by gently sloping pediments. No faults have been observed cutting either the pediments or their thin veneer of gravel.

Gravity data and well information indicate that the South Mountains are part of a larger Basin and Range horst block that includes the Sierra Estrella and Sacaton Mountains (Oppenheimer and Sumner, 1981). Throughout most of the horst block, bedrock is buried beneath 100 to 400 m of late Tertiary-Quaternary clastic deposits. Bedrock protrudes through its sedimentary cover in the South Mountains, probably due to the influence of the pre-Basin-and-Range South Mountains antiform.

Although the South Mountains and Sierra Estrella are clearly not separated by a deep basin or graben, it is possible that a Basin-and-Range-type fault extends between the two ranges and is partly responsible for the impressive east-facing escarpment of the topographically rugged Sierra Estrella. The amount of transcurrent movement on the fault would be limited by the apparent similarity between lithologies in the South Mountains and Sierra Estrella.

Economic Geology

The South Mountains contain the Salt River mining district, a past source of gold, silver, and copper (Wilson and others, 1934; Wilson, 1969). Mineral deposits were discovered before 1900 and recorded production occurred sporadically between 1913 and 1942. Nine mines yielded nearly 7,000 oz of gold, 5,000 oz of silver, and 28,000 lb of copper (Arizona Bureau of Geology and Mineral Technology, 1984, unpublished file data). These commodities would be worth approximately \$2.7 million at May 1984 prices, with gold accounting for 97.6 percent of the total value. Silver and copper represent 1.7 and 0.7 percent, respectively, of the net worth.

The Delta or Max Delta Mine, the largest producer in the district, accounted for nearly 90 percent of the gold, silver, and copper production. It yielded more than 6,200 oz of gold and 4,300 oz of silver. The average recovered grade of the mined ore was 0.45 oz of gold per ton, 0.32 oz of silver per ton, and 0.09 percent copper. The highest recorded

assays of shipped ore were evidently 2.5 oz of gold and 1.5 oz of silver per ton; however, some mineralized samples contained more than 14 oz of gold per ton. The average recovered grade of ore produced from mines other than the Delta Mine was 0.55 oz of gold and 0.45 oz of silver per ton.

Most gold mines and prospects are located in Precambrian Estrella Gneiss within several kilometers of Telegraph Pass Granite (Figure 65). Gold occurrences are aligned along a north-northwest trend that parallels the intrusive contact between gneiss and granite. This spatial distribution of gold occurrences is largely coincident with the western Tertiary dike swarm.

Mineralization is consistently associated with quartz veins and stockworks that are up to 8 ft in width. One of the mined stopes in the Delta Mine is reportedly 100 ft long, 100 ft along dip, and 5 ft wide. The ore contains pyrite, chalcopyrite, arsenopyrite, and minor amounts of galena. Limonite, hematite, and



Figure 65. Distribution of gold mines and prospects in the South Mountains. Areas with mines and prospects are shown in black. Tertiary plutonic rocks are patterned.

Selected dikes of the western dike swarm are shown with hatched lines.

several copper minerals, including chrysocolla, are present in ores that have been oxidized. Calcite, siderite, and gypsum are also locally associated with the gold-bearing quartz veins. Some veins have apparently been offset by gently dipping faults.

The age and orientation of the quartz veins are of particular interest in evaluating the relationship between mineralization and the various episodes of plutonism and deformation. Age of the veins is tightly constrained by crosscutting relationships between the veins, deformational fabric in the host rocks, and middle Tertiary dikes. The mineralized veins discordantly crosscut both the Precambrian crystalloblastic foliation and the Tertiary mylonitic fabric. A number of quartz veins are mylonitic, but it is uncertain whether these particular veins are mineralized. Several mine reports indicate that there is a close association between mineralized veins and the north-northwest-trending middle Tertiary felsic and dioritic dikes; one of the veins in the Delta Mine is reportedly crosscut by a diorite or microdiorite dike. These relationships suggest that mineralization is middle Tertiary in age, probably around 25 m.y. B.P.

Orientation of the veins is similar to the systematic orientation of middle Tertiary dikes, aplites, and extensional fractures. Most gold-bearing veins strike north-northwest or northwest, although other orientations are described in unpublished mine reports (Figure 66). Several veins dip approximately 60° to the east, an attitude that is essentially

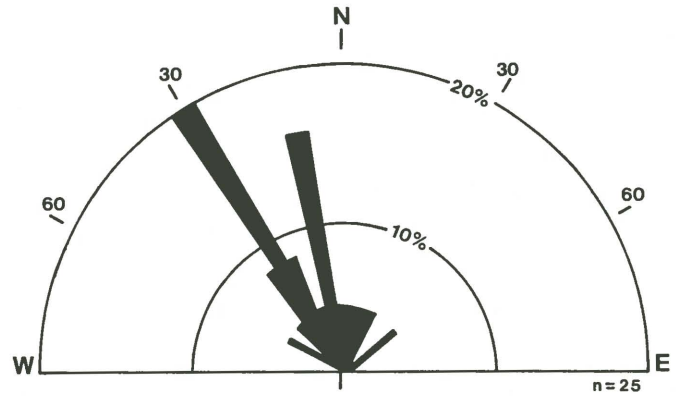


Figure 66. Strike-frequency diagram of gold-bearing veins in and near the Delta Mine.

perpendicular to the mylonitic foliation and lineation in the host rocks. The steep, easterly dip of the veins is geometrically coordinated with the gentle, westerly dip of the mylonitic foliation. The veins evidently are the same age as numerous dikes that are syn- to postkinematic with respect to mylonitization. The veins and dikes were both emplaced into north-northwest fractures that opened in response to east-northeast extension. In essence, the veins may be large gash fractures that formed during middle Tertiary extension. The gold ore was probably deposited by hydrothermal fluids that emanated from either the Telegraph Pass Granite or the related middle Tertiary dikes.

Summary and Conclusions

The South Mountains are composed of two distinct geologic terranes, each of which forms approximately half of the range. The northeastern half of the range is underlain by a composite middle Tertiary pluton that is approximately 25 m.y. old. Gently dipping, mylonitic foliation in the plutonic rocks defines a broad antiform that gently plunges to the east-northeast. Mylonitic fabric increases in intensity upward from nonmylonitic rocks in the core of the antiform. The mylonitic plutonic rocks are converted up-section into a gently dipping, tabular mass of chloritic breccia and microbreccia that formed in the footwall of a low-angle detachment fault.

In contrast, the southwestern half of the range is almost entirely composed of Precambrian Estrella Gneiss and Komatke Granite. Steep, northeast-striking Precambrian foliation in the gneiss is discordantly cut by a diffuse, moderately southwest-dipping zone of Tertiary mylonitic fabric. Gneissic rocks above and below the zone are lithologically identical and have retained their steep Precambrian foliation.

Geologic Evolution of the South Mountains

The geologic history of the South Mountains is dominated by two major tectonic episodes, one Precambrian and the other middle Tertiary. The Precambrian tectonic episode included regional metamorphism with concurrent deformation and granitic magmatism. Middle Tertiary tectonism consisted of pluton and dike emplacement, mylonitization, brecciation, detachment faulting, and broad folding. The chronology and nature of the major plutonic and deformational events are outlined below (see also Figure 67):

1) In middle Proterozoic time (1.7 - 1.6 b.y. B.P.), Estrella Gneiss was formed by amphibolite-grade metamorphism and accompanying deformation of a variety of protoliths. Precambrian Komatke Granite was emplaced during the late stages of this deformation. Steep, northeast-striking crystalloblastic foliation in the gneiss and granite was probably formed by regional, northwest-southeast-directed compression.

2) Middle Tertiary tectonism began with successive emplacement of the South Mountains Granodiorite, Telegraph Pass Granite, Dobbins Alaskite, and late-stage dikes at 25 m.y. B.P. Plutonism occurred in a regime of east-northeast extension, as indicated by the geometry of each intrusion and by the north-northwest strike of aplites, dikes, and mineralized fractures.

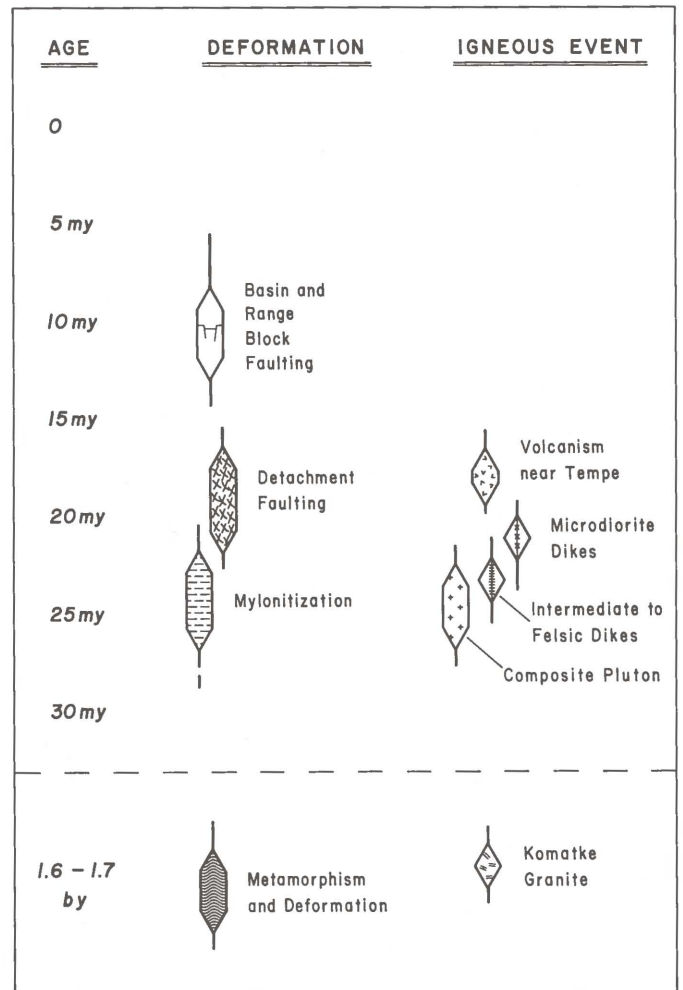


Figure 67. Chronology of geologic events in the South Mountains.

3) Middle Tertiary plutonism was closely accompanied by mylonitization that affected Precambrian, as well as middle Tertiary, rocks. Mylonitic fabrics are best developed within or near the Tertiary intrusions, which suggests that mylonitization was localized in areas of thermal weakening. As the rocks were heated or while they were still hot, they were extended parallel to east-northeast-trending lineation and flattened perpendicular to sub-horizontal foliation. Small-scale structures indicate that the overall sense of shear during mylonitization was toward the east-northeast. Antithetic, southwest-dipping, normal-slip shear zones (ductile normal faults) locally formed in mylonitic Tertiary dikes and in Precambrian Estrella Gneiss, probably due

to antithetic shear between synthetically rotating, dominolike blocks. Some mylonitic fabrics may have formed by coaxial deformation (i.e., pure shear), especially fabrics in late-kinematic dikes that were emplaced in extension fractures oriented perpendicular to the mylonitic stretching lineation.

4) Mylonitization was followed by intrusion of microdiorite dikes and by formation of chloritic breccia and microbreccia in the footwall of a low-angle detachment fault. Brecciation and associated detachment faulting probably started during, but continued after, emplacement of the dikes. The chloritic breccia and slightly younger microbreccia were formed by east-northeast-directed extension and shear, largely in response to east-northeast transport of upper-plate rocks relative to lower-plate rocks. The east-northeast-trending South Mountains antiform was possibly formed during detachment faulting.

5) Middle Tertiary tectonism was followed by an apparently unrelated episode of late Tertiary Basin and Range block faulting that formed the nearby Phoenix (Luke) and Higley Basins. It is likely that mylonitic rocks and detachment faults similar to those in the South Mountains underlie much of the Phoenix Basin.

Relationship Between Mylonitization, Brecciation, and Detachment Faulting

Plutonism, mylonitization, brecciation, and detachment faulting are clearly different manifestations of a single episode of middle Tertiary tectonism. Specifically, the overall structural evolution from mylonitization to formation of microbreccia represents a continuum of ductile to brittle extension and east-northeast-directed shear (Reynolds, 1982, 1983). Evidence for such a continuum includes the following:

- 1) close spatial and temporal association of mylonitization, brecciation, and detachment faulting;
- 2) precise kinematic coordination between mylonitization, brecciation, and detachment faulting;
- 3) consistent orientation of extension direction during the entire episode of middle Tertiary tectonism, as indicated by the orientations of aplites and other dikes, mineralized and chloritic fractures, and ductile to brittle normal faults; and
- 4) existence of a complete spectrum from ductile to brittle deformation from ductile to brittle deformation from ductile to brittle deformed mylonitic schist to more brittle deformed chloritic breccia, and microbreccia.

The continuum from ductile to brittle deformation represents a regime of consistent kinematics, but progressively decreasing temperature and pressure. Progressive decrease in temperature and pressure is reflected by the following: (1) decrease in grain size of successive synkinematic intrusions; (2) gradual transition from penetrative, ductile, mylonitic fabrics to more-localized, less-ductile, mylonitic fabrics; (3) change from mylonitization to brecciation with accompanying retrograde alteration; and (4) successive formation of chloritic breccia followed by microbreccia.

In essence, the ductile-to-brittle continuum is a response to passage of the rocks through the ductile-brittle transition. Penetrative mylonitic fabrics formed in relatively high-temperature, moderate-depth environments, whereas more localized, less ductile, mylonitic fabrics represent levels near the ductile-brittle transition. The chloritic breccia and younger microbreccia were formed in successively shallower, lower temperature environments above the brittle-ductile transition.

Implications for the Origin of Cordilleran Metamorphic Core Complexes

The structural evolution of the South Mountains as described above has significant implications for the evolution of Cordilleran metamorphic core complexes. Metamorphic core complexes are distinctive crystalline terranes that occur in a discontinuous belt between Sonora, Mexico and southern Canada (Coney, 1980; Crittenden and others, 1980). They are characterized by a crystalline core of metamorphic and plutonic rocks that generally display mylonitic fabrics at high structural levels. The upper limit of the crystalline core is commonly a zone of chloritic breccia and microbreccia that formed directly below a major low-angle normal fault or detachment fault. Rocks in the upper plate of the detachment fault are highly distended and rotated by numerous low- to high-angle normal faults. The detachment fault and lower-plate mylonitic fabrics are generally folded into perpendicular sets of broad, doubly plunging antiforms and synforms, one set of which is commonly aligned parallel to lower-plate mylonitic lineation and the transport direction for the detachment fault.

Recognition of metamorphic core complexes has largely come about in the last 10 years, and various models have been proposed to explain the observed features of the complexes (Crittenden and others, 1980). One major controversy concerns the age and kinematic significance of the mylonitic fabric and what genetic relationship, if any, exists between mylonitic deformation and detachment faulting. The South Mountains metamorphic core complex provides a unique opportunity to evaluate these controversies in a relatively uncomplicated geologic setting.

The clear association between plutonism and mylonitic deformation in the South Mountains has allowed the age of mylonitization to be precisely dated at 25 m.y. B.P. A documented, middle Tertiary age for mylonitization is strong evidence against the hypothesis that Late Cretaceous-early Tertiary overthrusting is responsible for similar mylonitic fabrics in other metamorphic core complexes of southern Arizona (Drewes, 1977; Thorman, 1977). Instead, all evidence indicates that mylonitic fabrics in the South Mountains were formed by middle Tertiary extension and shear in an east-northeast direction.

Of all the core complexes, the South Mountains contain the most compelling evidence for a genetic relationship between mylonitization and detachment faulting. Mylonitization and detachment faulting appear to have oc-

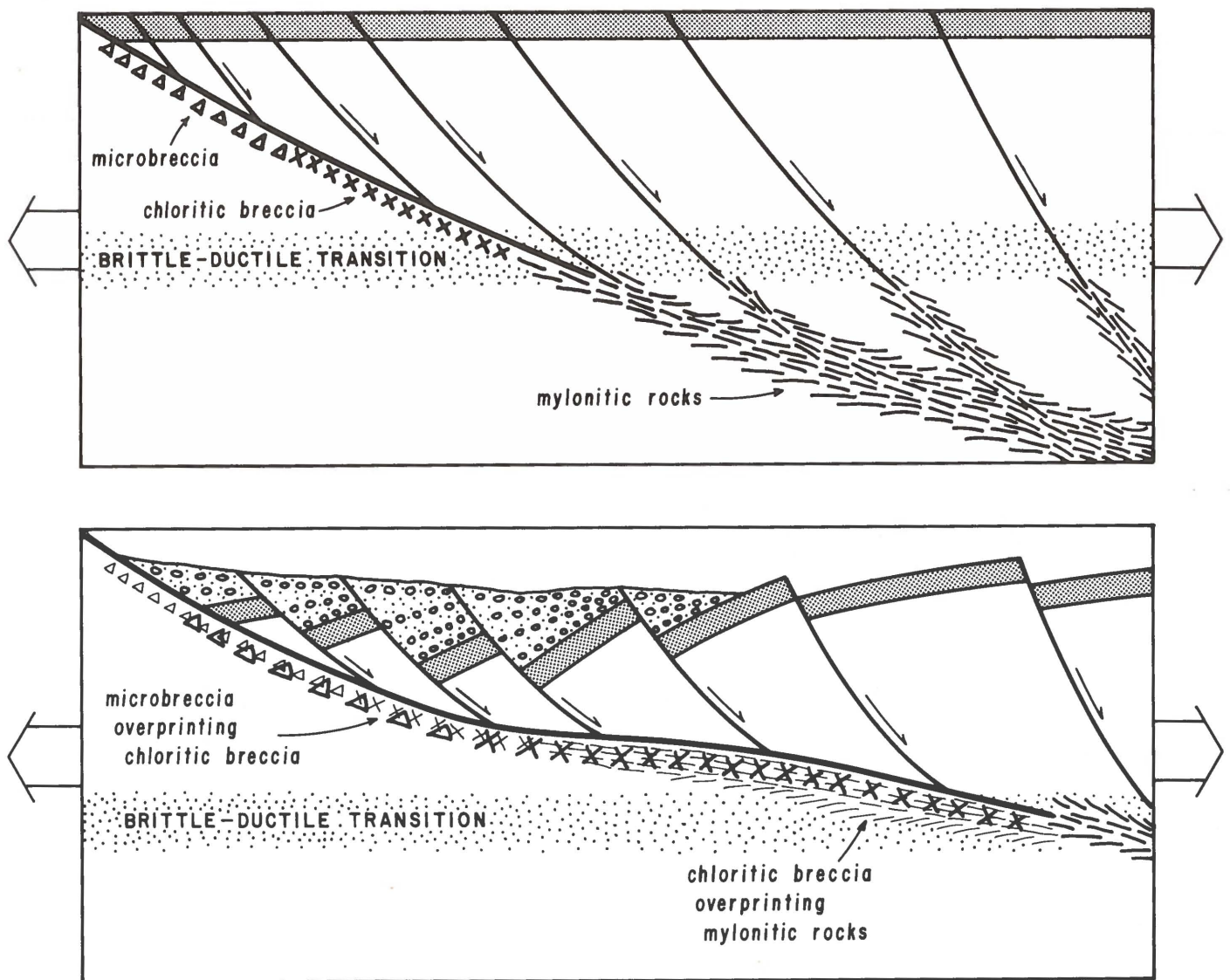


Figure 68. Schematic diagram depicting an evolving-shear-zone model for Cordilleran metamorphic core complexes.

curred within the ductile and brittle levels, respectively, of a gently dipping zone of east-northeast-directed shear and extension. An original northeast dip for the South Mountains shear zone is suggested by the following: (1) the predominant northeast dip of the main mylonitic zone; (2) the northeast dip of the South Mountains detachment fault, as inferred from the attitude of chloritic breccia; (3) regional relationships, including the distribution of upper- and lower-plate rocks adjacent to the South Mountains; and (4) comparison of the South Mountains with other core complexes in Arizona and California (Crittenden and others, 1980). The northeast dip of the shear zone, in conjunction with the east-northeast sense of shear, indicates that the shear zone has a normal sense of displacement.

Interpretation of metamorphic core complexes as low-angle, normal-slip, crustal shear zones explains most of the observed structural relationships (Davis, G. H., 1980, 1983; Wernicke, 1981; Reynolds, 1982; Davis, G. A., and others, 1983; Lister and Davis, 1983). The main features of an evolving shear-

zone model are shown in Figure 68. In this model, mylonitic fabrics in the core complexes are formed by normal slip along deeper levels of gently inclined, crustal-scale shear zones. Such mylonitic fabrics would reflect a strong component of noncoaxial strain (i.e., simple shear). Other mylonitic fabrics might be formed by localized or penetrative coaxial strain (i.e., pure shear). In either case, mylonitization would occur at depths great enough to sustain temperatures of approximately 350° to 500° C (Davis, G. A., and others, 1980). Mylonitization could occur at relatively shallow levels if plutons, such as the South Mountains Granodiorite, penetrated to high levels of the crust. The youngest, most-localized mylonitic fabrics would form at crustal depths within or slightly below the ductile-brittle transition.

Formation of chloritic breccia and microbreccia occurred mostly above the brittle-ductile transition, at lower temperatures and shallower depths than mylonitization. The breccia is the result of synchronous fracturing and hydrothermal alteration of hot plutonic rocks in the footwall of the detachment

fault. In this model, the breccia would form along segments of the shear zone that are intermediate in depth and temperature between mylonitization and the surface of the earth. Microbreccia, upper plate-fault gouge, and the actual detachment surface represent the most brittle and structurally highest levels of the crustal shear zone.

The model illustrated in Figure 68 predicts that the style of deformation within lower-plate rocks along the shear zone would change with time (Wernicke, 1981; Reynolds, 1982; Davis, G. H., 1983; Davis, G. A., and others, 1983). With progressive normal shear along the zone, lower-plate rocks along each segment of the shear zone would become less

deeply buried because of the tapered shape of the upper plate and because of brittle attenuation of upper-plate rocks (Wernicke, 1981). Lower-plate rocks would therefore become increasingly brittle with time. In this manner, mylonitic rocks formed at depth would pass upward through the brittle-ductile transition and be overprinted by brecciation and retrograde alteration. The resulting chloritic breccia would subsequently be overprinted by microbreccia at shallower crustal levels. It is this evolution toward progressively more brittle styles of deformation that produces the distinctive assemblage of rocks and structures that characterizes Cordilleran metamorphic core complexes.

References Cited

- Anderson, C. A., and Silver, L. T., 1976, Yavapai Series--a greenstone belt: *Arizona Geological Society Digest*, v. 10, p. 13-26.
- Avedisian, G. E., 1966, Geology of the western half of Phoenix South Mountain Park, Arizona: Tempe, Arizona State University, M.S. Thesis, 52 p.
- Banks, N. G., 1980, Geology of a zone of metamorphic core complexes in southeastern Arizona, in Crittenden, M. D., Jr., and others, eds., *Cordilleran metamorphic core complexes: Geological Society of America Memoir 153*, p. 177-215.
- Berthe, D., Choukroune, P., and Jegouzo, P., 1979, Orthogneiss, mylonite, and noncoaxial deformation of granites--the example of the South American shear zone: *Journal of Structural Geology*, v. 1, no. 1, p. 31-42.
- Champine, A. L., 1982, The microstructures and petrofabrics of the mylonite-chloritic breccia transition, South Mountains, Phoenix, Arizona: Tempe, Arizona State University, M.S. Thesis, 101 p.
- Christenson, G. E., Welsch, D. G., and Pewe, T. L., 1978, Environmental geology of the McDowell Mountains area, Maricopa County, Arizona: Arizona Bureau of Geology and Mineral Technology Folio Series No. 1, Map GI-1A, scale 1:24,000.
- Coney, P. J., 1973, Noncollision tectogenesis in western North America, in Tarling, D. H., and Runcorn, S. H., eds., *Implications of continental drift to the earth sciences*: New York, Academic Press, p. 713-727.
- _____, 1980, Cordilleran metamorphic core complexes--an overview, in Crittenden, M. D., Jr., and others, eds., *Cordilleran metamorphic core complexes: Geological Society of America Memoir 153*, p. 7-31.
- Cooley, M. E., and Davidson, E. S., 1963, The Mogollon Highlands--their influence on Mesozoic and Cenozoic erosion and sedimentation: *Arizona Geological Society Digest*, v. 6, p. 7-36.
- Crittenden, M. D., Jr., Coney, P. J., and Davis, G. H., eds., 1980, *Cordilleran metamorphic core complexes: Geological Society of America Memoir 153*, 490 p.
- Damon, P. E., 1968, Application of the potassium-argon method to the dating of igneous and metamorphic rock within the basin ranges of the Southwest, in Titley, S. R., ed., *Southern Arizona Guidebook III--1968*: Arizona Geological Society, p. 7-20.
- Darton, N. H., 1925, A resume of Arizona geology: Arizona Bureau of Mines Bulletin 119, 298 p.
- Davis, G. A., Anderson, J. L., Frost, E. G., and Shackelford, T. J., 1980, Mylonitization and detachment faulting in the Whipple-Buckskin-Rawhide Mountains terrane, southeastern California and western Arizona, in Crittenden, M. D., Jr., and others, eds., *Cordilleran metamorphic core complexes: Geological Society of America Memoir 153*, p. 79-129.
- Davis, G. A., Anderson, J. L., Martin, D. L., Krummenacher, Daniel, Frost, E. G., and Armstrong, R. L., 1982, Geologic and geochronologic relations in the lower plate of the Whipple detachment fault, in Frost, E. G., and Martin, D. L., eds., *Mesozoic-Cenozoic tectonic evolution of the Colorado River region, California, Arizona, and Nevada*: San Diego, Cordilleran Publishers, p. 408-432.
- Davis, G. A., Lister, G. S., and Reynolds, S. J., 1983, Interpretation of Cordilleran core complexes as evolving crustal shear zones in an extending orogen [abs.]: *Geological Society of America Abstracts With Programs*, v. 15, no. 5, p. 311.
- Davis, G. H., 1979, Laramide folding and faulting in southeastern Arizona: *American Journal of Science*, v. 279, p. 543-569.
- _____, 1980, Structural characteristics of metamorphic core complexes, southern Arizona, in Crittenden, M. D., Jr., and others, eds., *Cordilleran metamorphic core complexes: Geological Society of America Memoir 153*, p. 35-77.
- _____, 1983, Shear-zone model for the origin of metamorphic core complexes: *Geology*, v. 11, no. 6, p. 342-347.
- Davis, G. H., and Coney, P. J., 1979, Geological development of the Cordilleran metamorphic core complexes: *Geology*, v. 7, no. 3, p. 120-124.
- Drewes, Harald, 1977, Geologic map and sections of the Rincon Valley quadrangle, Pima County, Arizona: U.S. Geological Survey Miscellaneous Investigations Series Map I-997, scale 1:48,000.
- _____, 1978, The Cordilleran orogenic belt between Nevada and Chihuahua: *Geological Society of America Bulletin*, v. 89, no. 5, p. 641-657.
- Eberly, L. D., and Stanley, T. D., Jr., 1978, Cenozoic stratigraphy and geologic history of southwestern Arizona: *Geological Society of America Bulletin*, v. 89, no. 6, p. 921-940.
- Faure, G., 1977, *Principles of isotope geology*: New York, John Wiley and Sons, 464 p.
- Frost, E. G., 1981, Structural style of detachment faulting in the Whipple Mountains, California and Buckskin Mountains, Arizona: *Arizona Geological Society Digest*, v. 13, p. 25-29.
- Giletti, B. J., and Damon, P. E., 1961, Rubidium-strontium ages of some basement rocks from Arizona and northwestern Mexico: *Geological Society of America Bulletin*, v. 72, no. 4, p. 639-644.
- Harshbarger, J. W., Repenning, C. A., and Irwin, J. H., 1957, Stratigraphy of the uppermost Triassic and the Jurassic rocks of the Navajo country (Colorado Plateau): U.S. Geological Survey Professional Paper 291, 74 p.
- Haxel, Gordon, Wright, J. E., May, D. J., and Tosdal, R. M., 1980, Reconnaissance geology

- of the Mesozoic and Cenozoic rocks of the southern Papago Indian Reservation, Arizona --a preliminary report, *in* Jenney, J. P., and Stone, Claudia, eds., *Studies in western Arizona: Arizona Geological Society Digest*, v. 12, p. 17-29.
- Hayes, P. T., and Drewes, Harald, 1978, Mesozoic depositional history of southeastern Arizona, *in* Callender, J. F., and others, eds., *Land of Cochise--southeastern Arizona: New Mexico Geological Society Guidebook*, 29th Field Conference, p. 201-207.
- Higgins, M. W., 1971, Cataclastic rocks: U.S. Geological Survey Professional Paper 687, 97 p.
- Jahns, R. H., and Burnham, C. W., 1969, Experimental studies of pegmatite genesis--I. A model for the derivation and crystallization of granitic pegmatites: *Economic Geology*, v. 64, no. 8, p. 843-864.
- Keith, S. B., and Reynolds, S. J., 1980, Geochemistry of Cordilleran metamorphic core complexes, *in* Coney, P. J., and Reynolds, S. J., eds., *Cordilleran metamorphic core complexes and their uranium favorability: U.S. Department of Energy Open-File Report GJBX-256(80)*, 627 p.
- Keith, S. B., Reynolds, S. J., Damon, P. E., Shafiqullah, Muhammed, Livingston, D. E., and Pushkar, P. D., 1980, Evidence for multiple intrusion and deformation within the Santa Catalina-Rincon-Tortolita crystalline complex, southeastern Arizona, *in* Crittenden, M. D., Jr., and others, eds., *Cordilleran metamorphic core complexes: Geological Society of America Memoir* 153, p. 217-267.
- Lee, W. T., 1905, Underground waters of Salt River Valley, Arizona: U.S. Geological Survey Water-Supply Paper 136, 196 p.
- Lister, G. S., and Davis, G. A., 1983, Development of mylonitic rocks in an intracrustal laminar flow zone, Whipple Mountains, S.E. California [abs.]: *Geological Society of America Abstracts With Programs*, v. 15, no. 5, p. 310.
- Livingston, D. E., 1969, Geochronology of older Precambrian rocks in Gila County, Arizona: Tucson, University of Arizona, Ph.D. Dissertation, 224 p.
- Livingston, D. E., and Damon, P. E., 1968, The ages of stratified Precambrian rock sequences in central Arizona and northern Sonora: *Canadian Journal of Earth Science*, v. 5, p. 763-772.
- Oppenheimer, J. M., and Sumner, J. S., 1981, Gravity modeling of the basins in the Basin and Range Province, Arizona: *Arizona Geological Society Digest*, v. 13, p. 111-115.
- Peirce, H. W., 1976a, Elements of Paleozoic tectonics in Arizona: *Arizona Geological Society Digest*, v. 10, p. 37-57.
- _____, 1976b, Tectonic significance of Basin and Range thick evaporite deposits: *Arizona Geological Society Digest*, v. 10, p. 325-339.
- Pushkar, P. D., and Damon, P. E., 1974, Apparent Paleozoic ages from southern Arizona--K-Ar and Rb-Sr geochronology: *Isotopes West*, no. 10, p. 7-10.
- Ransome, F. L., 1903, Geology of the Globe copper district, Arizona: U.S. Geological Survey Professional Paper 12, 168 p.
- Rehrig, W. A., and Heidrick, T. L., 1976, Regional tectonic stress during the Laramide and late Tertiary intrusive periods, Basin and Range Province, Arizona: *Arizona Geological Society Digest*, v. 10, p. 205-228.
- Rehrig, W. A., and Reynolds, S. J., 1980, Geologic and geochronologic reconnaissance of a northwest-trending zone of metamorphic core complexes in southern and western Arizona, *in* Crittenden, M. D., Jr., and others, eds., *Cordilleran metamorphic core complexes: Geological Society of America Memoirs* 153, p. 131-157.
- Rehrig, W. A., Shafiqullah, Muhammed, and Damon, P. E., 1980, Geochronology, geology, and listric normal faulting of the Vulture Mountains, Maricopa County, Arizona, *in* Jenney, J. P., and Stone, Claudia, eds., *Studies in western Arizona: Arizona Geological Society Digest*, v. 12, p. 89-110.
- Reynolds, S. J., 1980, Geologic framework of west-central Arizona, *in* Jenney, J. P., and Stone, Claudia, eds., *Studies in western Arizona: Arizona Geological Society Digest*, v. 12, p. 1-16.
- _____, 1982, Geology and geochronology of the South Mountains, central Arizona: Tucson, University of Arizona Ph.D. Dissertation, 220 p.
- _____, 1983, A continuum of ductile to brittle extension in the South Mountains, central Arizona [abs.]: *Geological Society of America Abstracts With Programs*, v. 15, no. 5, p. 309.
- Reynolds, S. J., and Keith, S. B., 1983, Geochemistry and mineral potential of peraluminous granitoids: *Arizona Bureau of Geology and Mineral Technology Fieldnotes*, v. 12, no. 4, p. 4-6.
- Reynolds, S. J., and Rehrig, W. A., 1980, Mid-Tertiary plutonism and mylonitization, South Mountains, central Arizona, *in* Crittenden, M. D., Jr., and others, eds., *Cordilleran metamorphic core complexes: Geological Society of America Memoir* 153, p. 159-175.
- Reynolds, S. J., Rehrig, W. A., and Damon, P. E., 1978, Metamorphic core complex terrain at South Mountains, near Phoenix, Arizona [abs.]: *Geological Society of America Abstracts With Programs*, v. 10, no. 3, p. 143-144.
- Scarborough, R. S., and Peirce, H. W., 1978, Late Cenozoic basins of Arizona, *in* Callender, J. F., and others, eds., *Land of Cochise--southeastern Arizona: New Mexico Geological Society Guidebook*, 29th Field Conference, p. 157-163.
- Shafiqullah, Muhammed, Damon, P. E., Lynch, D. J., Reynolds, S. J., Rehrig, W. A., and Raymond, R. H., 1980, K-Ar geochronology and geologic history of southwestern Arizona and adjacent areas, *in* Jenney, J. P., and Stone, Claudia, eds., *Studies in western Arizona: Arizona Geological Society Digest*, v. 12, p. 201-260.
- Simpson, Carol, and Schmid, S. M., 1983, An evaluation of criteria to deduce the sense of movement in sheared rocks: *Geological Society of America Bulletin*, v. 94, no. 11, p. 1281-1288.
- Sommer, J. V., 1982, Structural geology and metamorphic petrology of the northern Sierra Estrella, Maricopa County, Arizona: Tempe, Arizona State University, M.S. Thesis, 127 p.

- Spencer, J. E., Reynolds, S. J., Anderson, Phillip, and Anderson, J. L., in preparation, Reconnaissance geology of the crest of the Sierra Estrella, central Arizona: Arizona Bureau of Geology and Mineral Technology Open-File Report.
- Streckeisen, A., 1976, To each plutonic rock its proper name: *Earth-Science Reviews*, v. 12, no. 1, p. 1-33.
- Thorman, C. H., 1977, Gravity-induced folding off a gneiss dome complex, Rincon Mountains, Arizona--discussion: *Geological Society of America Bulletin*, v. 88, no. 8, p. 1211-1212.
- Wasserburg, G. J., and Lanphere, M. A., 1965, Age determinations in the Precambrian of Arizona and Nevada: *Geological Society of America Bulletin*, v. 76, no. 7, p. 735-758.
- Wernicke, Brian, 1981, Low-angle faults in the Basin and Range Province--nappe tectonics in an extending orogen: *Nature*, v. 291, p. 645-648.
- Wilson, E. D., 1969, Mineral deposits of the Gila River Indian Reservation, Arizona: Arizona Bureau of Mines Bulletin 179, 34 p.
- Wilson, E. D., Cunningham, J. B., and Butler, G. M., 1934, Arizona lode gold mines and gold mining: Arizona Bureau of Mines Bulletin 137, 261 p.
- Wilson, E. D., Moore, R. T., and Peirce, H. W., 1957, Geologic map of Maricopa County, Arizona: Arizona Bureau of Mines, scale 1:375,000.

Appendix

SAMPLE LOCATIONS, FIELD NUMBERS, AND DECAY CONSTANTS USED

	<u>Field Numbers</u>	<u>Latitude (N)</u>	<u>Longitude (W)</u>
Estrella Gneiss			
EG-1	UARS 78-8	33°19.92'	112°05.32'
UAKA 78-27	UARS 78-8	33°19.92'	112°05.32'
South Mountains Granodiorite			
SMG-1	Sm-7	33°20.51'	112°02.81'
SMG-2	Sm-9	33°20.00'	112°04.17'
SMG-3	Sm-Sr-6	33°19.78'	112°04.38'
SMG-4	Sm-Rs-15	33°19.78'	112°04.38'
SMG-5	Sm-Sr-8	33°20.20'	112°03.95'
SMG-6	UARS 78-2	33°20.57'	112°02.52'
SMG-7	Sm-Sr-7	33°19.91'	112°04.14'
UAKA 78-80	UARS 78-2	33°20.57'	112°02.52'
UAKA 78-81	UARS 78-3	33°20.27'	112°03.23'
Telegraph Pass Granite			
TPG-1	Sm-Sr-2	33°19.90'	112°04.79'
TPG-2	UARS 78-6	33°20.33'	112°04.30'
TPG-3	UARS 78-9	33°20.70'	112°04.69'
TPG-4	Sm-Sr-1	33°20.15'	112°04.74'
UAKA 73-110	Sm-4	33°20.48'	112°04.87'
Microdiorite Dike			
UAKA 79-133	794-25-9	33°19.90'	112°00.77'

Decay constants are as follows:

$$\text{for Rb-Sr: } \lambda_B = 1.42 \times 10^{-11} \text{ yr}^{-1}$$

$$\text{for K-Ar: } \lambda_E = 0.581 \times 10^{-10} \text{ yr}^{-1}, \lambda_B = 4.963 \times 10^{-10} \text{ yr}^{-1},$$

$$^{40}\text{K}/\text{K} = 1.167 \times 10^{-4} \text{ mol/mol}$$

